Theses and Dissertations　　　　　　　Theses, Dissertations, and Senior Projects

January 2018

The Mobility Of Semi-Volatile Trace Elements From Size Segregated Fly Ash Particles Generated During Pulverized Coal Combustion

Prasanna Seshadri

How does access to this work benefit you? Let us know!

Follow this and additional works at: https://commons.und.edu/theses

THE MOBILITY OF SEMI-VOLATILE TRACE ELEMENTS FROM SIZE SEGREGATED FLY
ASH PARTICLES GENERATED DURING PULVERIZED COAL COMBUSTION

by

Prasanna Seshadri
Master of Science, University of North Dakota, 2006

A Dissertation

Submitted to the Graduate Faculty

of the

University of North Dakota

in partial fulfillment of the requirements

for the degree of

Doctor of Philosophy

Grand Forks, North Dakota
December
2018

This page was intentionally left blank

This dissertation, submitted by Prasanna Seshadri in partial fulfillment of the requirements for the degree of Doctor of Philosophy from the University of North Dakota, has been read by the Faculty Advisory Committee under whom the work has been done and is hereby approved.

_____
Dr. Frank Bowman, Committee Chairperson

_____
Dr. Steve Benson, Committee Co-chair

_____
Dr. Wayne Seames, Committee Co-chair

_____
Dr. Michael Mann, Committee Member

_____
Dr. Evgenii Kozliak, Member at large

This dissertation meets the standards for the appearance, conforms to the style and format requirements of the Graduate School of the University of North Dakota, and is hereby approved.

_____
Dr. William McGimpsey
Dean of the Graduate School

_____
December 7, 2018
Date

iii

PERMISSION

Title   The Mobility of Semi-Volatile Trace Elements From Size Segregated Fly Ash Particles Generated During Pulverized Coal Combustion

Program   Energy Engineering

Degree   Doctor of Philosophy

    In presenting this dissertation in partial fulfillment of the requirements for a graduate degree from the University of North Dakota, I agree that the library of this University shall make it freely available for inspection. I further agree that permission for extensive copying for scholarly purposes may be granted by the professor who supervised my dissertation work, or in his absence, by the Chairperson of the department or the dean of the Graduate School. It is understood that any copying or publication or other use of this dissertation or part thereof for financial gain shall not be allowed without my written permission. It is also understood that due recognition shall be given to me and to the University of North Dakota in any scholarly use which may be made of any material in my dissertation.

               Prasanna Seshadri
               December 2018

ACKNOWLEDGEMENT

TABLE OF CONTENTS

LIST OF TABLES

xii

LIST OF FIGURES

SUMMARY

INTRODUCTION

Coal-based power generation produces a significant amount of fly ash globally, but less than 50% of world production is utilized in other process industries. Large amounts of fly ash are either stored temporarily in stockpiles, disposed of in ash landfills or ash ponds. Whether ash is utilized or disposed of as waste, its chemical and physical properties must be evaluated in order to protect both health and environment. The physical nature of fly ash, especially its size distribution, is also of significant importance for both efficient design of air pollution control equipment and quantification of toxic species in ash. Fine particles, in particular, present an elevated risk of becoming air-borne particles because of their ability to escape particle capture devices and enter the atmosphere where their residence time can be as high as several weeks. Hence interest in the control of $PM_{2.5}$, denoting fine particles with aerodynamic diameters less than 2.5 μm, is motivated by health considerations as they present a respirable risk and also contain a relatively high concentration of toxic trace species.

The concentration of fine particles in the flue gas stream is dependent on a plethora of factors including coal rank, combustion system and plant operating conditions. For many coals, there are three distinct particle regions developed during combustion: 1) a submicron fume, 2) a fragmentation region, and 3) a bulk region. For most coal ashes, the combined distribution of the entire submicron fume and a major portion of the fragmentation mode constitutes $PM_{2.5}$. The controlling partitioning mechanisms for trace elements may be different in each of the three particle regions. Many trace elements (TEs) have a tendency to vaporize in the flame and as the flue gas cools, they will contact solid surfaces and undergo partitioning reactions. Most of the smaller sized submicron and fine fragment particles have fairly high surface to volume ratios and particle number densities (as compared to bulk ash particles) and hence can offer more active surface sites for trace elements heterogeneous transformation reactions. This causes TE enrichment in $PM_{2.5}$.

The three TEs of interest for this study are arsenic, selenium and antimony. All three are semi volatile in nature and are expected to undergo a vapor to solid transformation mechanism in combustion flue gas. The controlling partitioning mechanisms for the three elements may be different in each of the three particle size regions and are affected by factors such as their mode of occurrence, combustion conditions, elemental chemical properties, flue gas composition and gas cooling rates. Those TEs present on the smaller particles are typically derived from a surface chemical reaction of vapor with cation sites and they pose larger health and environmental concerns than those present in the larger bulk particles. One way to assess potential threats from trace elements is by conducting leaching tests to determine element solubility in various pH conditions. In particular it is important to determine element solubility as a function of ash particle size since each size fraction presents a different behavior that can impact the health and environment.

Laboratory leaching studies are a qualitative means to assess potential environmental impacts from combustion generated PM. Whether or not certain toxic elements in fly ash are stable and do not impact the surrounding environment depends on their solubility in the specific pH conditions encountered and data from leaching studies can be used to assess the impacts in particular environments.

The focus of the present work is to understand the factors driving TE mobility from size segregated fly ash for change in combustion conditions and coal type. The underlying hypothesis is changes to

combustion parameters are expected to change trace element speciation patterns and hence affect their final mobility from size-segregated ash particles. To achieve this objective, specific tests were designed and conducted including changes to peak combustion temperature, coal rank and ash chemistry to determine their effect on a given trace element's final mobility.

This research encompasses data from the testing and analysis of samples derived from a laboratory-combustion scale system as well as a commercial utility boiler. With respect to major limitations, a given elements speciation in ash is not identified even though it is a critical parameter in determining its overall toxicity.

MATERIALS & METHODS

Lab-scale experiments were conducted in a down-fired combustor located at the University of North Dakotas Chemical Engineering Department. A dilute stream of coal particles was burned under well controlled, reproducible conditions in this laminar flow furnace which simulates time-temperature history of a commercial boiler. Pulverized coal particles (with a fineness of 70% through a 200-mesh screen) were entrained with transport air and injected through a water-cooled feeder tube into the furnace hot zone. The coal and air were injected axially and mixed with secondary air/air+oxygen mixture flowing through a honeycomb structure. The honeycomb serves as a flow straightener to deliver combustion air at a uniform velocity. The flow rate and composition of air + oxygen mixture is regulated by both mass flow controller and rotameters. On entering the combustion zone of the furnace particles are rapidly heated and ignited producing a steady laminar flame.

Bulk gas temperature was measured using a portable, uncooled R type thermocouple. All the combustion products were withdrawn from the bottom most port (Port #10) of the furnace using a water-cooled probe. Combustion products were rapidly quenched and diluted by a high volumetric flow rate of nitrogen added at the entrance of the probe. Following the collection probe, gases and particulate matter directly enter the Dekati Low Pressure Impactor for on-line aerodynamic size classification of fly ash particles. This impactor can segregate ash particles between 0.03 and 10 micrometers in 13 different stages. During sample collection, each stage of the impactor was loaded with greased pre-weighed membranes to collect size segregated fly ash samples in the flue gas stream. In some experiments a pre-separator cyclone was employed before the impactor to remove larger particles and an impinge train was set-up downstream of the impactor to either measure flue gas moisture or gas phase concentration of metals in flue gas. Once samples were collected, they were re-weighed and carefully placed in petri dishes and stored in desiccators.

Fly ash particle size distributions (PSD) were determined by measuring the mass of particles impacted on the stages of the DLPI which was calculated as the difference in the weight of membranes prior to and after sampling. For each test, at least four sets of impactor samples were collected and data from each set was used to generate individual PSD curves. An overall typical PSD curve was then obtained by averaging data from individual runs. Four individual PSDs that most closely resembled the typical PSD were selected for further analysis.

One set of DLPI samples was extracted using an acid digestion method to determine the total concentration of major and TEs in ash. Three other sets of samples were extracted with acidic (pH = 2.88), neutral (pH = 7) or basic (pH = 11) solutions during the leaching studies conducted using a modified TCLP procedure. Major ash forming elements including Si, Ca and Fe were measured using

a Flame Absorption Spectrometer (FAA), while Graphite Furnace Atomic Absorption Spectrometry (GFAAS) was used to determine TE concentration in the sampled products. An elements overall mobility was expressed as the ratio of elemental concentration in the leaching fluid to its concentration in the totally digested sample.

The total concentration of elements of interest in the original coal was also determined using a microwave assisted acid digestion process. Additionally, a sequential leaching procedure, was used to estimate the TE associations in the test coal. This method uses solubility data to predict element mode of occurrence in coal. Similar to fly ash analysis, the FAA and GFAAS were used to determine the concentration of major and TEs, respectively. A computer controlled scanning electron microscopy (CCSEM) analysis was used to determine the principal mineralogical forms present in the test coals.

In addition to lab-scale experiments, fly ash samples were also collected from a commercial utility boiler burning a blend of two sub-bituminous coals from the Powder River Basin (PRB). Samples were collected both upstream and downstream of a wet scrubber, which was also employed as the primary particulate capture device. This study was conducted to determine if there are significant differences in fly ash TE mobility between upstream and downstream locations. Once samples were collected, aforementioned preparation and analysis methods were used to determine overall element concentration and mobility under particular leaching conditions.

RESULTS

For carefully controlled combustion conditions, some of the important variables (coal rank, combustion conditions and leaching environment) which govern the mobility of TEs in fly ash particles were examined. The results presented here will focus on the effect of some of these parameters in affecting trace element mobility in size segregated fly ash particles.

Effect of Combustion Temperature

An increase in peak combustion temperature (PCT) has been shown to affect TE partitioning and therefore is expected to influence its mobility from ash particles. This study was therefore aimed at studying this effect by varying the PCT without a significant change in flue gas residence time. The coal used for this study was a PRB subbituminous coal having a high concentration of calcium but low in iron. These two elements play a significant role in post combustion TE partitioning reactions. Test measurements included the PCT which was measured to be around 1350°C (1623 K), 1400°C (1673 K) and 1450°C (1723 K) for the three test conditions, respectively.

Fly ash PSD data for all three test conditions show a trimodal distribution namely submicron, fine fragment and bulk modes. This trimodal distribution is consistent with observations made by other researchers. Even though the difference in combustion temperature did not alter the overall PSD profile, the relative amount of ash loading for most of the stages in the submicron and fine fragment size fractions increased with increasing combustion temperatures. The mass size distributions of major elements (including Ca and Fe) and the three TEs also showed marked differences with changes to PCT, wherein their concentrations increased in the smaller submicron and fine fragment modes with increasing PCT.

Results for trace element mobility for the three size fractions under the three leaching environments indicates PCT not significantly affecting a given TEs mobility. Although there were differences in a TEs leaching behavior with respect to the size mode it resides in and the nature of the leaching fluid, these results were independent of PCT.

Effect of Coal Rank

TE mobility was determined in size segregated fly ash samples for two coals of different ranks, namely an Illinois #6 bituminous and a PRB sub bituminous, respectively. In order to better evaluate rank effect, the PCT was maintained the same for both test coals.

A trimodal ash distribution was observed for both PRB and Illinois # 6 fly ash samples with mode peaks observed at approximately the same average particle size (D_p) for both coal ashes. Even though the PSD curves for the two test coals are similar, they show some variation in the relative magnitude of peaks for the different size modes. Mass size distributions of minor and trace elements indicate contrasting trends, where the PRB ash had higher Ca loading while the Illinois # 6 ash had higher Fe distribution. As and Se loadings were higher for the Illinois # 6 ash than PRB ash in all size fractions, while only bulk mode Sb was significantly more for the Illinois # 6 ash than the PRB ash.

With respect to TE mobility from fly ash particles, there were differences in an elements leaching behavior based on the type of coal ash under consideration. While As had similar solubilities across submicron and fine fragment size fractions for both PRB and Illinois # 6 ashes, Se present in the Illinois #6 ash showed slightly higher solubility than the PRB ash for all three pHs in the smaller size ranges. Leaching studies for antimony showed a similar trend to selenium where Sb in the Illinois # 6 ash samples was found to be more soluble in most cases than Sb in the PRB ash samples. Also, irrespective of the type of coal ash, all three elements exhibited higher mobility under acidic leaching conditions compared to both neutral and basic conditions.

Effect of Wet Scrubber

Fly ash PSD results show a trimodal distribution – a smaller submicron mode, an intermediate fine fragment mode and a larger bulk mode - in both inlet and outlet samples. The scrubber removed particles across the entire size range of fly ash. However, the fine fragment mode with a peak at about 0.8 µm, was not removed as well as the other modes.

With respect to element mass size distribution, both Ca and Fe distribution mirrored overall PSD curves, especially for submicron and fine fragment particles. As and Sb had similar distributions at both inlet and outlet including matching peaks for both submicron and fine fragment regions. Se, on the other hand, exhibited anomalous behavior compared to both As and Sb, especially at the scrubber outlet. Data indicates a slight increase in submicron selenium at scrubber outlet compared to inlet concentrations indicating potential selenium re-emission. Overall, the scrubber was efficient in capturing a major portion of TE in fly ash.

Results from leaching studies indicate a trend also observed under lab-scale testing - solubility was much higher in the smaller submicron and fine particulate fractions as compared to the larger bulk fly ash particles. Additionally, all three TEs showed about equal solubility in the submicron and fine particulate size regimes under all three environmental conditions. Furthermore, with the exception of

selenium, there was no clear distinction in element solubility between scrubber inlet and outlet for both As and Sb in all three size modes. However, for Se, there was in increase in mobility for both submicron and fine fragment fractions across the scrubber and was mainly observed under acidic and neutral leaching conditions.

DISCUSSION

Effect of Combustion Temperature

The increase in submicron and fine fragment concentration of Ca and Fe with increasing PCT is mainly due to increased vaporization of mineral matter at higher combustion temperatures. Vaporized species will then undergo nucleation/ coagulation and condensation reactions during gas cooling on entrained fly ash particles creating active surface sites for TE partitioning reactions. Hence, increasing PCT would have increased the amount of active cation sites available for trace element partitioning reactions. This was verified by both TE mass distribution and their vapor phase concentration for the three test conditions.

All three TEs showed an increase in submicron and fine fragment mode concentrations with increasing PCT. The amount of trace elements that partitions to the small PM is expected to increase as PCT increases due to the increase in available Ca and Fe surface sites at elevated combustion temperatures. Vapor phase data for TEs support this hypothesis since lower amounts of TEs were present as vapor at higher PCTs, indicating increased vapor to solid transformation at these conditions.

Results of leaching studies show that combustion temperature did not have a pronounced effect on overall TE mobility. This indicates the possibility of the formation of similar chemical species at all three test conditions and in the respective size fractions. With respect to size mode, all three TEs had higher solubility in submicron and fine fragment modes compared to the bulk mode indicating surface presence on the smaller particles. Significant amount of TEs present in bulk particles are likely incorporated within the particulate matter structure and is expected to stay bound within the ash under most pH conditions.

While considering the effect of leaching environment, both As and Sb showed high mobility under acidic conditions and moderate mobility under neutral conditions. Arsenic was completely insoluble under basic conditions, while Sb was only slightly soluble. Selenium, on the other hand, showed particle-size based dependency in a given leaching environment. While submicron Se showed equal solubility in all three leaching environments, Se present on fine fragment particles showed pH-based dependence with high solubility in acidic medium and moderate solubilities in both neutral and basic medium.

Effect of coal rank

Results of fuel analysis shows the PRB coal having high calcium content and the Illinois # 6 coal to be iron rich, which is mainly derived from the pyrite grains. Additionally, Illinois # 6 coals had higher amounts of TEs than the PRB coal, as these elements are commonly associated with pyrite. Sequential leaching results of the coal samples does indicate significant pyrite association for all three TEs in the Illinois # 6 coal.

Fly ash PSD curves for the two test coals are similar but show some variation in the relative magnitude of peaks for the different size modes. Even though the tests were carried out at the same peak combustion temperature, differences in ash content, chemistry and mineralogy influence the overall PSD curves. For most low rank coals such as PRB, vaporized alkali and alkaline earth metals (Ca, Mg, Na and K) are expected to contribute significantly to the smaller submicron/ultrafine and fine fragment masses. Similarly, for the low calcium and pyrite rich Illinois #6 coal, the submicron mode is expected to be mostly composed of oxides of Si and Fe. Coarse mode ash for both coals is expected to be derived from clays such as kaolinite, illite etc.

With respect to elemental mass size distributions, the PRB ash had higher loading for calcium than Illinois # 6 for all the size fractions. The organic association of calcium, as determined by chemical fractionation analysis, will play a major role in its behavior during combustion and subsequent partitioning onto fly ash particles. Also, in the case of Illinois #6 coal, the combination of low calcium and high sulfur content will tend to reduce the availability of active cation sites on fly ash particle surfaces. This may reduce the fraction of trace elements that partition due to a surface reaction mechanism. However, unlike Ca, there were much higher amounts of Fe in Illinois # 6 ash compared to PRB ash. Most of the Fe in ash would have been derived from the high concentration pyrite in the raw coal.

While the forms of arsenic are different between the two coals, a significant portion of the arsenic in both coals will vaporize during the combustion process. Illinois # 6 ash samples had higher As for all particle sizes compared to the PRB samples. This is partly from the higher overall amounts of As present in the Illinois # 6 coal. Similar to arsenic distribution, the Illinois # 6 samples had more Se in all the reported size fractions. The partitioning of selenium is also very similar to arsenic for the different size fractions for the Illinois # 6 sample. However, unlike As and Se, there was not a significant difference in submicron antimony levels between both coal ashes even though the Iliinois #6 coal had twice as much antimony than the PRB coal. This indicates the possibility of lower Sb vaporization for the Illinois # 6 coal compared to the PRB coal or the possibility of vaporized species not transforming to solid surfaces mainly due to kinetic and or mass transfer limitations. Sb is the least reactive of all three TEs, it is the least likely to react with Fe and may not even have sufficient Ca sites for vapor phase partitioning. The coarse size fraction of Sb was much higher for Illinois # 6 samples compared to PRB samples indicating the presence of non-volatilizing fraction, mainly derived from bigger exclusions.

Data from leaching studies indicate that the mobility for As was very similar for both coal ashes especially under acidic and neutral conditions for both submicron and fine fragment modes. This indicates similar partitioning mechanisms across both size fractions, with calcium arsenate expected to dominate the particulate phase. However, under alkaline conditions there was more of a difference between the two coals. In the Illinois # 6 ash arsenic was not found to be very soluble for the smaller size fractions. This contrasts with the PRB ash which had somewhat higher arsenic solubility in the submicron and fine fragment size fractions. Chemical fractionation data for the bituminous coal shows mainly mineral association for As which can inhibit mobility under certain leaching environments. For Se, both submicron and fine fragment mode mobility was higher for the Illinois # 6 samples compared to PRB ash samples under all three leaching environments. Selenium undergoes a partitioning mechanism similar to arsenic and hence it was found to be more soluble in the smaller size range. While most of the selenium is expected to be complexing with Ca, high solubility data, especially for

the Illinois # 6 ash, indicates the possibility of Fe-Se complexes (selenates) which have been shown to have fairly high solubility than Ca-Se complexes (selenites). Leaching studies for Sb showed trends similar to Se, where Sb in the Illinois # 6 ash samples was found to be more soluble (for most cases) than the PRB ash samples. This indicates possible differences in Sb partitioning mechanism for the two fly ashes which mainly arises from the differences in coal ash chemistry. However, unlike Se, the PRB ash solubility remained fairly constant irrespective of pH.

Effect of Wet Scrubber

Based on overall PSDs and elemental mass size distributions, the scrubber was efficient in capturing a major portion of all three TEs in fly ash particles. With respect to individual elements, both As and Sb had distributions that mirrored calcium at inlet conditions indicating potential surface reactions with active Ca sites. As these two elements are present in the same group of the periodic table, they are expected to exhibit similar behavior in a combustion environment. While all three TEs also partition onto iron sites, calcium-based compounds and complexes are expected to dominate TE distribution in fly ash due to much higher amounts of calcium, in comparison to iron, both in the original fuel and final fly ash particles.

Fly ash data at the scrubber outlet shows an interesting trend for selenium, especially in the smaller submicron and fine particulate mode. For the smaller size fractions, between 0.1-0.5 µm, selenium showed increases in concentrations at the scrubber outlet compared to inlet levels. This could be attributed to any of the following factors or a combination there-of:

- Displacement reactions in the scrubber where sulfur present in the FGD solution reacts with the cations that were holding the selenium oxy-anion and thereby liberating Se back in the gas phase. Released Se vapor can then nucleate/coagulate or even condense forming very small particles.

- Gas-to-particle conversion of selenium vapor across the scrubber as evidenced by other researchers in a utility boiler burning bituminous coal.

- A significant portion of Se in the FGD can be associated with the gypsum and this can be entrained with the flue gas exiting the FGD and can be collected as fine PM.

Factors affecting Se partitioning on solid particulate surfaces in a wet scrubber are not fully understood yet and may require additional data on Se in the scrubber slurry, gypsum stream and chloride purge.

All three TEs showed about equal solubility in the submicron and fine particulate size regimes under the three environmental conditions. This indicates the possibility of the same partitioning mechanism for both size fractions for that particular TE. Since there was no clear distinction in element solubility between scrubber inlet and outlet for both As and Sb, it is clear these TEs haven't changed form/species across the scrubber and that the decrease in mass loading is solely due to the physical scrubbing of the PM out of the flue gas and not due to any effect from the FGD solvent. However, for Se, the increase in mobility for both submicron and fine fragment fractions across the scrubber is mainly due to change in speciation and thus Se is more soluble in all fluids.

CONCLUSIONS

Understanding the fate of trace elements (TEs) in fly ash generated during pulverized coal combustion is a necessary component in assessing potential risks, including health effects of any respirable ash particles, and in the subsequent implementation of suitable control measures. Their tendency to be enriched in the $PM_{2.5}$ size range makes them an even bigger threat since particulate capture devices have lower capture efficiencies for this size range. Of particular interest to this study is the leaching potential of the three TEs – As, Se and Sb - in size segregated coal combustion fly ash. Prior research has shown that fly ash particle size and chemistry plays a significant role in both TE partitioning reactions and the control of their overall mobility under different leaching environments.

A series of experiments were conducted to evaluate the environmental impact, in terms of element mobility, of these three important trace elements in coal. This study examined the effect of certain parameters affecting ash particle size distribution including changes to combustion temperature, difference in coal ash chemistries, particle size distribution, and its effect on both TE availability and its subsequent mobility. Some of the important conclusions include:

- In general, all three trace elements showed moderate to high mobility in the smaller submicron and fine fragment particles mainly under acidic and neutral environments, while bulk mode mobility was comparatively lower for all three TEs. This was observed irrespective of combustion conditions and coal rank.

- Bulk mode mobility was comparatively lower for all TEs under most test conditions.

- Changes to combustion temperature increased TE mass loadings in particle matter in the submicron and fine fragment regime size ranges. However, TE solubilities in a given leaching solution and for a particular size mode remained unaffected for the test coal. This suggests that the increase in mass loadings was due to an increase in available cation surface sites rather than from a change to TE partitioning mechanism.

- With respect to the effect of coal rank, differences in mobility were observed only for Se suggesting potential speciation differences for the two test coals. Arsenic mobility showed no significant difference between the two coals and antimony results were inconclusive.

- Tests conducted in a full-scale utility boiler showed the scrubber had an overall positive impact by removing a majority amount of all three elements. In the case of As and Sb, removal across the scrubber occurred without change in form (physical scrubbing) as evidenced by both mass distribution and mobility data. However, Se data indicates there has been a change in form from scrubber operating conditions resulting in slightly increased emissions for the submicron range. This was further confirmed by differences in mobility data between inlet and outlet conditions.

While this work demonstrated a relatively easy, inexpensive technique to qualitatively assess the environmental impact of PC combustion generated fly ash, one of the biggest drawbacks in this technique is the inability for direct measurements of an elements speciation in fly ash. Information on an elements solubility is important to assess potential threat, but knowledge of its oxidation state is critical to assess overall toxicity. This shortcoming is hereby acknowledged, and it is recommended that this technique is improved further to determine exact oxidation states, especially for TEs.

CHAPTER 1

INTRODUCTION

Coal is widely used as the primary fuel for power generation and accounted for over 40% of global power production in 2016. Even though coal usage has been in steady decline in developed nations, it still accounted for over 30% of electricity generated in the U.S. in 2016. China leads the world in coal usage followed by US and India. Concerns over the impact of fossil fuels on climate change has impacted coal use in developed nations, but it still remains a readily accessible source of energy and is expected to provide an inexpensive and reliable source of power across the globe. The advancement of clean and efficient coal combustion technologies including fluid bed systems and ultra-super critical boilers will help sustain coal-based power over the next few decades.

Aside from managing flue gas emissions, one of the other major challenges for coal power plants is the management of coal combustion wastes (CCWs) which includes fly ash, bottom ash/slag and wet scrubber effluents etc. Some of these byproducts, including fly ash, have economic value and are sold to various process industries, while others such as bottom ash are disposed of in landfills and ash ponds.

While most of the fly ash is captured by particulate capture devices (PCDs) such as Electrostatic Precipitators (ESPs) and Baghouses (BHs), a very small percentage of ash escape these devices and are emitted into the atmosphere with the flue gas. Most of the emitted particles are in the smaller size range (one micron or less) and can be enriched in trace metal species, most of which are classified environmental toxins. As fly ash gets carried downwind of the stack, toxic species present on fly ash surfaces can potentially harm living beings either directly or through indirect means.

Arsenic (As), Selenium (Se) and Antinomy (Sb) are three of the trace elements (TEs) emitted from coal fired plants and are classified hazardous air pollutants. Even though all three elements are present in only trace quantities (no more than 100ppm by weight) in most coals, their emission levels are still significant due to the large amount of coal being burnt in utilities across the country. All three elements are semi-volatile in nature and will exhibit varying degree of vaporization during combustion. Combustion zone transformations and subsequent post combustion partitioning of these elements may produce environmentally harmful forms which may be preferentially emitted from the stack.

Studies for the transformations of the major elements such as K, Na, and Fe in coal have shown that the form of occurrence of an element has a major influence on the volatility of that element during combustion. Similarly, the form of occurrence of trace elements will affect their volatility in a boiler and their subsequent transformations away from the flame as the flue gas cools. Aside from their original mode of occurrence, TE partitioning in coal fired boilers will also be affected by fuel rank, ash chemistry and firing conditions such as combustion temperature and percent excess air. TEs that penetrate PCDs and exit the stack as particles can pose potential risks to both human and environmental health. One way to assess such risks is by conducting leaching studies on fly ash particles and determining the overall solubility of TEs present in them. Depending on the size fraction in which they are present and for a given leaching fluid (acidic, neutral or basic), TE solubility data can be used to assess risk to both human and environmental health and in some cases, infer possible TE speciation in ash. The oxidation state of TE as well as other ash components is a critical parameter in determining overall TE mobility.

Data from leaching studies can also be used to assist in cost effective design of control strategies and subsequent element immobilization from fly ash utilization and disposal practices.

This dissertation addresses the solubility of the trace elements, As, Se, and Sb in coal fly ash collected under different experimental conditions which have been proven to impact TE partitioning. An understanding of how they are transformed during combustion is essential to assessing their environmental impact and developing effective control and immobilization strategies. The following chapters are organized as follows:

Chapter 2 – Background information on TE evolution during coal combustion and leaching from fly ash.

Chapter 3. The effect of combustion temperature was studied to understand its effect on both TE partitioning and subsequent solubility from fly ash surfaces. Change in combustion temperature will change the volatility of TEs and other ash forming species and this will affect TE speciation on fly ash surfaces.

Chapter 4. Coal rank was varied and fly ash samples were collected to study TE solubility as a function of coal rank. With a change in coal rank there will be change in coal chemistry and this will affect TE speciation even if all other conditions were held constant.

Chapter 5. Fly ash samples were collected across a Wet Flue Gas Desulfurization (WFGD) unit for a utility sized commercial boiler and TE solubility was assessed to study the effect of WFGD on any potential TE re-emission.

Chapter 6. Conclusions and suggestions for future work

CHAPTER 2

BACKGROUND

Ambient fine particulate matter (PM) concentrations are regulated as $PM_{2.5}$, denoting particles with aerodynamic diameters less than 2.5 μm [1]. Coal combustion derived flue gas is a significant source of $PM_{2.5}$, despite continuing improvements in boiler operation and implementation of technologies for particulate emission control. Factors such as particle chemical and physical characteristics, combustion system design and operating condition, and the choice of control technology tend to affect Particulate Capture Device (PCD) efficiencies resulting in $PM_{2.5}$ emission through the stack along with the flue gas stream. For example, electrostatic precipitators (ESPs) have an overall particulate collection efficiency of over 99% but have noticeably lower efficiencies in the $PM_{2.5}$ range [2]. The EPA estimates an ESP to have an overall efficiency of 99.2%, but a $PM_{2.5}$ efficiency of only 95.1% [2,3]. Because of an ESP's efficiency limits, $PM_{2.5}$ makes up around 68% of the total ash released from power plants through the exhaust gas stream [2,3]. Fly ash particles that escape PCDs can stay suspended in air or settle downwind of the stack onto soil surfaces and water bodies inducing adverse health effects. Potential health risks can be either through direct means (inhalation) or indirect means such as uptake by plants and waterbodies and subsequently affecting human and animal health through consumption. Therefore, controlling airborne fine particles emitted by power plants is of vital interest since some of these particles have long atmospheric residence times [1,4-6], can penetrate deep into the lungs [7-9], and can also contain relatively high concentrations of toxic trace species [10-15]. Research data shows that most of the ash generated during combustion is concentrated in a size range of 2.5 to 20 microns [16, 17] and only a small amount of the total ash (by weight) present in the $PM_{2.5}$ size range [16-19]. Determining fly ash Particle Size Distribution (PSD) is critical in evaluating PCD capture efficiency [20] as well as modeling the distribution of inorganic materials [,21, 22, 23], especially those that are classified as environmental toxins.

Majority of the particulate bound toxins from coal combustion are grouped under trace elements (TEs) since their original concentration in coal is orders of magnitude less than major species such as C,H,S and also other ash constituents like Si, Al, Ca etc [24,25]. Most TEs exiting the stack tend to be enriched in the $PM_{2.5}$ size range while others, such as mercury (Hg), leave mostly as vapor [26,27]. While Hg stack emission is regulated under the Mercury and Air Toxics Standards (MATS) rule [28], currently, there are no regulations governing the emission of other TEs from coal power plants making them an even bigger concern.

Of particular interest to this study is the fate of three TEs – Arsenic (As), Selenium (Se) and Antimony (Sb) - after combustion and their final transformation onto fly ash surfaces. All three elements are classified hazardous pollutants under the amended Clean Air Act [29] and their emission from coal-fired power plants cannot be always predicted from the collection efficiency of PCDs. Although significant amounts of all three TEs gets retained on fly ash surfaces [12,14,30] (and later captured in PCDs), a small portion can leave as vapor with the flue gas (as with Se) [31,32] and can come into direct contact with our environment through stack emissions. The fate of TEs present on fly ashes can be of major environmental concern depending on plant ash handling and disposal practices [33,34].

Whether fly ash is landfilled, disposed in surface impoundments, lagooned or recycled into ash-based products, the total concentration of an element is not an accurate indicator of the potential environmental impact. Assessing environmental performance of products based on total concentration

in fly ash would provide unreliable and highly overestimated predictions of the risk level which would restrict any fly ash application opportunities. Therefore metal (including TEs) characterization based on solubility/mobility will serve as a better indicator for risk assessment especially when there is a growing concern about health effects of exposure to heavy metals. Knowledge of the reasons underlying element mobility can also help to achieve better control over environmental impacts in the wide variety of utilization and disposal practices. This in turn will assist in cost-effective design of management strategies and in the decision making of regulatory agencies.

TRACE ELEMENTS IN COAL

Health Impacts of Trace Elements

Coal is a heterogeneous fuel containing varying amounts of inorganic substances, including an array of TEs. Depending on their source, they can be present in variable concentrations even though their levels usually do not typically exceed 100 ppmw [27,35,36]. The harmful toxicological and bio-accumulation effects of TEs from coal combustion have been found in many studies. For instance, As is both a carcinogen and mutagen that leads to dangerous dermatological, respiratory and digestive system diseases [37-39]. Selenium, on the other hand, is an essential element but is also toxic above certain levels. Long term exposure to Se causes irritation of the mucous membranes, pulmonary edema, severe bronchitis, and bronchial pneumonia and may adversely affect nervous, cardiovascular, dermal, respiratory and immune systems [40,41,42]. Research also shows that chronic exposure to Sb causes inflammation of the lungs, alterations in pulmonary function, chronic bronchitis, chronic emphysema, inactive tuberculosis and irritation [43,44].

Since all three TEs are shown to be enriched in $PM_{2.5}$ [11,12,14,15,21], they are likely to be present in significant concentrations in the atmosphere. Once emitted, they may have severe adverse impact on human health as they have high probability to deposit in lungs [7,10,12,13,14] or they may deposit to the earth's surface resulting in elevated levels of TEs in soil, vegetation and water [14,214546]. Because of these detrimental effects on humans and environment, there is a need to further understand the fate of TEs present on fly ash surfaces. A thorough knowledge on the modes of occurrence of TEs in coal will facilitate the understanding of both TE transformation during coal combustion and post partitioning in the flue gas where a major portion of them will likely be retained on fly ash particles.

Mode of Occurrence of Trace Elements in Coal

All three TEs (As, Se and Sb) are semi-volatile in nature and are expected to vaporize during combustion, primarily forming oxy-anions [12,14,23,47,48]. The extent of volatilization primarily depends on their mode of occurrence in coal [21,49,50] and the nature of the combustion system. Hence, a thorough knowledge on the modes of occurrence of TEs in coal will facilitate the understanding of the transformation of TEs during both combustion and in post-combustion flue gas. For example, the original form of occurrence can influence how TEs partition during combustion and will ultimately influence the fraction of TEs that exit the combustion system in vapor form compared to TEs associated with particulate matter [14,23,48].

TEs have a variety of ways in which they are associated within coal but are generally categorized as belonging to one of three forms of occurrence: organically associated, contained in mineral inclusions,

or contained in mineral exclusions [14,23,47,48]. Organically bound TEs include those elements that are bonded to carbon-based compounds within the coal, whereas included TEs are elements found within inorganic minerals that were encapsulated by the coal carbon matrix during coalification. Finally, TEs in exclusions are found within inorganic constituents that may be mixed with the coal after coalification but are not intrinsic parts of the coal [23,48].

TEs in each of these regimes will experience different conditions that will affect vaporization. Typically, TE associated with the organic structure of the coal or in small inclusions will experience reducing environments and very high temperatures and can vaporize with a high efficiency as it diffuses out of the burning char particle and into the bulk gas phase. Elements associated with excluded mineral grains experience a neutral/oxidizing atmosphere and not as high a temperature as organically associated materials. TEs contained in them are less likely to volatilize and may remain trapped in these particles [14,21,23,45]. Different analytical techniques, including scanning electron microscope (SEM), X-ray absorption fine structure spectroscopy(XAFSS), instrumental neutron activation analysis (INAA), have been extensively used to investigate modes of occurrence of TEs in coal. A sequential leaching procedure, known as chemical fractionation, of the raw fuel can also be used to determine TE original mode of occurrence and is a relatively cheaper analytical technique than XFAAS and INAA.

Based on their original association with coal, combustion system design and operating conditions, TEs get emitted (i) as flue gas vapor, (ii) in smaller submicron and fine fragment fly ash particles and (iii) with the larger bulk particles which make up the majority of fly ash particles [14,21,45].

Once deposited on fly ash particles, TEs can have multiple oxidation states just as they do in the original fuel. For example, As can exist in three valences states (−3, +3, and +5) in coal [51] while the +3 and +5 states are the most prevalent forms in combustion fly ash [52,53,54]. The +3 form of As is also more toxic than the +5 state [51,53]. Selenium, on the other hand, can be present as elemental Se (0), Selenite (+4), Selenate (+6) or a hydrogen selenide (-2) in coal [51,55]. Selenium in coal ash occurs mostly as Se (+4) or Se (+6), but Se (+4) is the most common form [55,56,57] and is also more toxic than Se (+6) [12,53,58]. Antimony is similar to arsenic and is commonly present in coal ash in the +3 and +5 forms [59] with the +3 form believed to be more toxic than the +5 state [60,61]. The mode of partitioning also determines a TEs final oxidation state in ash, thereby directly influencing its impact on the environment [14,21].

Post Combustion Partitioning of Trace elements

Prior research [12,14,21,62] has shown that it is the interaction of fly ash particles with TE vapor that determines the final partitioning in these respective phases. TE partitioning is mainly controlled by reactions with active cation (calcium and/or iron) surface sites indicating that surface reaction is the dominant mechanism for the heterogeneous partitioning of volatilized TE to fly ash surfaces. If enough active sites aren't available (as in the case of a high S and low Ca and/or Fe coal) sorption on existing fly ash particles, aerosols or within its pores will become the preferred method of TE partitioning from vapor to solid phase [12,14,21,45,62,63,64].

Enrichment of TEs in the smaller sized particles is not uncommon due to the availability of active sites (that are formed by condensation reactions) and also due to surface morphology considerations. Most of the smaller sized particles have fairly high surface to volume ratios and particle number densities

(as compared to bulk ash particles) and depending on coal type and combustion conditions, can either offer more active surface sites for TE heterogeneous transformation reactions or surface for sorption reactions. This results in significant TE presence in $PM_{2.5}$ particles making all three of them an environmental concern. A detailed study on TE partitioning reactions is shown here [14,21,65].

Based on published findings, some of the key parameters affecting the partitioning of trace elements during pulverized coal combustion are [14,21,62,63]:

- The forms of occurrence of trace elements and major inorganic elements (i.e., calcium, iron, and aluminum) in the feed coal.

- The maximum combustion temperature (affected primarily by the carbon content and moisture content of the feed coal).

- The air-to-coal ratio and staging combustion.

- The ratio of oxy-anion trace elements (volatilized) to surface active cations (i.e., calcium and iron).

- The ratio of cationic trace elements (volatilized) to surface active anions (i.e., aluminum).

- The sulfur content of the feed coal.

While TE transformation reactions are extremely important, the behavior of major ash forming elements, such as Si, Al, Fe, Ca, S, K, Na, Mg and others is also of equal importance. And, similar to TEs, mode of occurrence of major elements plays an important role in their combustion zone transformation reactions [14,21]. With respect to TE partitioning, an understanding of the combustion zone transformation of major ash elements helps predicting TEs distribution in the different size modes/fractions of fly ash. This in turn can help understand mechanisms driving TE vapor to solid reactions. Each size mode in fly ash is formed as a result of the various mechanisms involving major inorganic element transformation in the combustor and is discussed below.

MODES OF FLY ASH DISTRIBUTION

Numerous studies have been conducted over the years to study fly ash PSD from pulverized coal (PC) combustion. In most lab scale studies, two distinct modes – a larger bulk size mode and a smaller submicron (or) ultrafine mode - have been observed in PSDs generated during PC combustion. Field data of McElroy et al. [66] support this finding, showing a submicron/ultrafine ash vaporization mode centered at approximately 0.1 µm diameter and a coarse fragmentation mode apparently centered at approximately 20 µm diameter. It has also been well established that these two modes are produced by different mechanisms [16,17,67]. Submicron mode is mainly formed by the vaporization–condensation mechanism where highly volatile alkali metals (Na and K) vaporize in the flame and later homogeneously nucleate to form very fine sulfate aerosols. The very small particles grow by a combination of coagulation and heterogeneous condensation forming very fine particles [14,16,67,68].

Even oxides of major elements such as Si, Ca, Al, Fe, K, Na, Mg and others will partially volatilize during ash vaporization. forming extremely reactive suboxides (or pure elements) under reducing conditions encountered in the burning char particle [16,17,68]. Once formed, these species diffuse away from the parent particle and re-oxidize in the oxygen-rich atmosphere of the surrounding bulk gas. Subsequent oxidation of the reduced species could produce supersaturation without any

decrease in temperature [68]. If the saturation ratio (the ratio of vapor pressure to the equilibrium vapor pressure) becomes sufficiently high, new particle formation can take place even though the residual ash particles present a large surface area for heterogeneous condensation [68]. When supersaturated they too will homogeneously nucleate to form very fine aerosols. which grows by a combination of coagulation and heterogeneous condensation of vapors, which condense after the initial nucleation [16,17,68].

In contrast, the dominant formation mechanisms for particles in the bulk mode (supermicron) has been recognized as fragmentation, melting and coalescence [14,69,70], for the vaporization–condensation mechanism cannot possibly produce such large ash particles. Bulk particles have been characterized as predominantly individual, almost spherical particles, with a rather smooth surface, sometimes with discrete submicron particles sintered onto the surface. As the char particle burns, mineral grains present on the surface experiences high temperatures and will melt forming spherical droplets. Once char burnout is complete, these droplets can come into contact with each other and coalesce to form larger sized particles. However, some mineral grains (exclusions) do not experience temperatures high enough to melt and they tend to soften and rearrange into thermodynamically favorable structures. This gives rise to the characteristic spherical shape of bulk fly ash particles [14,21,45,48].

Later studies suggested that pulverized-coal combustion will yield three, rather than two, primary ash aerosol size modes. Kang [71] is probably the first to declare that ash particles from pulverized coal combustion may have a trimodal size distribution. Kang found that, besides an ultrafine mode, there were two other distinct modes present in coal fly ash derived PSD. Joutsensaari et al. [72] also observed a third (or central) mode in PSDs generated in a full-scale power plant. Experimental results by Linak et al., [67] and Seames et al. [12,14] confirmed that coal fly ash particle formation is more accurately described by a trimodal particle size distribution which includes a distinct central or fine fragment mode centered at approximately 2.0 μm. By re-examination of literature data Linak et al. [67] found that three particle modes were in fact the rule, not the exception. Compared to both submicron and bulk size modes, the formation of the fine fragment mode might be the consequence of multiple mechanisms including heterogeneous vapor condensation, shedding ash particles from burning char, fragmenting of larger fly ash particles and particle-to-particle impaction [2,12,14]. Prior to this, Smith et al. [73] had also observed two fragmentation modes. One was a fine fragmentation mode due to bursting of hollow ash spheres, and a coarse fragmentation mode due to coalesced ash formed during char burnout. However, their research did not emphasize the additional importance of the ultrafine vaporization mode and only considered particles larger than 1μm. Besides the number of particle modes, the mode size boundary is also an important parameter for modeling, risk assessment and development of mitigation strategies. Since all the inorganic elements in coal exhibit varying degree of volatility (including TEs) their solid phases will be distributed across all three size modes.

However, the vaporized concentration of all three TEs are often not in sufficient concentration to homogeneously nucleate and hence, as mentioned earlier, heterogeneous chemical reaction or sorption on the surface of existing fly ash particles is the likely mechanism of vapor to solid transformation. The gas-solid partitioning mechanisms of TEs have an impact on the solubility of trace element-containing species formed during combustion [45,46]. One way to assess potential TE threats to environment is by conducting leaching tests on fly ash particles of different sizes under different pH conditions.

LEACHING STUDIES OF TRACE ELEMENTS

Laboratory leaching studies are a qualitative means to assess potential environmental impacts from combustion generated PM. Leaching tests can simulate environments encountered by fly ash particles and provides information on element mobility for that particular environment. They are simple lab scale tests, wherein a sample of collected PM is dissolved under different pH conditions and the mass of each element in solution is then measured. Whether or not certain toxic elements in fly ash are stable and do not impact the surrounding environment depends on their solubility in the specific pH conditions encountered. Data from leaching studies can be used to assess the severity of threat for particular environments. Fly ash enters the environment through three main pathways: bulk ash piles, deposition downwind and inhalation.

Bulk ash particles collected by pollution control equipment are typically disposed of in landfills or utilized as a sheetrock or asphalt filler material [33,45,74]. During rainstorms, water percolates through the ash pile, absorbing water-soluble material and thereby changing water pH. Depending on the pH of the ash, the pH of water can be lower than the original rain source (acidic ash) or higher (basic ash). Water leaving the ash pile may then percolate downwards to the water table, thereby increasing the amount of dissolved contaminants in the surrounding water cycle [14,45,46]. The solubility of TEs from the ash pile will depend on the pH of water within the pile. Fly ash solubility from both acidic and basic leachates can be used to assess the potential for TE leaching from ash piles.

Fine particulate mode particles account for only a small portion of the mass of ash disposed of in the landfill, which is dominated by bulk ash particles, but trace elements contained in the fine particulate mode have the potential to be easily dissolved as a result of their presence on the surface of particles. These particles have a tendency to settle out onto the ground downwind of the combustor. Ground moisture and rainfall may dissolve soluble trace element-containing compounds and carry them into the soil. These compounds may then be absorbed into plants through roots in the soil or percolate downwards to the water table. The solubility will depend primarily upon the pH of the soil where the particles deposit, rather than the pH of the ash itself [33,45,46]. Fine particulate solubility data in an acidic medium can demonstrate TE solubility in acidic soil, such as that in the eastern United States, whereas solubility data in a basic medium can represent TE solubility in more alkaline soils, such as that typical of the western U.S.

Finally, airborne particles that have not yet settled to the ground can be inhaled into human and animal respiratory systems [14,45]. Particles in the submicron mode pose the greatest inhalation health risk due to their longer atmospheric residence times (mean residence times of 100-1000 hours compared to 10-100 hours for super-micron particles) [75,76] and their ability to penetrate deeper into the lungs. Solubility data under neutral conditions represents the pH environment of respiratory fluids and can be used to determine potential TE exposure through inhalation.

In general, elements present on the surface of ash particles (such as TEs on submicron and fine fragment particles) are more readily soluble than those trapped inside bigger coarse particles [45,46]. Additionally, the chemical form of the trace element on the particle surface can substantially affect the solubility of that TE in aqueous environments [33,45,46,77]. Hence TE solubility studies as a function of particle size are important to assess specific risks for a given pH condition.

The overall fly ash solubility for a given TE is affected by multiple parameters such as combustion temperature, fuel rank, mode of occurrence of TEs and some of these factors, including the effect of combustion temperature, differences in coal ash chemistry (resulting from change in rank) are addressed in the work presented herein.

PRIOR WORK & KNOWLEDGE GAPS

While extensive research data is available for TE leaching from fly ashes [33,53,77-81], knowledge gaps still exists in a few areas and addressing them can be critical for developing enhanced control technologies and immobilization strategies. For example, a host of researchers [33,57,77,82-85] have published TE leaching data from coal fly ash but without taking into consideration the effect of particle size. Their results were based on leaching data for bulk ash samples collected directly from PCD hoppers. A batch sample collected from PCD hoppers could skew the particle size towards bulk fraction and this will not be representative of the actual ash distribution in the flue gas. As explained earlier, TEs present in bulk size mode are not as mobile compared to TEs present in the smaller sized submicron and fine fragment particles. Hence, there exists the possibility of obtaining incorrect results leading to wrong conclusions. This research addresses this concern by reporting leaching data for each fly ash size mode under all the test conditions.

However, some studies have reported coal fly ash TE mobility as a function of particle size [45,46]. For example, Seames et al., have reported mobility data for lab-scale fly ash samples collected from two different combustors [46]. In the first study, size segregated fly ash samples were analyzed for the combustion of five different coals (with overlapping ranks) and TE mobility was reported under two pH conditions (2.88 and 4.9) [21,46]. In the latter study conducted at the University of North Dakota combustion facility, fly ash samples were analyzed for the combustion of a bituminous coal and its co-combustion with biomass. In this study TE mobility was reported under three pH conditions (2.88,7 and11) [45,86]. However, in both studies, only selected impactor stages from a given size mode were leached to determine an elements mobility for that size mode. Even though TEs are expected to have nearly the same mobility for all the impactor stages making up a given size mode, analyzing only select stages can increase uncertainty in reported data. Additionally, peak combustion temperatures reported in both studies were lower than what would be expected of a typical coal fired boiler. As previously explained, combustion temperature can have a significant effect on TE partitioning and by extension, its mobility from fly ash particles.

Research work conducted herein addresses the aforementioned issues through carefully constructed experiments and sampling techniques both in lab scale and commercial systems. In this research:

- Experiments were designed to closely simulate conditions in commercial utilities including combustion temperature and % excess oxygen. The lab-scale furnace mirrors time–temperature history of a commercial boiler which is critical to collecting representative samples of actual fly ash distribution in the flue gas.

- A study was specifically conducted to understand the effect of combustion temperature on TE mobility. The underlying hypothesis is TE mobility will be influenced by differences in combustion temperature.

- TE mobility was reported for each of the three size modes and not just for the bulk ash. During leaching studies, all the impactor stages were analyzed to report overall mobility including uncertainty in reported values.

- In addition to lab scale experiments, TE leaching studies were also carried out for size segregated fly ash samples collected from a commercial utility boiler equipped with a wet scrubber. This aspect of this research is unique since, to the best of my knowledge, there is no current published data on TE mobility for size segregated fly ashes from a commercial boiler.

REFERENCES

1. Linak, William P., and Thomas W. Peterson. "Effect of coal type and residence time on the submicron aerosol distribution from pulverized coal combustion." Aerosol Science and Technology 3.1 (1984): 77-96.

2. Fix, G., Seames, W., Mann, M., Benson, S. and Miller, D., 2013. The effect of combustion temperature on coal ash fine-fragmentation mode formation mechanisms. Fuel, 113, pp.140-147.

3. U.S. EPA. Compilation of air pollution emission factors. In: Stationary point and area sources, AP-42, 5th ed., vol. 1; 1998 [chapter 1].

4. Esmen, N.A. and Corn, M., 1971. Residence time of particles in urban air. Atmospheric Environment (1967), 5(8), pp.571-578.

5. Häkkinen, S.A.K., Äijälä, M., Lehtipalo, K., Junninen, H., Backman, J., Virkkula, A., Nieminen, T., Vestenius, M., Hakola, H., Ehn, M. and Worsnop, D.R., 2012. Long-term volatility measurements of submicron atmospheric aerosol in Hyytiälä, Finland. Atmospheric Chemistry and Physics, 12(22), pp.10771-10786.

6. Chen, Q., Farmer, D.K., Rizzo, L.V., Pauliquevis, T., Kuwata, M., Karl, T.G., Guenther, A., Allan, J.D., Coe, H., Andreae, M.O. and Pöschl, U., 2015. Submicron particle mass concentrations and sources in the Amazonian wet season (AMAZE-08). Atmospheric Chemistry and Physics, 15(7), pp.3687-3701.

7. Linak, W.P., Yoo, J.I., Wasson, S.J., Zhu, W., Wendt, J.O., Huggins, F.E., Chen, Y., Shah, N., Huffman, G.P. and Gilmour, M.I., 2007. Ultrafine ash aerosols from coal combustion: Characterization and health effects. Proceedings of the Combustion Institute, 31(2), pp.1929-1937.

8. USEPA. 1998. Particulate matter research needs for human health risk assessment to support future reviews of the national ambient air quality standards for particulate matter. U.S. Environmental Protection Agency, Report No. EPA/600/R97/132F.

9. Schwartz, J. and Neas, L.M., 2000. Fine particles are more strongly associated than coarse particles with acute respiratory health effects in schoolchildren. Epidemiology, Pages 6-10.

10. Senior, C.L., Helble, J.J. and Sarofim, A.F., 2000. Emissions of mercury, trace elements, and fine particles from stationary combustion sources. Fuel Processing Technology, 65, Pages 263-288.

11. Wang, C., Liu, H., Zhang, Y., Zou, C. and Anthony, E.J., 2018. Review of arsenic behavior during coal combustion: Volatilization, transformation, emission and removal technologies. Progress in Energy and Combustion Science, 68, pp.1-28.

12. Seames, W.S., 2003. An initial study of the fine fragmentation fly ash particle mode generated during pulverized coal combustion. Fuel Processing Technology, 81(2), Pages 109-125.

13. Linak, W.P. and Wendt, J.O., 1993. Toxic metal emissions from incineration: mechanisms and control. Progress in Energy and Combustion Science, 19(2), Pages 145-185.

14. Seames, W.S., 2000.The partitioning of trace elements during pulverized coal combustion, Ph.D. dissertation, University of Arizona, Tucson, AZ.

15. Yan, R., Gauthier, D. and Flamant, G., 2001. Volatility and chemistry of trace elements in a coal combustor. Fuel, 80(15), Pages 2217-2226.

16. Neville, M., 1982. Formation of inorganic submicron particles under simulated pulverized coal combustion conditions (Doctoral dissertation, Massachusetts Institute of Technology).

17. Quann, R.J., 1982. Ash vaporization under simulated pulverized coal combustion conditions (Doctoral dissertation, Massachusetts Institute of Technology).

18. Gilmour, M.I., O'Connor, S., Dick, C.A., Miller, C.A. and Linak, W.P., 2004. Differential pulmonary inflammation and in vitro cytotoxicity of size-fractionated fly ash particles from pulverized coal combustion. Journal of the Air & Waste Management Association, 54(3), pp.286-295.

19. Duan, F.K., He, K.B., Ma, Y.L., Yang, F.M., Yu, X.C., Cadle, S.H., Chan, T. and Mulawa, P.A., 2006. Concentration and chemical characteristics of PM2. 5 in Beijing, China: 2001–2002. Science of the Total Environment, 355(1-3), pp.264-275.

20. Liu, H., Wang, Y. and Wendt, J.O., 2017. Particle size distributions of fly ash arising from vaporized components of coal combustion: A comparison of theory and experiment. Energy & Fuels, 32(4), pp.4300-4307.

21. Senior, C.L., et.al., 1999. Toxic Substances from Coal Combustion – A Comprehensive Assessment. Final Report, July 2001, pp 1-786.

22. Wang, C., Seames, W.S., Gadgil, M., Hrdlicka, J. and Fix, G., 2007. Comparison of coal ash particle size distributions from Berner and Dekati low pressure impactors. Aerosol Science and Technology, 41(12), pp.1049-1062.

23. James, D.W., Krishnamoorthy, G., Benson, S.A. and Seames, W.S., 2014. Modeling trace element partitioning during coal combustion. Fuel Processing Technology, 126, pp.284-297.

24. Mokhtar, M.M., Taib, R.M. and Hassim, M.H., 2014. Understanding selected trace elements behavior in a coal-fired power plant in Malaysia for assessment of abatement technologies. Journal of the Air & Waste Management Association, 64(8), pp.867-878.

25. Font, O., Córdoba, P., Leiva, C., Romeo, L.M., Bolea, I., Guedea, I., Moreno, N., Querol, X., Fernandez, C. and Díez, L.I., 2012. Fate and abatement of mercury and other trace elements in a coal fluidised bed oxy combustion pilot plant. Fuel, 95, pp.272-281.

26. Meij, R., Vredenbregt, L.H. and Winkel, H.T., 2002. The fate and behavior of mercury in coal-fired power plants. Journal of the Air & Waste Management Association, 52(8), pp.912-917.

27. Nalbandian, H., 2012. Trace element emissions from coal. IEA Clean Coal Centre, 601.

28. Driscoll, C.T., Buonocore, J.J., Levy, J.I., Lambert, K.F., Burtraw, D., Reid, S.B., Fakhraei, H. and Schwartz, J., 2015. US power plant carbon standards and clean air and health co-benefits. Nature Climate Change, 5(6), p.535.

29. Geiger, A. and Cooper, J., 2010. Overview of airborne metals regulations, exposure limits, health effects, and contemporary research. Environmental Protection Agency, Air Quality: Washington, DC, USA.

30. Meij, R., 1994. Trace element behavior in coal-fired power plants. Fuel processing technology, 39(1-3), pp.199-217.

31. Yan, R., Gauthier, D., Flamant, G., Peraudeau, G., Lu, J. and Zheng, C., 2001. Fate of selenium in coal combustion: volatilization and speciation in the flue gas. Environmental science & technology, 35(7), pp.1406-1410.

32. Senior, C.L., Tyree, C.A., Meeks, N.D., Acharya, C., McCain, J.D. and Cushing, K.M., 2015. Selenium partitioning and removal across a wet FGD scrubber at a coal-fired power plant. Environmental science & technology, 49(24), pp.14376-14382.

33. Izquierdo, M. and Querol, X., 2012. Leaching behaviour of elements from coal combustion fly ash: an overview. International Journal of Coal Geology, 94, pp.54-66.

34. Yao, Z.T., Ji, X.S., Sarker, P.K., Tang, J.H., Ge, L.Q., Xia, M.S. and Xi, Y.Q., 2015. A comprehensive review on the applications of coal fly ash. Earth-Science Reviews, 141, pp.105-121.

35. Zhao, Y., Yang, J., Ma, S., Zhang, S., Liu, H., Gong, B., Zhang, J. and Zheng, C., 2018. Emission controls of mercury and other trace elements during coal combustion in China: a review. International Geology Review, 60(5-6), pp.638-670.

36. Swaine, D.J., 1994. Trace elements in coal and their dispersal during combustion. Fuel Processing Technology, 39(1-3), pp.121-137.

37. Tchounwou, P.B., Centeno, J.A. and Patlolla, A.K., 2004. Arsenic toxicity, mutagenesis, and carcinogenesis–a health risk assessment and management approach. Molecular and cellular biochemistry, 255(1-2), pp.47-55.

38. Jomova, K., Jenisova, Z., Feszterova, M., Baros, S., Liska, J., Hudecova, D., Rhodes, C.J. and Valko, M., 2011. Arsenic: toxicity, oxidative stress and human disease. Journal of Applied Toxicology, 31(2), pp.95-107.

39. Steinmaus, C., Ferreccio, C., Acevedo, J., Yuan, Y., Liaw, J., Durán, V., Cuevas, S., García, J., Meza, R., Valdés, R. and Valdés, G., 2014. Increased lung and bladder cancer incidence in adults after in utero and early-life arsenic exposure. Cancer epidemiology and prevention biomarkers.

40. Grandjean, P. and Landrigan, P.J., 2006. Developmental neurotoxicity of industrial chemicals. The Lancet, 368(9553), pp.2167-2178.

41. Vinceti, M., Wei, E.T., Malagoli, C., Bergomi, M. and Vivoli, G., 2001. Adverse health effects of selenium in humans. Reviews on environmental health, 16(4), pp.233-252.

42. MacFarquhar, J.K., Broussard, D.L., Melstrom, P., Hutchinson, R., Wolkin, A., Martin, C., Burk, R.F., Dunn, J.R., Green, A.L., Hammond, R. and Schaffner, W., 2010. Acute selenium toxicity associated with a dietary supplement. Archives of internal medicine, 170(3), pp.256-261.

43. Cooper, R.G. and Harrison, A.P., 2009. The exposure to and health effects of antimony. Indian journal of occupational and environmental medicine, 13(1), p.3.

44. Léonard, A. and Gerber, G.B., 1996. Mutagenicity, carcinogenicity and teratogenicity of antimony compounds. Mutation Research/Reviews in Genetic Toxicology, 366(1), pp.1-8.

45. Seames, W.S., Gadgil, M., Wang, C. and Fetsch, J., 2006, September. Impacts on trace metal leaching from fly ash due to the co-combustion of switch grass with coal. In Proceedings of 23rd Pittsburgh coal Conference paper (pp. 40-4).

46. Seames, W.S., Sooroshian, J. and Wendt, J.O., 2002. Assessing the solubility of inorganic compounds from size-segregated coal fly ash aerosol impactor samples. Journal of aerosol science, 33(1), pp.77-90.

47. Raeva, A.A., Klykov, O.V., Kozliak, E.I., Pierce, D.T. and Seames, W.S., 2011. In situ evaluation of inorganic matrix effects on the partitioning of three trace elements (As, Sb, Se) at the outset of coal combustion. Energy & Fuels, 25(10), pp.4290-4298.

48. Raeva, A.A., Pierce, D.T., Seames, W.S. and Kozliak, E.I., 2011. A method for measuring the kinetics of organically associated inorganic contaminant vaporization during coal combustion. Fuel processing technology, 92(7), pp.1333-1339.

49. Finkelman, R.B., 1999. Trace elements in coal. Biological trace element research, 67(3), pp.197-204.

50. Tian, H.Z., Lu, L., Hao, J.M., Gao, J.J., Cheng, K., Liu, K.Y., Qiu, P.P. and Zhu, C.Y., 2013. A review of key hazardous trace elements in Chinese coals: abundance, occurrence, behavior during coal combustion and their environmental impacts. Energy & fuels, 27(2), pp.601-614.

51. Shah, P., Strezov, V., Stevanov, C. and Nelson, P.F., 2007. Speciation of arsenic and selenium in coal combustion products. Energy & Fuels, 21(2), pp.506-512.

52. Deonarine, A., Kolker, A., Foster, A.L., Doughten, M.W., Holland, J.T. and Bailoo, J.D., 2016. Arsenic speciation in bituminous coal fly ash and transformations in response to redox conditions. Environmental science & technology, 50(11), pp.6099-6106.

53. Wang, T., Wang, J., Tang, Y., Shi, H. and Ladwig, K., 2009. Leaching characteristics of arsenic and selenium from coal fly ash: role of calcium. Energy & Fuels, 23(6), pp.2959-2966.

54. Schwartz, G.E., Rivera, N., Lee, S.W., Harrington, J.M., Hower, J.C., Levine, K.E., Vengosh, A. and Hsu-Kim, H., 2016. Leaching potential and redox transformations of arsenic and selenium in sediment microcosms with fly ash. Applied Geochemistry, 67, pp.177-185.

55. Sun, W., Renew, J.E., Zhang, W., Tang, Y. and Huang, C.H., 2017. Sorption of Se (IV) and Se (VI) to coal fly ash/cement composite: Effect of Ca 2+ and high ionic strength. Chemical Geology, 464, pp.76-83.

56. Huggins, F.E., Senior, C.L., Chu, P., Ladwig, K. and Huffman, G.P., 2007. Selenium and arsenic speciation in fly ash from full-scale coal-burning utility plants. Environmental science & technology, 41(9), pp.3284-3289.

57. Liu, Y.T., Chen, T.Y., Mackebee, W.G., Ruhl, L., Vengosh, A. and Hsu-Kim, H., 2013. Selenium speciation in coal ash spilled at the Tennessee Valley Authority Kingston site. Environmental science & technology, 47(24), pp.14001-14009.

58. Roy, B., Choo, W.L. and Bhattacharya, S., 2013. Prediction of distribution of trace elements under oxy-fuel combustion condition using Victorian brown coals. Fuel, 114, pp.135-142.

59. Tian, H., Zhou, J., Zhu, C., Zhao, D., Gao, J., Hao, J., He, M., Liu, K., Wang, K. and Hua, S., 2014. A comprehensive global inventory of atmospheric antimony emissions from anthropogenic activities, 1995-2010. Environmental science & technology, 48(17), pp.10235-10241.

60. Matusiewicz, H. and Krawczyk, M., 2008. Determination of total antimony and inorganic antimony species by hydride generation in situ trapping flame atomic absorption spectrometry: a new way to (ultra) trace speciation analysis. Journal of Analytical Atomic Spectrometry, 23(1), pp.43-53.

61. Varrica, D., Bardelli, F., Dongarra, G. and Tamburo, E., 2013. Speciation of Sb in airborne particulate matter, vehicle brake linings, and brake pad wear residues. Atmospheric environment, 64, pp.18-24.

62. Seames, W.S. and Wendt, J.O., 2000. Partitioning of arsenic, selenium, and cadmium during the combustion of Pittsburgh and Illinois# 6 coals in a self-sustained combustor. Fuel Processing Technology, 63(2-3), pp.179-196.

63. Seames, W.S. and Wendt, J.O., 2007. Regimes of association of arsenic and selenium during pulverized coal combustion. Proceedings of the combustion institute, 31(2), pp.2839-2846.

64. Zhao, Y., Zhang, J., Huang, W., Wang, Z., Li, Y., Song, D., Zhao, F. and Zheng, C., 2008. Arsenic emission during combustion of high arsenic coals from Southwestern Guizhou, China. Energy Conversion and Management, 49(4), pp.615-624.

65. Liu, J., Dai, S., He, X., Hower, J.C. and Sakulpitakphon, T., 2017. Size-dependent variations in fly ash trace element chemistry: examples from a Kentucky power plant and with emphasis on rare earth elements. Energy & Fuels, 31(1), pp.438-447.

66. McElroy, M.W., Carr, R.C., Ensor, D.S. and Markowski, G.R., 1982. Size distribution of fine particles from coal combustion. Science, 215(4528), pp.13-19.

67. Linak, W.P., Miller, C.A., Seames, W.S., Wendt, J.O., Ishinomori, T., Endo, Y. and Miyamae, S., 2002. On trimodal particle size distributions in fly ash from pulverized-coal combustion. Proceedings of the Combustion Institute, 29(1), pp.441-447.

68. Flagan, R.C. and Taylor, D.D., 1981, January. Laboratory studies of submicron particles from coal combustion. In Symposium (International) on Combustion (Vol. 18, No. 1, pp. 1227-1237). Elsevier.

69. Quann, R. J., Neville, M., Janghorbani, M., Mims, C. A., Sarofim, A. F., 1982. Mineral Matter and Trace Element Vaporization in a Laboratory-Pulverized Coal Combustion System. Environ.Sci.Technol 16, pp. 776-781.

70. Yu, D., Xu, M., Yao, H., Liu, X., Zhou, K., Li, L. and Wen, C., 2009. Mechanisms of the central mode particle formation during pulverized coal combustion. Proceedings of the Combustion Institute, 32(2), pp.2075-2082.

71. Kang, S.G., 1991. Fundamental studies of mineral matter transformation during pulverized coal combustion: Residual ash formation, PhD dissertation, Massachusetts Institute of Technology.

72. Joutsensaari, J., Kauppinen, E.I., Ahonen, P., Lind, T.M., Ylätalo, S.I., Jokiniemi, J.K., Hautanen, J. and Kilpeläinen, M., 1992. Aerosol formation in real scale pulverized coal combustion. Journal of Aerosol Science, 23, pp.241-244.

73. Smith, R.D., Campbell, J.A. and Nielson, K.K., 1979. Characterization and formation of submicron particles in coal-fired plants. Atmospheric Environment (1967), 13(5), pp.607-617.

74. Jones, C., Hahn, J., Magee, B., Yuen, N., Sandefur, K., Tom, J. and Yap, C., 1999. Utilization of ash from municipal solid waste combustion (No. NREL/SR-570-26068). National Renewable Energy Lab., Golden, CO (US).

75. Karjalainen, P., Timonen, H., Saukko, E., Kuuluvainen, H., Saarikoski, S., Aakko-Saksa, P., Murtonen, T., Bloss, M., Maso, M.D., Simonen, P. and Ahlberg, E., 2016. Time-resolved characterization of primary particle emissions and secondary particle formation from a modern gasoline passenger car. Atmospheric Chemistry and Physics, 16(13), pp.8559-8570.

76. Zhou, Y., 2013. The Problems of Sulphur: Reviews in Coal Science. Butterworth-Heinemann.

77. Schwartz, G.E., Hower, J.C., Phillips, A.L., Rivera, N., Vengosh, A. and Hsu-Kim, H., 2018. Ranking Coal Ash Materials for Their Potential to Leach Arsenic and Selenium: Relative Importance of Ash Chemistry and Site Biogeochemistry. Environmental Engineering Science, 35(7), pp. 728-738

78. Akar, G., Polat, M., Galecki, G. and Ipekoglu, U., 2012. Leaching behavior of selected trace elements in coal fly ash samples from Yenikoy coal-fired power plants. Fuel processing technology, 104, pp.50-56.

79. Singh, R.K., Gupta, N.C. and Guha, B.K., 2012. The leaching characteristics of trace elements in coal fly ash and an ash disposal system of thermal power plants. Energy Sources, Part A: Recovery, Utilization, and Environmental Effects, 34(7), pp.602-608.

80. Neupane, G. and Donahoe, R.J., 2013. Leachability of elements in alkaline and acidic coal fly ash samples during batch and column leaching tests. Fuel, 104, pp.758-770.

81. Jones, K.B., Ruppert, L.F. and Swanson, S.M., 2012. Leaching of elements from bottom ash, economizer fly ash, and fly ash from two coal-fired power plants. International Journal of Coal Geology, 94, pp.337-348.

82. Jegadeesan, G., Al-Abed, S.R. and Pinto, P., 2008. Influence of trace metal distribution on its leachability from coal fly ash. Fuel, 87(10-11), pp.1887-1893.

83. Jones, D.R., 1995. The leaching of major and trace elements from coal ash. In Environmental aspects of trace elements in coal (pp. 221-262). Springer, Dordrecht.

84. Pathan, S.M., Aylmore, L.A.G. and Colmer, T.D., 2003. Properties of several fly ash materials in relation to use as soil amendments. Journal of environmental quality, 32(2), pp.687-693.

85. Huggins, F.E., Senior, C.L., Chu, P., Ladwig, K. and Huffman, G.P., 2007. Selenium and arsenic speciation in fly ash from full-scale coal-burning utility plants. Environmental science & technology, 41(9), pp.3284-3289.

86. Gadgil, M.R., Leachability of Trace Elements From Biomass Fly Ash Samples, 2006, M.S Thesis, University of North Dakota.

CHAPTER 3

THE MOBILITY OF SEMI-VOLATILE TRACE ELEMENTS FROM THE FLY ASH GENERATED BY THE COMBUSTION OF A SUBBITUMINOUS COAL – THE EFFECTS OF COMBUSTION TEMPERATURE

Prasanna Seshadri, Dennis Sisk, Frank Bowman, Steve Benson, and Wayne Seames*

University of North Dakota, Department of Chemical Engineering, 241 Centennial Drive Stop 7101, Grand Forks, ND 58201

ABSTRACT

The effect of combustion temperature on the mobility of three semi-volatile trace elements (TEs), arsenic, selenium and antimony, from the fly ash generated from the combustion of a pulverized subbituminous coal was assessed using a modified toxicity characteristic leaching procedure protocol. Multiple sets of size segregated fly ash samples were collected from the combustion of a Powder River Basin subbituminous coal in a laboratory scale self-sustaining combustor at Peak Combustion Temperatures of 1623 K, 1673 K and 1723 K. TEs were extracted from representative ash samples from each particle size mode (submicron, fine fragment, and bulk) in acidic (pH=2.88), neutral (pH=7) and basic (pH=11) solvents and the concentrations were compared to the concentration of TEs from complete digestion to determine fly ash TE mobility under various conditions. It was observed that an increase in the peak combustion temperature increased the distribution of minor elements and TEs in the smaller size modes, potentially influencing their final partitioning mechanisms. However, leaching results suggest that peak combustion temperature had no significant effect on TE mobility for a given size mode under a particular leaching fluid. In a majority of the cases, the fraction present in the smaller sized submicron and fine fragment particles were found to be more leachable compared to the larger bulk particles.

INTRODUCTION

Coal is one of the primary fuels for power production and accounted for about 30% electricity produced in the United States in 2017 [1]. More specifically, the subbituminous coals mined in the Powder River Basin (PRB) regions of Wyoming and Montana account for over 45% of all coal used to produce power in America and are the most mined coals in the United States [2]. Although coal-based power is economically attractive, stack emissions from coal fired plants are a concern, including aerosols and small fly ash particles that are not completely captured by particle capture devices [PCD] such as electrostatic precipitators and baghouses [3,4]. The EPA estimates that a typical ESP has an overall efficiency of 99.2%, but a PM$_{2.5}$ efficiency of only 95.1%. Therefore, for units equipped with ESPs, PM$_{2.5}$ makes up around 68% of the total ash released from a power plant [5]. Further, particulate matter less than 2.5 µm has been linked to adverse health effects in humans [4,5,6,7,8].

Even though the levels of trace elements in the original coal are small when compared to species such as Calcium (Ca), Iron (Fe), Sodium (Na) and Potassium (K) [9,10], the large-scale consumption of coal in commercial scale power plants results in a significant emission of TEs, including those which are

classified as environmental toxins. Trace elements exiting the stack are typically enriched in the smaller sized particles while others, such as mercury (Hg), leave mostly as vapor. While Hg stack emission is regulated under the U.S. Mercury and Air Toxics Standards (MATS) rule [11], there are currently no U.S. regulations governing the emission of other TEs from coal power plants. Studying the fate of TEs, especially those which leave the stack on/within particulate matter, can help us to understand their potential impact to both human and environmental health, and can help guide the development of more effective control strategies.

The three trace elements of interest to this study are arsenic (As), selenium (Se), and antimony (Sb). All three elements are semi-volatile [4,12,13,14] and their emission from coal-fired power plants cannot always be reliably predicted from the collection efficiency of PCDs. Once emitted, they can have an adverse impact on human health (through subsequent inhalation) [13,15,16,17,18] or may deposit to the earth's surface resulting in elevated levels of TEs in soil, vegetation and water [4,18,19,20]. The harmful toxicological and bio-accumulation effects of TEs from coal combustion have been shown in many studies. For instance, As is both a carcinogen and mutagen [21, 22, 23] whereas long term exposure to Se can cause severe bronchitis and bronchial pneumonia [15,24,25]. It has also been shown that chronic exposure to Sb can cause inflammation of the lungs and could lead to chronic bronchitis [26,27]. Because of these detrimental effects, there is a need to further understand the potential impacts of these particular TEs as they get distributed in our environment through anthropogenic means including from fuel combustion and other energy conversion technologies.

All three TEs can have multiple oxidation states in both coal and combustion-generated fly ash. Arsenic can exist in three valences states (−3, +3, and +5) in coal [28] while the +3 and +5 states are the most prevalent forms in combustion fly ash [29,30,31]. The +3 form of As is also more toxic than the +5 state [28,30,32]. Selenium can be present as elemental Se (0), Selenite (+4), Selenate (+6) or a hydrogen selenide (-2) in coal [28,33] and occurs mostly as Se (+4) or Se (+6) in coal ash. Se (+4) is the most common form [33,34,35] and is also more toxic than Se(+6) [4,30,36]. Antimony is similar to arsenic and is commonly present in coal ash in the +3 and +5 forms [37] with the +3 form believed to be more toxic than the +5 state [38,39]. Knowing a given TEs oxidation state is essential to assess its level of toxicity and also, like with As (+3), potential impacts to plant pollution control devices such as Selective Catalytic Reduction (SCR) [40].

Several factors affect the fate of TEs in combustion systems including their original mode of occurrence in the as-fired coal. TE modes of occurrence can significantly influence their combustion zone behavior and this in turn affects TE fraction partitioning between vapor and particulate phase. The forms of occurrence will also impact TE concentration in size segregated fly ash, which, to a large extent, determines their fate in our environment. It is therefore important that the modes of occurrence of TEs in coal be understood in order to develop effective control strategies.

TEs in coal are not uniformly distributed and can be associated in more than one form in the parent coal. Typically, they are categorized as belonging to one of three forms of occurrence: present in coal mineral inclusions, be associated with the coal's organic matrix, or be present within excluded minerals [41,42,43].

TEs present in each of the three association regimes (organic, inclusions, exclusions) will experience different conditions that will affect vaporization. Organically associated TEs are exposed to very high

temperatures and a highly reducing environment and will be released from the coal matrix when TE-C bonds break. As this material volatilizes it will diffuse out of the surrounding structure in order to enter the bulk gas phase. By contrast, TEs present as mineral inclusions are associated with specific minerals such as pyrite, mono- and di-sulfides and carbonates [44,45]. They too are exposed to high temperatures, but not as high as the organically associated TEs. At these temperatures inclusions melt and the degree of volatilization of trace elements will be determined by the vapor pressure of that specific trace element over the melt solution at the localized conditions [4,13]. Finally, TEs associated with excluded minerals are exposed to lower temperatures and experience neutral/oxidizing environments during combustion. TEs incorporated with exclusions may vaporize when the minerals melt and vaporize, albeit at slower release rates than for inclusions. Therefore, based on their original association with coal, combustion system design and operating conditions, TEs can leave (i) as flue gas vapor, (ii) in smaller submicron and fine fragment particles [4,18] and (iii) with the bulk particles which make up the major portion of fly ash particles [4,13, 46].

Each size mode in fly ash is formed as a result of the various mechanisms involving inorganic element transformation in the combustor. The dominant formation mechanism for the bulk mode (supermicron) particles is the softening/reorganization of mineral inclusions and exclusions present in the original coal. These particles have been characterized as predominantly individual, almost spherical particles, with a rather smooth surface, sometimes with discrete submicron particles sintered onto the surface. Typically, particles in the bulk mode are dominated by oxides of refractory elements such as Si, Al, Fe etc [42,47].

Particles in the intermediate fine fragmentation mode come from a number of different formation mechanisms. The largest (1-2.5 μm) of these particles form via softening/reorganization of small mineral inclusions/exclusions, often after they have shed significant volatile material. Particles in the 0.8-1.2 μm range may be formed from char cenospheres, particle fragmentation, ash ejection from rapidly rotating char particles [46,48], or from the bursting of hollow ash spheres [49]. The smallest of the fine fragmentation mode particles (0.4-0.8 μm) are most likely due to the agglomeration and coagulation of nucleated refractory minerals which vaporized from the coal at higher temperatures. Other particles in this size range may originate as the residue of particle shedding or fragmentation.

Seames et al [4] studied fly ash morphology and observed particles in the fine fragment region appear to have a much larger effective surface area compared to bulk particles due to irregularities such as fractures, stretching, and shedding. This is important when considering TE partitioning via surface reactions of vaporized TES with active sites present on solid ash particle surfaces.

The submicron particles, on the other hand, are formed predominantly by vaporization, nucleation, coagulation and condensation mechanisms. Highly volatile alkali refractory minerals (such as Na and K) can have high vaporization rates and usually forms the bulk of the submicron fume. As the flue gas cools, the gas phase concentration of the least volatile elements can become sufficient to exceed saturation and can homogeneously nucleate forming very fine particles in the order of 0.02 μm [41,42,47]. Once nuclei have formed, they can grow by collision and coagulation forming slightly larger particles in the order of 0.2 - 0.5 μm.

For less volatile minerals and heavy metals, such as Ca, Mg, Al, Si, etc. only a small fraction vaporizes. These will also condense as they move out of the pyrolysis zone of the burning coals and encounter

oxygen-deficient conditions where they are reduced by CO to more volatile species (suboxides). Because their melting temperatures are so low, they become supersaturated at extremely low concentrations and can form submicron particles through nucleation and subsequent condensation [42,47].

As semi-volatile elements, As, Se and Sb, are often typically not present in sufficient concentrations to homogeneously nucleate even at stack temperatures. Therefore, partitioning out of the flue gas to particles occurs via heterogeneous sorption of vaporized species on the surface of existing fly ash particles and/or by reaction with active sites on particle surfaces [4,13,28,53]. The partitioning mechanism of TEs in different fly ash regimes has been explained in detail elsewhere [4,13,54]. The mode of partitioning of TE determines their final oxidation state in the ash thereby directly influencing its impact on the environment [4,17].

Regardless of how TEs partition back to ash particles, they will only be harmful to the environment if they are mobile, i.e. they can leach out/off of the ash particle and into the environment. Therefore, one way to assess potential TE impacts to the environment is by conducting leaching tests on fly ash particles from the different modes of occurrence under different pH conditions. Leaching tests can simulate environments encountered by fly ash particles and provides information on element mobility for that particular environment. In general, element mobility largely depends on geochemical conditions like the pH of the water (or moist soil) they settle onto rather the pH of the ash itself [4,10].

Fly ash can enter the environment through three main pathways: inhalation, deposition downwind and bulk ash piles. Submicron and fine fragment particles can escape the PCDs and leave the stack along with the flue gas. Submicron particles present a bigger risk to human and animal health as a result of direct inhalation through the air passages and deposition in the lungs since they can stay in the air much longer than fine fragment or bulk ash particles. Hence trace element solubility results under neutral conditions (pH = 7) are important for this size fraction given the pH environment of respiratory fluids is close to 7.

Fine fragmentation particles tend to settle downwind of the stack and over a period of time can significantly increase in levels to cause potential harm. As the fine particles settle downwind of the combustor they come into contact with the moisture on wet ground or may settle in water bodies such as lakes and rivers. Once they are on the ground, the moisture in the soil (or in the water body) may act as a solvent for TE extraction, depending upon local conditions (i.e. acidic or alkaline soil). For example, soil pH. in the eastern part of the US is mostly acidic while in the west it is more likely to be alkaline [4,18,55]. Therefore, mobility data at pH 2.88 and pH 11 can provide insight into the mobility and hence the environmental impact of this size fraction.

Bulk particles are usually disposed of in landfills or used in byproducts such as road asphalt, sheetrock, etc. [4,18,56,57]. When bulk ash is deposited in a landfill, rain water may percolate through the ash pile and the pH of the rain can change substantially depending upon the pH of the ash (which was very alkaline in this study). Only the TEs present on the surface of bulk particles are generally mobile, as most of the TEs in these particles are fused within the refrozen solid spheres that characterize this ash fraction. Since the ash in this study was alkaline, alkaline leaching results from bulk particles will be the most important for this size fraction.

Previous researchers have studied fly ash TE mobility in both lab scale systems [4,17,18] as well as commercial plants [30,31,57]. Past work from lab scale systems addressed mobility as a function of particle size at a particular combustion temperature [4,17,18], whereas data reported for commercial unit samples addressed element solubility without taking particle size into consideration [30,31,57]. To the best of our knowledge, no studies to date have examined the influence of an increased combustion temperature (characterized here using the PCT) on TE speciation and mobility from size segregated fly ash particles. This study is therefore aimed at studying this effect by varying the peak combustion temperature without a significant change in flue gas residence time.

An increase in PCT has been shown to affect TE partitioning [4]. There are two effects at work. First, higher combustion temperatures increase the rate of diffusion of TEs to the surface of inclusions as well as the rate of vaporization [44]. Additionally, the quantity of major elements (Ca and Fe) that vaporize is also expected to increase with increasing combustion temperatures due to increases in the vapor-liquid equilibrium driving force. This is important because the more Ca and Fe that vaporizes, the more that will condense onto particle surfaces (or in the form of nuclei) and form reactive sites to react with As, Se, and Sb.

Additionally, fine fragment particle generation increases with increasing combustion temperature [5] producing a very high number density of small particles which in turn leads to a high surface area density. Therefore, at higher temperatures, the combination of increased TE vaporization and a high number density of small particles will increase TE enrichment in smaller sized particles compared to lower temperatures

Gas-solid partitioning reactions are important when considering the mobility of TEs from particles generated during combustion [4,17,18]. First, elements present on the surface of ash particles (such as TEs on submicron and a portion of the fine fragment particles) are generally more readily soluble than those trapped inside bigger bulk particles [4,18,57]. Second, the chemical form of the trace element on the particle surface can substantially affect the solubility of that TE in aqueous environments [4,17]. Changes in peak combustion temperature may affect which partitioning mechanisms control the transfer of vaporized semi-volatile TEs to solid surfaces and the chemical forms of occurrence present on the particles.

COMBUSTION SYSTEM AND EXPERIMENTS

Figure 1 shows a schematic of the lab-scale vertical laminar regime tube down-flow combustor used in this study. The combustor was operated at approximately 15.2 kW for all tests. The combustor is 6 m tall with a 0.15 m ID and consists of a burner cap, 1.8 m long combustion zone with 4 sample ports, a 4.2 m long post combustion zone with 6 additional sample ports, and a bottom ash trap located before a dual baghouse system. The burner cap houses a water-cooled fuel injection probe on the top and a side port through which primary air was introduced at temperatures over 700K. Air to the system was delivered by a compressor operating between 1100 - 1200 kPa. Rotameters (Series RM, Dwyer Inc, IN, USA) control the rate of air flow into the system.

A honeycomb flow straightener (0.08 m long and 0.16 m diameter) helps streamline the flow of primary air as it enters the combustor. It is made from alumina and can withstand temperatures as high as 2000 K. The top half of the flow straightener is encased in the furnace cap and the other half of the flow straightener sits inside the combustion chamber. The flow straightener has a 0.03 m opening in the

center through which the water-cooled fuel injector is inserted into the furnace. The fuel injector is about 0.72 m long and has an inner diameter of 0.015 m. It is surrounded by a water-cooled jacket on the outside.

As received coal was crushed and pulverized to deliver a particle fineness of at least 70% through a 200 mesh (U.S, 75×10^{-6} m) screen. A volumetric solids feeder (Acrison Series, 105-BC double concentric auger type) delivered pulverized coal to an entrainer with bottom fed transport air. The entrainer is designed in such a way that it provides a swirl when the fuel mixes with the air stream and this reduced pulsing in the combustor. Transport air was usually between 20 – 30 % of the total air requirement (including 20% excess) and the fuel-air mix from the entrainer was directly introduced at the top of the fuel injection probe. A detailed description of the facility and the combustor are provided by Seames [18].

After reaching steady state conditions, the centerline gas temperature was measured along the length of the furnace using a portable, uncooled R type thermocouple. Peak combustion temperatures, as measured at the nearest sample port (port 2), of around 1350°C (1623 K), 1400°C (1673 K) and 1450°C (1723 K) were achieved at a constant coal inlet flow rate of about 2.25 kg/hr and an excess oxygen value of 3% (as measured using a gas sample probe at the bottom port of the combustion zone, port 4) by adjusting the inert gas concentration/composition in the combustion air mixture. The self-sustaining bulk peak combustion temperature (PCT) achieved with no external heating was 1623 K. Raising the PCT to 1673 K and 1723 K was accomplished by replacing some of the combustion air with pure oxygen while maintaining the same coal-to-oxygen ratio. The addition of oxygen reduced the amount of sensible heat required to raise the temperature of the inert gas and resulted in increased combustion temperatures. Although gas residence times varied slightly for oxygen addition tests, it was not expected to significantly influence TE transformation reactions in the post combustion zone.
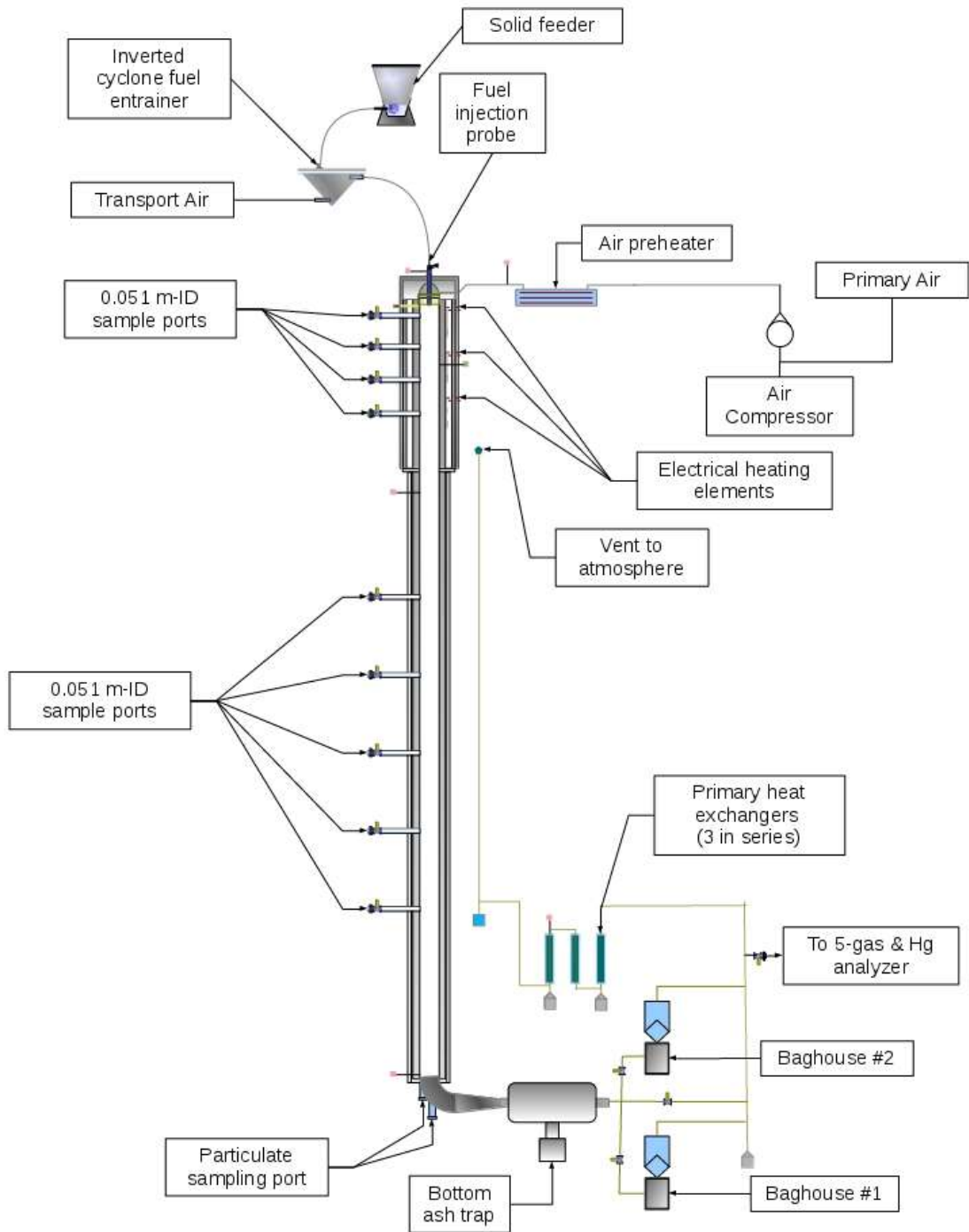
Figure 1: The University of North Dakota Chemical Engineering Department Vertical Downflow Combustion Research System.

Fly ash samples were pulled from the last sampling port using a Dekati Low Pressure Impactor (DLPI, Dekati Ltd, Finland) holding greased polycarbonate membranes. High purity Apiezon "L" type grease dissolved in toluene in a ratio of 4 mg of grease to 20 ml of toluene was sprayed on the membranes (Millipore 25x0.4 mm) using an air paint sprayer. The membranes were then dried in an oven at 65-70 °C for 24 hours to evaporate the toluene present in the spray leaving behind only the grease on the surface. Coating with grease helps to reduce particle bounce off during sampling. Dried membranes were then weighed on a microbalance having a minimum measurement of 0.01 mg. Each membrane was weighed in a temperature and humidity-controlled environment at least four times and if any readings deviated from others by a value of ± 0.05 mg or more, they were reweighed. These membranes were then loaded on impactor plates to collect fly ash samples. The DLPI uses momentum to aerodynamically segregate fly ash particles between 0.03 and 10 microns in 13 different stages with a maximum flow rate of 29.01NL/min [8]. The entire DLPI assembly was heated using an electric muff to prevent water condensation on the sample membranes.

An EPA Method 29 impinger train was used downstream of the DLPI to collect TEs present in the vapor phase. A vacuum pump was connected downstream of the impinger train and the off gases were safely vented into a fume hood.

Fly ash particle size distributions (PSD) were determined by measuring the mass of particles impacted on the stages of the DLPI which was calculated as the difference in the weight of membranes prior to and after sampling. The PSD curves were constructed following the method described by Markowski and Ensor [59] where the differential mass loading per normalized gas volume (dM) divided by the differential log10 of the particle diameter ($dlog_{10}Dp$) was plotted against the average particle diameter (D_p,avg). D_p,avg represents the average aerodynamic particle size of particles collected on a given stage and is calculated as the average of the aerodynamic diameters of the given impactor stage and the adjacent larger stage, and $dlogD_p$ is calculated as the difference between the log_{10} of the aerodynamic diameters of these two adjacent impactor stages.

For each test, at least four sets of impactor samples were collected and data from each set was used to generate individual PSD curves. An overall typical PSD curve was then obtained by averaging data from individual runs. Four individual PSDs that most closely resembled the typical PSD were selected for further analysis, as described below.

One set of DLPI samples was used to determine the total concentration of elements in ash and three other sets were extracted with acidic (pH = 2.88), neutral (pH = 7) or basic (pH = 11) solutions during the leaching studies. Ash loaded membranes from stages 3-12 of the DLPI were used for both total concentration and leaching analyses. Stages 1 and 2 were not analyzed because they represent a mixed ash that contains both submicron particles plus particles that were generated in the sampling probe via condensation/nucleation as the flue gas sample cooled [13]. In addition, the quantity of ash collected was extremely small, rendering the TE concentrations in the leaching fluid too low to be detected by GFAAS. An acid digestion method [4,13] developed by Wendt and co-workers was used to extract the total concentration of both TEs and other selected metals from ash [60]. A SOLAAR Flame Atomic Absorption Spectrometer (FAAS) (M6 Spectrometer, Thermo Electron Corporation, United Kingdom) was then used to determine the concentrations of major species (calcium and iron) and a Graphite Furnace Atomic Absorption Spectrometer (GFAAS), with Zeeman background correction, was used to determine TEs (As, Se and Sb) in both fly ash and vapor phase samples. All

the digested samples were analyzed multiple (at least three) times to ensure quality assurance and control.

The total concentration of TEs in the original coal was determined using a microwave assisted acid digestion process following EPA SW – 846 Test Method 3052 [61]. Additionally, a sequential leaching procedure, as recommended by Senior et.al., [13], was used to estimate the TE associations in the test coal. This method uses solubility data to predict TE mode of occurrence in coal. 5g samples of coal were sequentially leached with solutions of 1N Ammonium acetate, 3N hydrochloric acid, concentrated hydrofluoric acid (HF 48%) and finally using 2N nitric acid. Each of these solvents digest a specific portion of the coal sample. Ammonium acetate removes elements bonded onto ion-exchangeable sites and some carbonates. Hydrochloric acid dissolves carbonates, iron oxides, monosulfides, and certain chelated organic compounds. Hydrofluoric acid digests silicates, and nitric acid dissolves disulfides, especially pyrite. The entire test procedure, including details on the leaching fluids and their respective roles is shown here [13]. Results from this procedure provides basic information on the distribution of TEs in coal and can be used to predict TE transformations during combustion.

A modified TCLP procedure, as suggested by Seames [18], was used to determine trace element mobility in the fly ash. The EPA recommended TCLP Improved Method 1311 requires the use of about 100 g of loose fly ash and a liquid-to-solid (L/S) ratio of 20 [17]. This procedure was modified by Seames [4,18] for use with mg-size samples of ash affixed to greased membranes. Ash loaded membranes were extracted individually in a particular medium (acidic, neutral, or basic) while the sample pH was continuously monitored. Individual impactor membranes were placed in 10ml polycarbonate vials and 5 ml of the leaching fluid was then added and the pH was checked. If there was a drift from the original pH, appropriate buffers were added right away to return the pH back to its target pH condition. Capped vials were placed in a continuous rocking type shaker (Thermo Scientific™, Catalog No 13-687-11Q, USA) for 18 ± 2 hours. The pH was rechecked after 20 minutes initially and then every hour to make sure it remained constant. After 18 hours the samples were removed from the shaker and allowed to rest for an hour. The solution was then decanted from this vial into a clean vial and trace amounts of fluid entrained in the membranes were removed by placing the membrane into a syringe without a tip and squeezing the moisture out into the leachate vial.

This procedure was repeated with two more sets of impactor samples for the other two pH conditions. After a period of 18-24 hours, all sample leachates were analyzed for TE concentration using a GFAAS. Mobility was expressed as the ratio of elemental concentration in the leaching fluid to its concentration in the totally digested sample. Absolute elemental concentration was expressed as mg (or) µg of element in ash/Nm3 of gas sampled depending on element of interest. For metals such a Ca and Fe whose composition in ash is so much higher than TEs, concentration was usually expressed as mg/Nm3. Concentration for TEs was usually expressed as µg/ Nm3 due to their relatively low concentrations in coal ash

RESULTS – PSD AND ASH COMPOSITION DISTRIBUTION

The coal used for this study was a PRB subbituminous coal that had high concentrations of sodium and calcium but a low concentration of iron which may be due to the low levels of pyrite in the coal. Some of the relevant properties of the coal used are shown in Table 1.

Table 1: Proximate, Ultimate and major element ash analysis of the PRB Test Coal

Analyte	As rec.	Dry	Mineral analysis of ash	% wt.*
Moisture	22.5		Silicon dioxide	39.3
Volatile	31.3	40.4	Aluminum oxide	17.5
Fixed carbon	41.9	54.1	Ferric oxide	6.4
Ash	4.3	5.5	Titanium dioxide	1
			Phosphorous pentoxide	0.6
Carbon	56.1	72.4	Calcium oxide	19.1
Hydrogen	6.4	8.3	Magnesium oxide	6
Nitrogen	0.8	1.0	Sodium oxide	5.8
Sulfur	0.4	0.5	Potassium oxide	1.8
Oxygen	13.8	17.8	Others	2.5
BTU/lb	10015	12923		

* - Weight percent equivalent oxide on a SO_3 free basis

Data from the sequential leaching procedure conducted on the as-received test coal are shown in Table 2. As mentioned previously, these data can be used to estimate forms of occurrence of TEs in coal. Elements not leached by any of the four reagents may be present in the organic portions of the coal, or other insoluble phases such as zircon or titanium dioxides [13]. Additionally, where mineral grains are completely encased by the organic matrix, these shielded grains may not be completely digested.

Based on the results obtained, it was observed that selenium mostly had organic association, Data in Table 2 shows only about 24% of the total Se was recovered in the four leaching reagents. Se not liberated by any of the four solvents (about 75%) was assumed to have an organic association in the coal. Based on the mass fraction leached in the four solvents, the largest fraction of As (about 40%) was assumed to be organically associated while pyritic association was also significant around 25%. Sb, in particular, was mostly associated with pyrite with some organic association.

Table 2: Sequential leaching data to determine TE mode of association in the test coal

Element	Total (ppm)*	% Leached					% Not leached
		Acetate	HCl	HF	HNO$_3$	Total	
Arsenic	2.1	10	12	12	24	58	42
Selenium	1.8	7	0	6	11	24	76
Antomony	0.34	11	0	19	44	74	26

* As determined using EPA SW – 846 Test Method 3052

Test measurements included the peak combustion temperature, which was assumed to occur at the second available sample port (0.6 m from the top of the furnace). However, the actual peak may have occurred either prior to or after this point, introducing a minor level of uncertainty into the results. The measured PCT was 1350°C (1623 K), 1400°C (1673 K) and 1450°C (1723 K) for the three test conditions, respectively. Temperature profiles, including the PCT, were measured by recording the

centerline temperature of the flue gas at every available port for each experiment (Figure 2). Raising the PCT required replacing some of the combustion air with pure oxygen which slightly increased the gas residence time for the higher temperature tests.
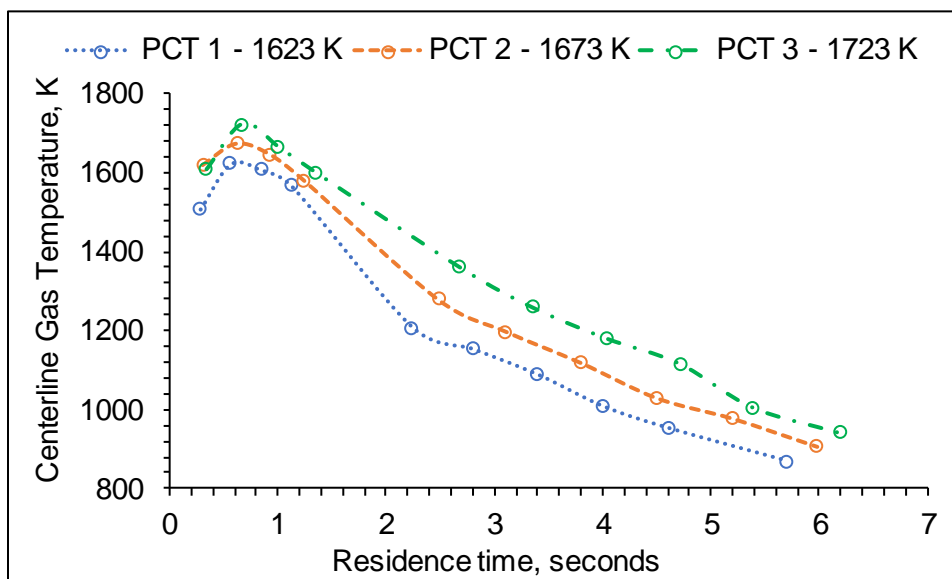
Figure 2: Flue gas temperature vs. gas residence time. Individual data points represent the actual measurements from the combustor and demonstrate the slight shift in gas residence time due to the partial replacement of air with oxygen in the higher PCT tests.

Fly ash samples were collected from the last port of the post combustion zone which is located about 6 m from the top of the furnace. Individual ash PSDs for the samples collected at the three combustion temperatures (in decreasing order of PCT) are shown in Appendix A, Figures 4-6, respectively. All the individual runs showed a consistent trend as observed by the presence of a multimodal ash distribution. PSDs for any run that showed a trend different from the other runs was not shown in either figure nor included while averaging data for the overall distribution.

Typical PSDs generated by averaging the data from all included PSDs are shown in Figure 3. All three PSDs show a trimodal distribution namely submicron, fine fragment and bulk modes. This trimodal distribution is consistent with observations made by other researchers [46,48,62,63]. The submicron regime peaks for all three tests at 0.22 μm. The peak for the fine fragment mode occurred within the range of 1.3 μm to 2.1 μm. This was observed under all three test conditions. For the bulk mode both 1673 and 1623 K test conditions showed a peak at 5.6 μm, but at 1723 K the maximum occurred at a larger particle size of 8.4 μm. In general there was no shift observed in the ash overall PSDs as a result of differences in peak combustion temperature.

Even though the difference in combustion temperature did not alter the overall PSD profile, the relative amount of ash loading for most of the stages in the submicron and fine fragment size fractions increased with increasing combustion temperatures even whilst considering uncertainty in data measurements. This possibly was the result of increased mineral vaporization with increasing PCT which in turn increased fine particle formation. Additionally, bulk mode loading (for particles over 5 μm in size) was higher for 1623 K samples than 1723 K samples indicating lower vaporization at lower PCT.

Based on the average PSDs (figure 3), DLPI stages 3, 4 and 5 (corresponding to aerodynamic particle diameters in the range from 0.11 to 0.4 µm), stages 6 – 9 (corresponding to aerodynamic particle diameters in the range from 0.4 to 2.5 µm), and stages 10 – 12 (corresponding to aerodynamic particle diameters of 2.5 to 10 µm) were chosen to represent the submicron, fine fraction and bulk size modes for mobility studies. Particles collected on stages 1 and 2 of the DLPI are likely to contain "mixed material" phase as a result of vapor phase material condensation in the sampling probe and will not be representative of submicron mode in the furnace flue gas [8]. Hence these two stages were not included in sample analysis for leaching studies.
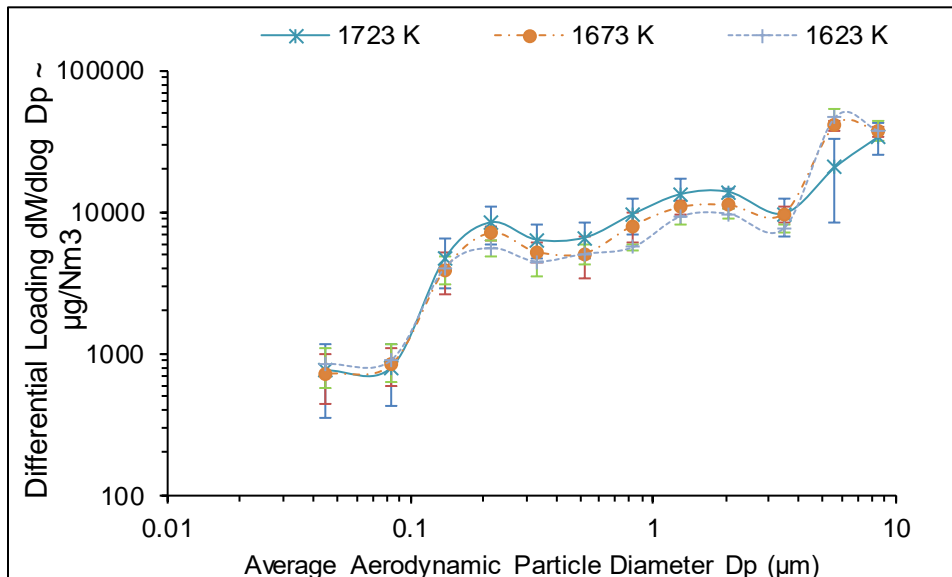
Figure 3: Average Flue Gas Fly Ash Particle Size Distributions for each set of peak combustion temperature experiments

Fly ash minor and trace element concentrations

As mentioned earlier, vaporized forms of all three TEs may partition onto fly ash particles via a heterogeneous surface chemical reaction. The degree of partitioning depends on the number of active cation sites available [14]. Calcium and iron are expected to provide the majority of these sites and this mechanism has been explained in detail elsewhere [4,64]. For this test coal, calcium is expected to be the major site provider since its concentration is much higher in the coal (and subsequently in the ash) when compared to iron. Thus, active Ca sites are expected to play a major role in the partitioning reactions of all three TEs. There is expected to be competition for these active Ca sites, between vapor phase TEs and SO2 in the flue gas, since flue gas sulfur levels are significantly higher (by several factors) than TE levels and sulfation reactions (for Ca sites) are likely to proceed much quicker than TE vapor - sorption reactions.

Active cation sites are formed when supersaturated vaporized species nucleate and coagulate or condense on the surface of existing ash particles. Active sites produced by this mechanism primarily include those in the submicron and fine fragment modes where this pathway is the most dominant. The size segregated typical composition distributions for Ca, Fe, As, Se, and Sb are shown in Appendix A, Figures 7-11, respectively.

Vapor phase concentration for all the three TEs is shown in Table 4. As combustion temperature increases, gas phase concentrations of all three TEs start to decrease. This supports the earlier hypothesis that combustion temperature will increase gas to solid partitioning mechanisms.

Table 3: Vapor phase concentration of As, Se and Sb measured for the three PCT test conditions

TE	Vapor phase concentration (µg/l)		
	1723 K	1673 K	1623 K
As	54±12	131±9	167±26
Se	188±41	223±19	282±62
Sb	21±11	53±6	99±14

RESULTS - LEACHING STUDIES

Results from the leaching studies are shown in Tables 4-6. The mass fraction soluble values (reported as % soluble), was calculated as the ratio of a given TE's concentration from any given DLPI stage to its concentration for the same DLPI stage as determined by the total digestion method. These are shown as a function of PCT for all three TEs under acidic, neutral and basic environments and for the three size modes. It is important to interpret these data as qualitative in nature due to the extremely small amounts of ash involved in the smaller particle modes and large uncertainty in the data. BD indicates below detection limit of TE in that particular leaching fluid only. Individual DLPI stages were analyzed separately in triplicates and then an average solubility for each mode was calculated from the average mobilities of all the individual stages constituting that mode. Additionally, data shown in tables 4, 5 & 6 also includes uncertainty in reported values calculated at a 95% confidence interval. In general, an elements' solubility should be similar for all the stages comprising a given size mode.

Table 4: Percentage solubility of TEs in submicron mode for the three PCTs and under the three pH conditions

Submicron mode	Acidic pH = 2.88	Neutral pH = 7	Basic pH = 11
Arsenic			
1723 K	91±5	61±10	BD
1673 K	80±9	64±4	BD
1623 K	76±4	45±4	BD
Selenium			
1723 K	51±8	42±5	46±4
1673 K	63±9	45±9	51±4
1623 K	47±4	51±5	52±4
Antimony			
1723 K	81±5	59±7	22±6
1673 K	86±10	48±7	12±3
1623 K	75±7	61±4	23±3

Table 5: Percentage solubility of TEs in fine fragment mode for the three PCTs and under the three pH conditions

Fine fragment mode	Acidic pH = 2.88	Neutral pH = 7	Basic pH = 11
Arsenic			
1723 K	90±6	64±8	BD
1673 K	84±7	56±6	BD
1623 K	77±4	48±4	BD
Selenium			
1723 K	87±6	72±8	62±4
1673 K	81±8	76±10	54±6
1623 K	76±3	67±4	53±3
Antimony			
1723 K	86±9	56±4	44±4
1673 K	91±7	56±4	41±4
1623 K	77±4	47±3	45±3

Table 6: Percentage solubility of TEs in the bulk mode for the three PCTs and under the three pH conditions

Bulk mode	Acidic pH = 2.88	Neutral pH = 7	Basic pH = 11
Arsenic			
1723 K	30±5	16±6	BD
1673 K	21±5	12±5	BD
1623 K	26±4	11±2	BD
Selenium			
1723 K	56±7	39±6	10±3
1673 K	47±6	41±6	3±2
1623 K	47±3	33±2	2±1
Antimony			
1723 K	76±8	60±11	BD
1673 K	79±7	47±5	BD
1623 K	72±5	52±3	BD

Submicron Mode

Data presented in Table 4 for submicron mode particles show that combustion temperature did not have a pronounced effect on TE mobility for this size fraction. This indicates the likelihood of formation of similar chemical species under all three PCTs. Both As and Sb showed high mobility under acidic conditions and moderate mobility under neutral conditions. Arsenic was completely insoluble under basic conditions, while Sb was only slightly soluble. Thus, for both As and Sb, as pH increased, solubility decreased. This finding is consistent with the work conducted by Seames et. al [18] to study TE leaching in combustion and co-combustion coal ashes. The precipitation of ettringite (calcium aluminate sulfate hydroxide hydrate) may account for the reduced solubility of both As and Sb in a basic solution [57,58,68,69]. Calcium based metalloids such as ettringite can incorporate and also

retain some of the arsenic [57]. Although the formation of ettringite has been observed only at pHs >11 [57,58], reduced solubility at alkaline pHs may have also been the result of oxyanions as silicate fractions which are not very soluble under these conditions [18,71]. Sb solubility data under acidic and neutral conditions is consistent with data reported by Norman et al. [72] where it was shown to be very mobile under acidic conditions and moderately solubile in a neutral medium.

Se data showed a different trend to As and Sb with respect to solubility in the three leaching solutions. Like As and Sb, PCT did not show any effect on its overall solubility, but unlike those other TEs, Se was found to be equally soluble in all three leaching solutions for all three PCTs.

Since submicron particles present an inhalation risk, it is important to evaluate solubility data for TEs in a neutral environment for potential health hazards. All three TEs were found to be partially soluble at pH = 7 indicating potential health risks from inhalation.

Fine fragment Mode

Solubility results for the fine fragment mode, as shown in Table 5, indicate a trend similar to TE solubility in submicron particles, especially for As and Sb. Both elements had very high solubility in an acidic medium and moderate solubility in a neutral medium. Antimony, in the smaller sized submicron and fine fragment particles can either have a Sb, Sb_2O_4 or a Sb_2O_6 association and all these compounds usually show high mobility under acidic conditions and are partially mobile in neutral pHs [17,68,72]. Arsenic was completely insoluble in the basic medium, while Sb was moderately soluble.

Similar to TE solubility results for the submicron mode, PCT did not influence mobility of either As or Sb under any of the leaching conditions and their mobilities decreased as pH approached basic conditions. The similarities between submicron and fine fragment mobility data for As and Sb indicate the possibility of similar partitioning mechanisms for these two TEs in both size fractions and hence, the same chemical state in both size fractions. Researchers [38] have shown that differences in partitioning mechanisms has a greater effect on TE solubility from fly ash than the size mode where the trace element resides.

Selenium also showed very high solubility in an acidic medium and moderate solubility in neutral and basic mediums. Unlike Se present in submicron particles, there seems to be a small dependence on pH for this size fraction. Like As and Sb, PCT did not seem to affect Se mobility for a given leaching solution. This indicates the possibility of the formation of similar chemical species at the three test conditions. However, Se mobility was higher for both acidic and neutral leaching solutions than their respective submicron values indicating the possibility of different species between the two modes. Seames et al. have shown that selenium present as Fe-Se complexes (selenates) have fairly high solubility in both acidic and neutral conditions, whereas Ca-Se complexes (selenites) have low solubility at both conditions [17].

Regarding the potential impact on the environment, it is important to take into consideration TE solubility data for fine fragment particles from both acidic and basic leaching solutions since soil can be either acidic (Eastern United States) or basic (Western United States) depending on the geographic location. Data presented indicates all three TEs could be of environmental concern under acidic conditions while Sb and Se but not As could also be of concern under basic conditions.

Bulk mode

TE solubility data for bulk mode particles are shown in Table 6. Similar to submicron and fine fragment modes the effect of PCT on TE mobility was not significant and all three elements had similar solubilities in a given leaching fluid irrespective of combustion temperature. Unlike its mobility in both submicron and fine fragment modes, bulk particle arsenic did not show high mobility. Submicron and fine fragment As is mostly held on the surface of the particle and is available for leaching, whereas a significant portion of As present in the bulk mode is likely incorporated within the PM structure and is expected to stay bound within the ash under most pH conditions. Arsenic had only slight solubility in acidic medium and was not very soluble in a neutral medium. It was completely insoluble in the basic leaching solution which mirrors both submicron and fine fragment data. Antimony had a high solubility in the acidic medium and was slightly soluble in the neutral medium. These data closely mirror Sb mobility data for both submicron and fine fragment particles. However, it was found to be completely insoluble under basic conditions for the bulk mode.

Selenium data for the bulk mode indicates slight mobility under both acidic and neutral conditions, while it was mostly immobile under basic conditions. Mobility data for Se in acidic and neutral solutions closely mirrors its mobility in submicron mode, whereas basic solution data aligns closely with As and Sb mobility.

The major environmental impact from bulk ash particles is primarily related to disposal since these particles are normally placed in landfills or used in by-products such as road asphalt, sheetrock, etc. Due to the basic nature of the PRB ash, rain water pH will rise as it seeps through the ash pile. Based on data presented in Table 6, all three TEs mobility were found to be immobile under a basic environment and are not expected to pose a major risk.

CONCLUSIONS

Size segregated fly ash samples were collected from the combustion of a PRB coal at three different combustion temperatures. The mobility of As, Se, and Sb in the submicron, fine and bulk particle size fractions were determined under three different pH conditions using a modified TCLP protocol. Even though an increase in combustion temperature increased TE mass loadings in particle matter in the submicron and fine fragment regime size ranges, their solubilities in a given leaching solution and for a particular size mode remained unaffected by the change in combustion temperature for this test coal. This suggests that the increase in mass loadings was due to an increase in available Ca and Fe surface sites rather than from a change to partitioning mechanism.

For both submicron and fine fragment modes, As and Sb showed significant mobility especially under acidic and neutral leaching solutions. Bulk mode solubility for these two leaching solutions was still significant for antimony, but arsenic was only slightly soluble in an acidic medium and even less in a neutral medium. However, both As and Sb showed lower solubility under basic leaching conditions. Arsenic was found to be completely insoluble for all three size modes whereas Sb showed slight mobility for submicron and fine fragment modes. However, like As Sb was found to be completely insoluble for the bulk mode fraction. Se solubility data indicates moderate to high mobility under all leaching conditions and particle sizes, except for bulk mode particles in a basic solution where Se was found to be mostly insoluble. Se solubility varied little with pH for the submicron mode and showed a slight increase in solubility as acidity increased for the fine fragment mode.

Based on solubility data, it appears that all three TEs may be solubilized in lungs after inhalation. Further, a portion of the TEs in fine fragment ash PM may be mobile in acidic soils with Se and Sb also partially mobile in alkaline soils. Bulk mode TE mobility was not significant and is not expected to pose a risk.

APPENDIX A

SUPPLEMENTARY FIGURES, TABLES AND DISCUSSION FOR CHAPTER 3
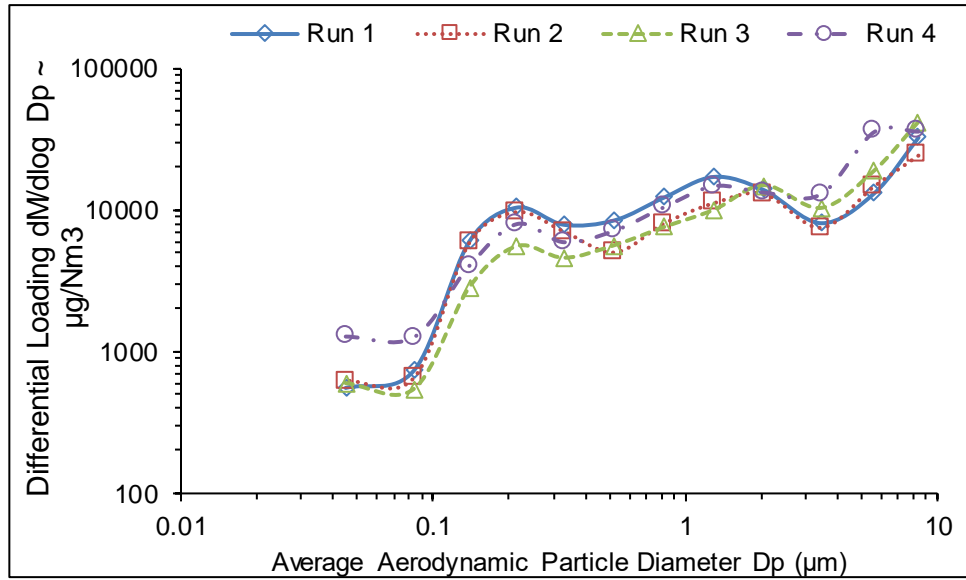
Figure 4: Flue Gas Fly Ash Particle Size Distribution replicates for PCT 1723 K experimental runs
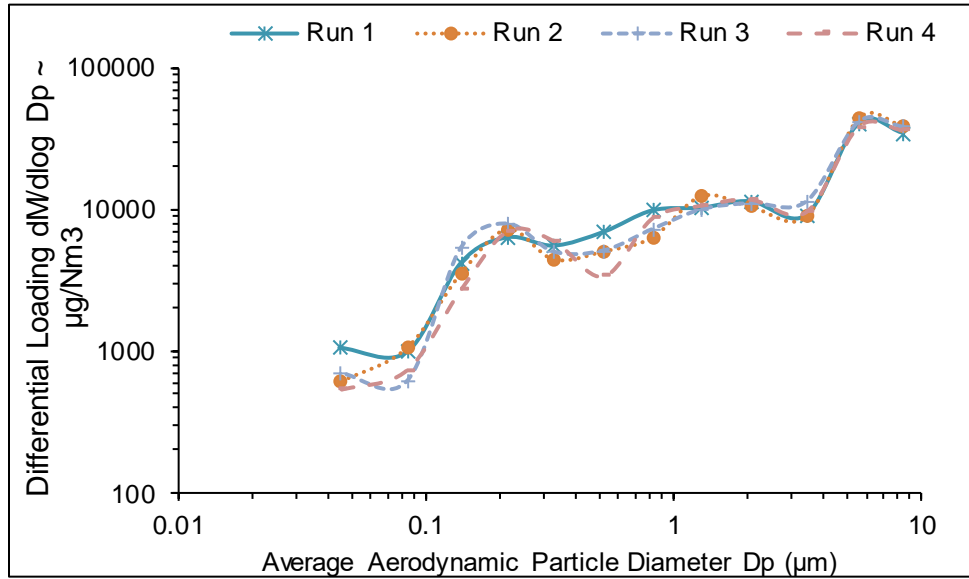
Figure 5: Flue Gas Fly Ash Particle Size Distribution replicates for PCT 1673 K experimental runs
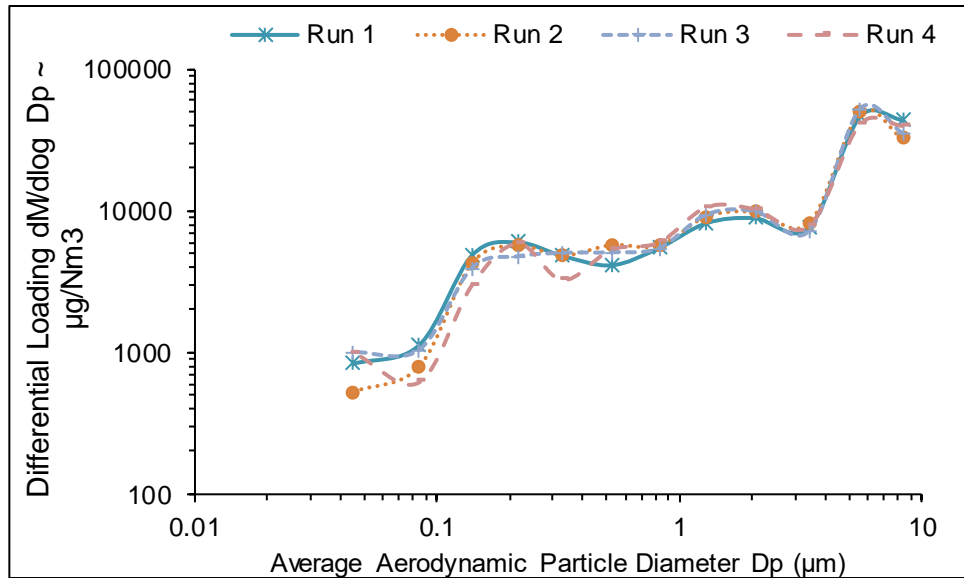
Figure 6: Flue Gas Fly Ash Particle Size Distribution replicates for PCT 1623 K experimental runs

Calcium and Iron

Data presented in Figures 7 and 8 shows the effect of PCT on calcium and iron mass distributions for the given test coal. Both data sets closely represent the average PSDs for a given PCT, including individual modal peaks at the same particle diameter. With respect to the effect of increasing combustion temperature, mass distribution of Ca and Fe for both submicron and fine fragment modes increased with increasing PCT. This indicates a higher degree of element vaporization and subsequent nucleation/ coagulation and condensation reactions. As expected, the bulk fly ash mode showed a reverse trend with higher elemental loadings from the lower temperature tests. Since the bulk mode is mostly derived from mineral matter, this further shows that an increase in PCT increased mineral vaporization which eventually contributed to higher concentrations of Ca and Fe in the smaller submicron and fine fragment particles. Even though PCT affected mass distributions for both Ca and Fe, the general shape of the mass distribution curve did not change with changing combustion temperature. This indicates similar partitioning mechanisms for a given size mode which was independent of PCT.

Typically, in low rank coals (such as the one in this test study) most of the Ca is present either as an ion-exchangeable or organically associated cation [65,66]. Under flame conditions, both forms are extremely reactive and all of Ca present in these two forms is expected to volatilize fully [13]. However, a portion of Ca is also present in the mineral form and those are the ones that are likely to be most affected by changes to PCT. Figure 7 shows changes to both submicron and fine fragment size modes at higher PCTs and this was probably the result of increased mineral source Ca vaporization at higher temperatures. Since an increase in PCT increased Ca distribution in submicron and fine fragment particles, it is therefore expected to contribute more active sites at higher combustion temperatures for TE partitioning reactions.
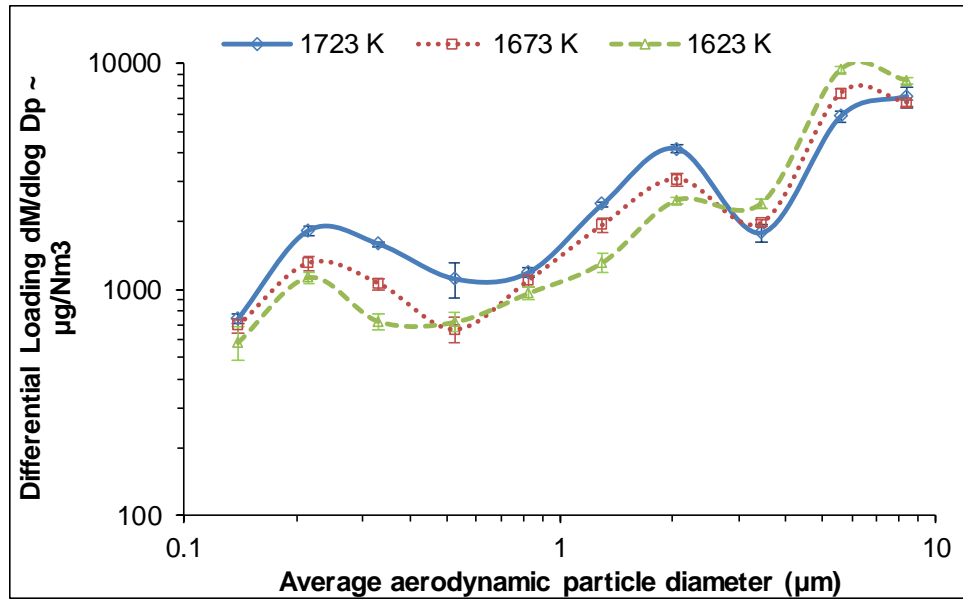
Figure 7: Differential mass distribution of calcium in fly ash for the three PCT runs

The Fe mass distributions, shown in Figure 8, exhibit a similar trend to the Ca distributions, but had comparatively lower overall ash loading. The total amount of calcium was almost three times more than the total amount of iron in the test coal. However, unlike Ca, most of the Fe present in ash is expected to be derived from mineral grains (such as pyrite etc) which would account for the major portion of iron distributed in all size modes. The distribution of Fe in the submicron and fine fragment regions (between 0.3 - 3 µm) increased with increasing PCT indicating the likelihood of increased mineral source Fe vaporization at higher PCTs and subsequent nucleation/ condensation forming small particles. These likely became active sites for TE vapor sorption reactions. However, the fine fragment peak for Fe distribution seems to be at a smaller particle size than Ca.
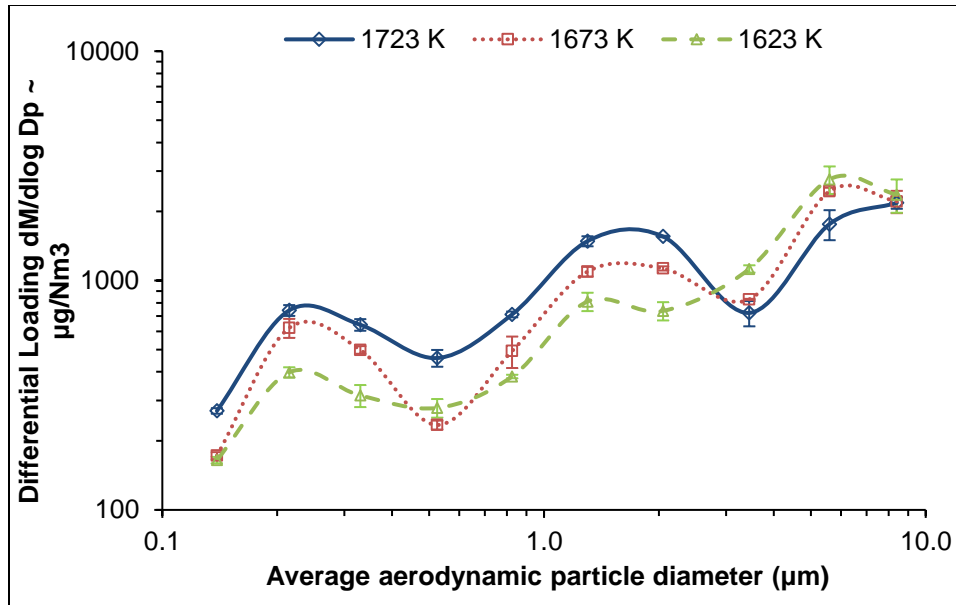
Figure 8: Differential mass distribution of iron in fly ash for the three PCT runs

Arsenic, Selenium & Antimony

Similar to Ca and Fe, all three TEs showed an increase in submicron and fine fragment mode concentrations with increasing PCT. This is expected since all three TEs have higher volatility than both Ca and Fe and with increasing PCTs, more of the TEs (especially those present in the mineral fraction such as silicates) are expected to vaporize and subsequently react with active Ca/Fe sites to make the bulk of TEs present in small particles, although the portion that vaporizes may still be a very small fraction of the TEs contained in these minerals. The bulk fraction will mainly consist of the non-vaporizing fraction from quartz and clay minerals present in coal ash [4,13,18,66]. However, only those Ca and Fe present on the surface, either from direct sorption or from the merger of smaller particles onto the bulk particle surfaces, will serve as active reaction sites for the partitioning of As, Se, and/or Sb. Bulk mode TE distribution will have a similar dependency on PCT as the less volatile Ca and Fe compounds.

The arsenic mass distributions shown in Figure 9 illustrate the effect of PCT on As distribution across the various fly ash size fractions. In general, an increase in PCT results in an increase in the mass of As in the submicron and fine fragment PM. The amount of As that partitions to the small PM is expected to increase as PCT increases due to the increase in available Ca and Fe surface sites at elevated combustion temperatures (Figures 6a and 6b). This explains the higher loading of As in both submicron and fine fragment modes as temperature increases. The overall shape of the distributions looks generally similar for all three samples indicating similar partitioning mechanisms which suggests that the chemical state of arsenic will be the same for a given particle size mode and was not influenced by change in PCT. However, there may be slight variations in peak locations for a given size mode depending on test conditions. For example, there was a clear submicron peak at 0.22 μm for both 1723 K and 1673 K samples whereas for the 1623 K sample it occurred at 0.3 μm.

45
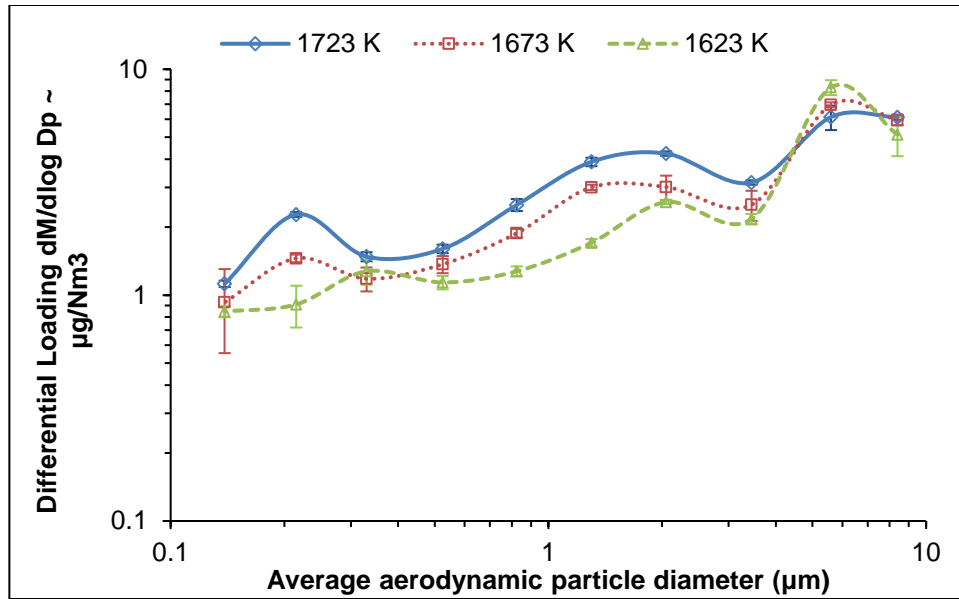
Figure 9: Differential mass distribution of arsenic in fly ash for the three PCT runs

Figure 10 shows the selenium distribution in the fly ash for the three test conditions. Compared to arsenic, selenium does not show a clear trend of increased concentrations at higher PCTs for most size fractions. Only at the smallest sizes do Se concentrations seem to increase with temperature. This is understandable considering Se is more volatile than the other two TEs [67] and almost 75% of the Se in coal was found to be organically bound (Table 2). In addition, vaporized SeO_2 is much more volatile than the corresponding As and Sb species, leading to higher Se vapor phase concentrations and consequently lower effects as a result of Ca and Fe surface site availability. Data in table 4 shows vapor phase Se concentration to also decrease with PCT indicating increased vapor to solid partitioning.
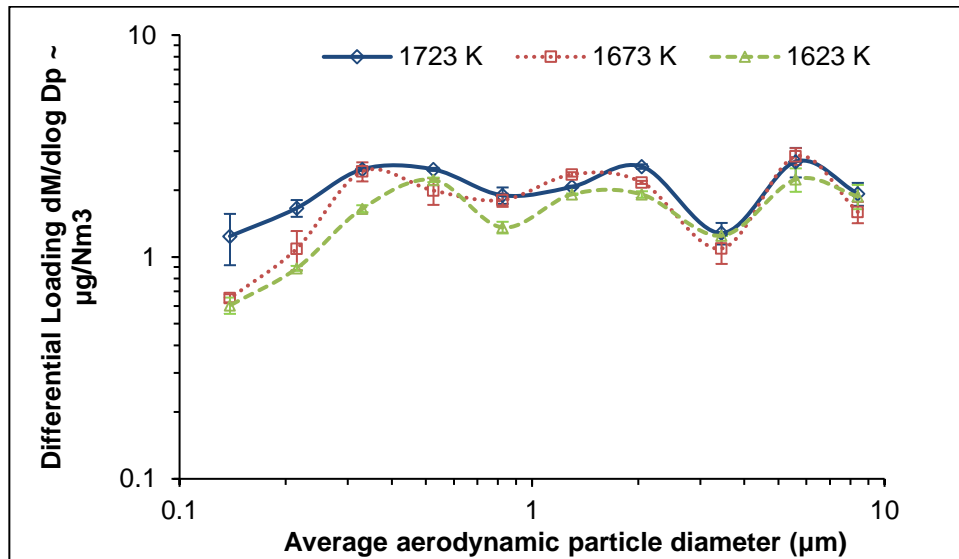
Figure 10: Differential mass distribution of selenium in fly ash for the three PCT runs

Fly ash antimony distributions for the three PCT conditions are shown in Figure 11. The distribution profiles showed mostly similar trends for the three test conditions. For example, Sb mass distribution

for all three PCT tests had size mode peaks and minimums at the same particle diameters, with the exception of the fine fragment mode at 1623 K. This suggests the possibility of a common partitioning mechanism for that given mode even under different test conditions. The effect of PCT on Sb distribution was more pronounced than for the other elements and was mostly similar to As, Ca and Fe distributions. At higher PCTs, Sb distribution was also higher for the smaller size fractions indication higher vaporization from the mineral fraction and subsequent vapor – active cation sorption reactions. Data from Table 2 shows that over 60% of the Sb was associated with coal minerals (HNO3 and HF solubility) and hence an increase in PCT will increase the amount as well as the rate of ash vaporization. Coarse mode Sb was the highest for the 1623 K samples which also had the lowest submicron and fine fragment loadings. This shows that increasing PCT primarily affected Sb present in the larger sized particles which is mostly composed of ash minerals. Vapor phase Sb data shown in table 4 shows a very clear trend of higher concentrations at lower combustion temperature. This is somewhat similar to As vapor data and indicates increased conversion of vapor to solid at higher combustion temperatures.
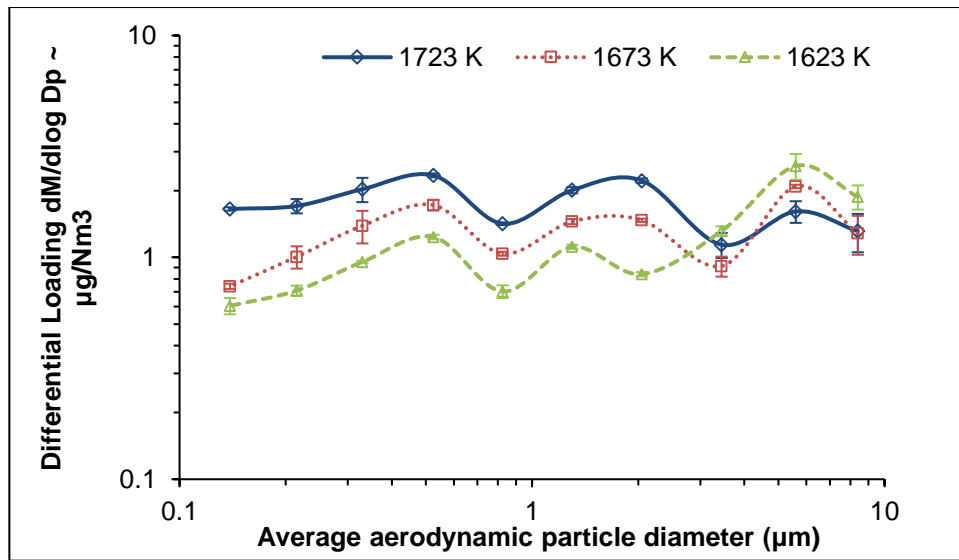
Figure 11: Differential mass distribution of antimony in fly ash for the three PCT runs

Table 7: Percentage solubility of TEs in the three size modes for 1723K PCT samples under acidic (pH = 2.88) condition

Particle regime	Element	DLPI Stage	Cut point (µm)	% Mobility				Uncertainty in mobility (95% CL)
				Run 1	Run 2	Run 3	Average	
Submicron	Arsenic	3	0.108	92	95	91	91	4
		4	0.17	99	84	86		
		5	0.26	86	102	83		
	Selenium	3	0.108	58	39	36	51	6
		4	0.17	66	52	51		
		5	0.26	49	61	46		
	Antimony	3	0.108	91	84	82	81	4
		4	0.17	82	76	75		
		5	0.26	71	88	83		
Fine fragment	Arsenic	6	0.4	106	89	92	90	5
		7	0.65	83	107	87		
		8	1	95	91	97		
		9	1.6	81	78	76		
	Selenium	6	0.4	109	88	91	87	5
		7	0.65	84	81	76		
		8	1	96	88	84		
		9	1.6	83	79	84		
	Antimony	6	0.4	96	82	81	86	7
		7	0.65	74	87	71		
		8	1	83	97	85		
		9	1.6	122	73	77		
Bulk	Arsenic	10	2.5	33	41	31	30	4
		11	4.4	26	28	36		
		12	6.8	22	19	35		
	Selenium	10	2.5	66	61	49	56	6
		11	4.4	42	57	53		
		12	6.8	71	55	48		
	Antimony	10	2.5	78	101	74	76	6
		11	4.4	72	75	79		
		12	6.8	64	71	73		

Table 8: Percentage solubility of TEs in the three size modes for 1723K PCT samples under neutral (pH = 7) condition

Particle regime	Element	DLPI Stage	Cut point (μm)	% Mobility				Uncertainty in mobility (95% CL)
				Run 1	Run 2	Run 3	Average	
Submicron	Arsenic	3	0.108	52	65	67	61	8
		4	0.17	77	54	51		
		5	0.26	46	84	49		
	Selenium	3	0.108	38	41	53	42	4
		4	0.17	47	41	44		
		5	0.26	47	32	34		
	Antimony	3	0.108	68	66	61	59	6
		4	0.17	73	51	54		
		5	0.26	62	49	46		
Fine fragment	Arsenic	6	0.4	78	59	74	64	7
		7	0.65	61	69	66		
		8	1	64	83	77		
		9	1.6	41	44	56		
	Selenium	6	0.4	94	83	87	72	6
		7	0.65	71	77	72		
		8	1	68	65	51		
		9	1.6	62	61	76		
	Antimony	6	0.4	49	48	61	56	3
		7	0.65	54	58	51		
		8	1	66	49	61		
		9	1.6	61	53	57		
Bulk	Arsenic	10	2.5	31	21	24	16	5
		11	4.4	8	13	11		
		12	6.8	12	9	15		
	Selenium	10	2.5	38	41	55	39	5
		11	4.4	33	44	46		
		12	6.8	31	37	29		
	Antimony	10	2.5	79	72	78	60	9
		11	4.4	64	55	57		
		12	6.8	52	41	43		

Table 9: Percentage solubility of TEs in the three size modes for 1723K PCT samples under basic (pH = 11) condition

Particle regime	Element	DLPI Stage	Cut point (μm)	% Mobility				Uncertainty in mobility (95% CL)
				Run 1	Run 2	Run 3	Average	
Submicron	Arsenic	3	0.108	1	1	2	2	1
		4	0.17	2	2	1		
		5	0.26	3	0	2		
	Selenium	3	0.108	46	54	51	46	3
		4	0.17	42	50	48		
		5	0.26	41	39	46		
	Antimony	3	0.108	16	13	19	22	4
		4	0.17	34	27	31		
		5	0.26	22	19	16		
Fine fragment	Arsenic	6	0.4	1	1	0	0	0
		7	0.65	1	1	1		
		8	1	0	0	0		
		9	1.6	0	0	0		
	Selenium	6	0.4	68	53	66	62	4
		7	0.65	56	72	59		
		8	1	48	67	64		
		9	1.6	59	66	65		
	Antimony	6	0.4	56	48	46	44	4
		7	0.65	39	40	51		
		8	1	46	41	43		
		9	1.6	44	29	47		
Bulk	Arsenic	10	2.5	0	0	0	1	1
		11	4.4	3	0	1		
		12	6.8	4	0	1		
	Selenium	10	2.5	8	14	11	10	2
		11	4.4	11	4	16		
		12	6.8	11	6	7		
	Antimony	10	2.5	4	2	0	2	1
		11	4.4	3	1	1		
		12	6.8	2	0	1		

Table 10: Percentage solubility of TEs in the three size modes for 1673K PCT samples under acidic (pH = 2.88) condition

Particle regime	Element	DLPI Stage	Cut point (µm)	% Mobility				Uncertainty in mobility (95% CL)
				Run 1	Run 2	Run 3	Average	
Submicron	Arsenic	3	0.108	103	85	81	80	7
		4	0.17	76	78	92		
		5	0.26	63	74	72		
	Selenium	3	0.108	56	61	83	63	7
		4	0.17	71	64	73		
		5	0.26	46	58	55		
	Antimony	3	0.108	99	109	94	86	8
		4	0.17	83	68	71		
		5	0.26	79	81	92		
Fine fragment	Arsenic	6	0.4	97	91	93	84	6
		7	0.65	83	84	102		
		8	1	77	73	86		
		9	1.6	71	66	88		
	Selenium	6	0.4	83	85	71	81	7
		7	0.65	86	89	95		
		8	1	87	101	84		
		9	1.6	63	66	61		
	Antimony	6	0.4	96	93	116	91	6
		7	0.65	103	84	81		
		8	1	78	90	96		
		9	1.6	82	81	88		
Bulk	Arsenic	10	2.5	29	26	31	21	4
		11	4.4	22	18	16		
		12	6.8	12	17	19		
	Selenium	10	2.5	58	47	49	47	5
		11	4.4	40	53	55		
		12	6.8	36	42	39		
	Antimony	10	2.5	93	90	86	79	6
		11	4.4	81	72	74		
		12	6.8	83	66	69		

Table 11: Percentage solubility of TEs in the three size modes for 1673K PCT samples under neutral (pH = 7) condition

Particle regime	Element	DLPI Stage	Cut point (μm)	% Mobility			Average	Uncertainty in mobility (95% CL)
				Run 1	Run 2	Run 3		
Submicron	Arsenic	3	0.108	71	73	64	64	3
		4	0.17	68	57	59		
		5	0.26	66	63	59		
	Selenium	3	0.108	56	61	63	45	7
		4	0.17	37	40	44		
		5	0.26	31	33	39		
	Antimony	3	0.108	38	49	47	48	5
		4	0.17	51	56	53		
		5	0.26	63	37	39		
Fine fragment	Arsenic	6	0.4	51	57	54	56	5
		7	0.65	66	68	76		
		8	1	54	49	47		
		9	1.6	41	53	56		
	Selenium	6	0.4	94	93	108	76	8
		7	0.65	76	77	81		
		8	1	69	66	77		
		9	1.6	56	58	61		
	Antimony	6	0.4	52	59	61	56	3
		7	0.65	66	49	63		
		8	1	44	51	53		
		9	1.6	53	58	62		
Bulk	Arsenic	10	2.5	13	21	18	12	4
		11	4.4	9	14	16		
		12	6.8	3	11	4		
	Selenium	10	2.5	46	41	39	41	5
		11	4.4	54	36	52		
		12	6.8	36	33	31		
	Antimony	10	2.5	54	51	48	47	4
		11	4.4	53	45	56		
		12	6.8	42	37	39		

Table 12: Percentage solubility of TEs in the three size modes for 1673K PCT samples under basic (pH = 11) condition

Particle regime	Element	DLPI Stage	Cut point (µm)	% Mobility			Average	Uncertainty in mobility (95% CL)
				Run 1	Run 2	Run 3		
Submicron	Arsenic	3	0.108	4	3	1	2	1
		4	0.17	0	0	0		
		5	0.26	2	4	0		
	Selenium	3	0.108	54	51	49	51	3
		4	0.17	53	46	48		
		5	0.26	44	49	62		
	Antimony	3	0.108	13	9	11	12	3
		4	0.17	15	14	17		
		5	0.26	8	19	6		
Fine fragment	Arsenic	6	0.4	9	7	7	3	2
		7	0.65	1	2	4		
		8	1	0	3	4		
		9	1.6	0	0	0		
	Selenium	6	0.4	42	59	57	54	5
		7	0.65	56	61	66		
		8	1	48	63	64		
		9	1.6	49	44	37		
	Antimony	6	0.4	38	31	39	41	3
		7	0.65	33	41	36		
		8	1	44	42	49		
		9	1.6	51	47	43		
Bulk	Arsenic	10	2.5	0	1	1	0	0
		11	4.4	1	1	0		
		12	6.8	0	0	0		
	Selenium	10	2.5	6	5	8	3	2
		11	4.4	1	1	3		
		12	6.8	1	2	0		
	Antimony	10	2.5	0	3	1	1	1
		11	4.4	1	1	0		
		12	6.8	0	0	4		

Table 13: Percentage solubility of TEs in the three size modes for 1623K PCT samples under acidic (pH = 2.88) condition

Particle regime	Element	DLPI Stage	Cut point (µm)	% Mobility				Uncertainty in mobility (95% CL)
				Run 1	Run 2	Run 3	Average	
Submicron	Arsenic	3	0.108	69	81	79	76	4
		4	0.17	74	86	73		
		5	0.26	68	77	75		
	Selenium	3	0.108	43	49	48	47	3
		4	0.17	54	52	47		
		5	0.26	44	46	39		
	Antimony	3	0.108	91	79	74	75	5
		4	0.17	69	73	82		
		5	0.26	66	74	63		
Fine fragment	Arsenic	6	0.4	71	76	77	77	3
		7	0.65	81	73	89		
		8	1	74	79	68		
		9	1.6	81	79	72		
	Selenium	6	0.4	84	76	74	76	3
		7	0.65	77	78	81		
		8	1	69	67	81		
		9	1.6	83	74	72		
	Antimony	6	0.4	69	66	73	77	3
		7	0.65	69	77	78		
		8	1	81	84	85		
		9	1.6	81	83	79		
Bulk	Arsenic	10	2.5	22	26	24	26	3
		11	4.4	19	28	31		
		12	6.8	33	31	24		
	Selenium	10	2.5	41	43	49	47	2
		11	4.4	44	46	51		
		12	6.8	52	51	49		
	Antimony	10	2.5	69	61	68	72	4
		11	4.4	79	77	73		
		12	6.8	71	72	82		

Table 14: Percentage solubility of TEs in the three size modes for 1623K PCT samples under neutral (pH = 7) condition

Particle regime	Element	DLPI Stage	Cut point (µm)	% Mobility				Uncertainty in mobility (95% CL)
				Run 1	Run 2	Run 3	Average	
Submicron	Arsenic	3	0.108	38	44	42	45	4
		4	0.17	51	55	49		
		5	0.26	43	41	39		
	Selenium	3	0.108	42	44	47	51	4
		4	0.17	51	59	56		
		5	0.26	58	53	51		
	Antimony	3	0.108	56	64	62	61	3
		4	0.17	51	63	61		
		5	0.26	59	69	67		
Fine fragment	Arsenic	6	0.4	57	55	51	48	3
		7	0.65	42	44	49		
		8	1	46	48	54		
		9	1.6	41	43	41		
	Selenium	6	0.4	73	71	69	67	3
		7	0.65	64	59	66		
		8	1	62	78	77		
		9	1.6	64	66	59		
	Antimony	6	0.4	33	49	48	47	3
		7	0.65	46	54	52		
		8	1	49	47	47		
		9	1.6	44	46	43		
Bulk	Arsenic	10	2.5	14	11	12	11	1
		11	4.4	10	8	7		
		12	6.8	13	12	9		
	Selenium	10	2.5	29	28	31	33	2
		11	4.4	32	34	36		
		12	6.8	33	37	36		
	Antimony	10	2.5	59	51	53	52	2
		11	4.4	47	49	49		
		12	6.8	54	53	54		

Table 15: Percentage solubility of TEs in the three size modes for 1623K PCT samples under basic (pH = 11) condition

Particle regime	Element	DLPI Stage	Cut point (μm)	% Mobility				Uncertainty in mobility (95% CL)
				Run 1	Run 2	Run 3	Average	
Submicron	Arsenic	3	0.108	2	0	0	2	1
		4	0.17	4	4	5		
		5	0.26	1	1	0		
	Selenium	3	0.108	56	51	51	52	3
		4	0.17	44	44	48		
		5	0.26	59	57	56		
	Antimony	3	0.108	27	22	21	23	3
		4	0.17	21	18	18		
		5	0.26	23	29	28		
Fine fragment	Arsenic	6	0.4	4	2	2	1	1
		7	0.65	1	0	0		
		8	1	1	2	2		
		9	1.6	1	0	0		
	Selenium	6	0.4	61	63	58	53	3
		7	0.65	48	52	54		
		8	1	46	49	49		
		9	1.6	54	53	54		
	Antimony	6	0.4	36	38	41	45	2
		7	0.65	47	47	48		
		8	1	48	53	49		
		9	1.6	46	46	44		
Bulk	Arsenic	10	2.5	1	0	0	0	0
		11	4.4	1	0	0		
		12	6.8	0	0	1		
	Selenium	10	2.5	3	3	1	2	1
		11	4.4	6	2	0		
		12	6.8	1	1	0		
	Antimony	10	2.5	1	1	0	0	0
		11	4.4	1	0	0		
		12	6.8	0	0	0		

REFERENCES

1. EIA Report, Electricity Net Generation: Total (All Sectors), Table 7.2a - https://www.eia.gov/totalenergy/data/monthly/pdf/sec7_5.pdf

2. EIA Report, Coal Production and Number of Mines by State and Coal Rank, 2016, Table 6 - https://www.eia.gov/coal/annual/pdf/table6.pdf

3. Li, Z.M., Sun, F.Z., Ma, L., Wei, W. and Li, F., 2016. Low-pressure economizer increases fly ash collection efficiency in ESP. Applied Thermal Engineering, 93, pp.509-517.

4. Seames, W.S., 2000. The partitioning of trace elements during pulverized coal combustion, Ph.D. dissertation, University of Arizona, Tucson, AZ.

5. Fix, G., Seames, W., Mann, M., Benson, S. and Miller, D., 2013. The effect of combustion temperature on coal ash fine-fragmentation mode formation mechanisms. Fuel, 113, pp.140-147.

6. Zellagui, S., Trouvé, G., Schönnenbeck, C., Zouaoui-Mahzoul, N. and Brilhac, J.F., 2017. Parametric study on the particulate matter emissions during solid fuel combustion in a drop tube furnace. Fuel, 189, pp.358-368.

7. Linak, W.P., Yoo, J.I., Wasson, S.J., Zhu, W., Wendt, J.O., Huggins, F.E., Chen, Y., Shah, N., Huffman, G.P. and Gilmour, M.I., 2007. Ultrafine ash aerosols from coal combustion: Characterization and health effects. Proceedings of the Combustion Institute, 31(2), pp.1929-1937.

8. Wang, C., Seames, W.S., Gadgil, M., Hrdlicka, J. and Fix, G., 2007. Comparison of coal ash particle size distributions from Berner and Dekati low pressure impactors. Aerosol Science and Technology, 41(12), pp.1049-1062.

9. Yan, R., Gauthier, D., Flamant, G. and Badie, J.M., 1999. Thermodynamic study of the behaviour of minor coal elements and their affinities to sulphur during coal combustion. Fuel, 78(15), pp.1817-1829.

10. Schwartz, G.E., Hower, J.C., Phillips, A.L., Rivera, N., Vengosh, A. and Hsu-Kim, H., 2018. Ranking Coal Ash Materials for Their Potential to Leach Arsenic and Selenium: Relative Importance of Ash Chemistry and Site Biogeochemistry. Environmental Engineering Science, 35(7), pp. 728-738

11. Environmental Protection Agency, Mercury and Air Toxics Standards (MATS) Electronic Reporting Requirements., 2017. 40 CFR Part 63, https://www.gpo.gov/fdsys/pkg/FR-2017-04-06/pdf/2017-06884.pdf.

12. Zhu, C., Tian, H., Cheng, K., Liu, K., Wang, K., Hua, S., Gao, J. and Zhou, J., 2016. Potentials of whole process control of heavy metals emissions from coal-fired power plants in China. Journal of Cleaner Production, 114, pp.343-351.

13. Senior, C.L., Huggins, F., Huffman, G.P., Shah, N., Yap, N., Wendt, J.O., Seames, W., Ames, M.R., Sarofim, A.F., Swenson, S. and Lighty, J.S., 2001. Toxic substances from coal combustion- a comprehensive assessment. Physical Sciences Inc. pp. 1-786.

14. Huang, Q., Li, S., Li, G. and Yao, Q., 2017. Mechanisms on the size partitioning of sodium in particulate matter from pulverized coal combustion. Combustion and Flame, 182, pp.313-323.

15. De Santiago, A., Longo, A.F., Ingall, E.D., Diaz, J.M., King, L.E., Lai, B., Weber, R.J., Russell, A.G. and Oakes, M., 2014. Characterization of selenium in ambient aerosols and primary emission sources. Environmental science & technology, 48(16), pp.8988-8994.

16. USEPA. 1998. Particulate matter research needs for human health risk assessment to support future reviews of the national ambient air quality standards for particulate matter. U.S. Environmental Protection Agency, Report No. EPA/600/R97/132F

17. Seames, W.S., Sooroshian, J. and Wendt, J.O., 2002. Assessing the solubility of inorganic compounds from size-segregated coal fly ash aerosol impactor samples. Journal of aerosol science, 33(1), pp.77-90.

18. Seames, W.S., Gadgil, M., Wang, C. and Fetsch, J., 2006, September. Impacts on trace metal leaching from fly ash due to the co-combustion of switch grass with coal. In Proceedings of 23rd Pittsburgh coal Conference paper (pp. 40-4).

19. David W. Evans, James G. Wiener & John H. Horton., 2012. Trace Element Inputs from a Coal Burning Power Plant to Adjacent Terrestrial and Aquatic Environments, Journal of the Air Pollution Control Association, 30(5), pp. 567-573.

20. Yao, Z.T., Ji, X.S., Sarker, P.K., Tang, J.H., Ge, L.Q., Xia, M.S. and Xi, Y.Q., 2015. A comprehensive review on the applications of coal fly ash. Earth-Science Reviews, 141, pp.105-121.

21. Wang, C., Liu, H., Zhang, Y., Zou, C. and Anthony, E.J., 2018. Review of arsenic behavior during coal combustion: Volatilization, transformation, emission and removal technologies. Progress in Energy and Combustion Science, 68, pp.1-28.

22. Hu, G., Liu, G., Wu, D. and Fu, B., 2018. Geochemical behavior of hazardous volatile elements in coals with different geological origin during combustion. Fuel, 233, pp.361-376.

23. Bustaffa, E., Stoccoro, A., Bianchi, F. and Migliore, L., 2014. Genotoxic and epigenetic mechanisms in arsenic carcinogenicity. Archives of toxicology, 88(5), pp.1043-1067..

24. Agency for Toxic Substances and Disease Registry (ATSDR). 2003. Toxicological profile for Selenium. Atlanta, GA: U.S. Department of Health and Human Services, Public Health Service.

25. Sun, H.J., Rathinasabapathi, B., Wu, B., Luo, J., Pu, L.P. and Ma, L.Q., 2014. Arsenic and selenium toxicity and their interactive effects in humans. Environment international, 69, pp.148-158.

26. De Miguel, E., Izquierdo, M., Gómez, A., Mingot, J. and Barrio‑Parra, F., 2017. Risk assessment from exposure to arsenic, antimony, and selenium in urban gardens (Madrid, Spain). Environmental toxicology and chemistry, 36(2), pp.544-550.

27. Zhao, X., Xing, F., Cong, Y., Zhuang, Y., Han, M., Wu, Z., Yu, S., Wei, H., Wang, X. and Chen, G., 2017. Antimony trichloride induces a loss of cell viability via reactive oxygen species-dependent autophagy in A549 cells. The international journal of biochemistry & cell biology, 93, pp.32-40.

28. Shah, P., Strezov, V., Stevanov, C. and Nelson, P.F., 2007. Speciation of arsenic and selenium in coal combustion products. Energy & Fuels, 21(2), pp.506-512.

29. Deonarine, A., Kolker, A., Foster, A.L., Doughten, M.W., Holland, J.T. and Bailoo, J.D., 2016. Arsenic speciation in bituminous coal fly ash and transformations in response to redox conditions. Environmental science & technology, 50(11), pp.6099-6106.

30. Wang, T., Wang, J., Tang, Y., Shi, H. and Ladwig, K., 2009. Leaching characteristics of arsenic and selenium from coal fly ash: role of calcium. Energy & Fuels, 23(6), pp.2959-2966.

31. Schwartz, G.E., Rivera, N., Lee, S.W., Harrington, J.M., Hower, J.C., Levine, K.E., Vengosh, A. and Hsu-Kim, H., 2016. Leaching potential and redox transformations of arsenic and selenium in sediment microcosms with fly ash. Applied Geochemistry, 67, pp.177-185.

32. Hu, H., Liu, H., Chen, J., Li, A., Yao, H., Low, F. and Zhang, L., 2015. Speciation transformation of arsenic during municipal solid waste incineration. Proceedings of the Combustion Institute, 35(3), pp.2883-2890.

33. Sun, W., Renew, J.E., Zhang, W., Tang, Y. and Huang, C.H., 2017. Sorption of Se (IV) and Se (VI) to coal fly ash/cement composite: Effect of Ca 2+ and high ionic strength. Chemical Geology, 464, pp.76-83.

34. Huggins, F.E., Senior, C.L., Chu, P., Ladwig, K. and Huffman, G.P., 2007. Selenium and arsenic speciation in fly ash from full-scale coal-burning utility plants. Environmental science & technology, 41(9), pp.3284-3289.

35. Liu, Y.T., Chen, T.Y., Mackebee, W.G., Ruhl, L., Vengosh, A. and Hsu-Kim, H., 2013. Selenium speciation in coal ash spilled at the Tennessee Valley Authority Kingston site. Environmental science & technology, 47(24), pp.14001-14009.

36. Roy, B., Choo, W.L. and Bhattacharya, S., 2013. Prediction of distribution of trace elements under oxy-fuel combustion condition using Victorian brown coals. Fuel, 114, pp.135-142.

37. Tian, H., Zhou, J., Zhu, C., Zhao, D., Gao, J., Hao, J., He, M., Liu, K., Wang, K. and Hua, S., 2014. A comprehensive global inventory of atmospheric antimony emissions from anthropogenic activities, 1995–2010. Environmental science & technology, 48(17), pp.10235-10241.

38. Matusiewicz, H. and Krawczyk, M., 2008. Determination of total antimony and inorganic antimony species by hydride generation in situ trapping flame atomic absorption spectrometry: a new way to (ultra) trace speciation analysis. Journal of Analytical Atomic Spectrometry, 23(1), pp.43-53.

39. Varrica, D., Bardelli, F., Dongarra, G. and Tamburo, E., 2013. Speciation of Sb in airborne particulate matter, vehicle brake linings, and brake pad wear residues. Atmospheric environment, 64, pp.18-24.

40. Peng, Y., Li, J., Si, W., Luo, J., Wang, Y., Fu, J., Li, X., Crittenden, J. and Hao, J., 2015. Deactivation and regeneration of a commercial SCR catalyst: Comparison with alkali metals and arsenic. Applied Catalysis B: Environmental, 168, pp.195-202.

41. Niu, Y., Wang, S., Shaddix, C.R. and Hui, S.E., 2016. Kinetic modeling of the formation and growth of inorganic nano-particles during pulverized coal char combustion in O 2/N 2 and O 2/CO 2 atmospheres. Combustion and Flame, 173, pp.195-207.

42. Quann, R. J., Neville, M., Janghorbani, M., Mims, C. A., Sarofim, A. F., 1982. Mineral Matter and Trace Element Vaporization in a Laboratory-Pulverized Coal Combustion System. Environ.Sci.Technol 16, pp. 776-781

43. Raeva, A.A., Pierce, D.T., Seames, W.S. and Kozliak, E.I., 2011. A method for measuring the kinetics of organically associated inorganic contaminant vaporization during coal combustion. Fuel processing technology, 92(7), pp.1333-1339.

44. Raeva, A.A., Klykov, O.V., Kozliak, E.I., Pierce, D.T. and Seames, W.S., 2011. In situ evaluation of inorganic matrix effects on the partitioning of three trace elements (As, Sb, Se) at the outset of coal combustion. Energy & Fuels, 25(10), pp.4290-4298.

45. James, D.W., Krishnamoorthy, G., Benson, S.A. and Seames, W.S., 2014. Modeling trace element partitioning during coal combustion. Fuel Processing Technology, 126, pp.284-297.

46. Linak, W.P., Miller, C.A., Seames, W.S., Wendt, J.O., Ishinomori, T., Endo, Y. and Miyamae, S., 2002. On trimodal particle size distributions in fly ash from pulverized-coal combustion. Proceedings of the Combustion Institute, 29(1), pp.441-447.

47. Yu, D., Xu, M., Yao, H., Liu, X., Zhou, K., Li, L. and Wen, C., 2009. Mechanisms of the central mode particle formation during pulverized coal combustion. Proceedings of the Combustion Institute, 32(2), pp.2075-2082.

48. Seames, W.S., 2003. An initial study of the fine fragmentation fly ash particle mode generated during pulverized coal combustion. Fuel Processing Technology, 81(2), pp.109-125.

49. Smith, R.D., Campbell, J.A. and Nielson, K.K., 1979. Characterization and formation of submicron particles in coal-fired plants. Atmospheric Environment (1967), 13(5), pp.607-617.

50. Baxter, L.L., 1992. Char fragmentation and fly ash formation during pulverized-coal combustion. Combustion and Flame, 90(2), pp.174-184.

51. Yu, D., Xu, M., Yao, H., Liu, X. and Zhou, K., 2008. A new method for identifying the modes of particulate matter from pulverized coal combustion. Powder Technology, 183(1), pp.105-114.

52. Taylor, D.D. and Flagan, R.C., 1981. The influence of combustor operation on fine particles from coal combustion. Aerosol Science and Technology, 1(1), pp.103-117.

53. Zeng, T., Sarofim, A. F., Senior, C. L., 2001. Vaporization of arsenic, selenium and antimony during coal combustion. Combustion and Flame 126, pp. 1714-1724.

54. Liu, J., Dai, S., He, X., Hower, J.C. and Sakulpitakphon, T., 2017. Size-dependent variations in fly ash trace element chemistry: examples from a Kentucky power plant and with emphasis on rare earth elements. Energy & Fuels, 31(1), pp.438-447.

55. Wortmann, C.S., Mamo, M. and Shapiro, C.A., 2003. Management strategies to reduce the rate of soil acidification. Cooperative Extension, Institute of Agriculture and Natural Resources, University of Nebraska-Lincoln.

56. Jones, C., Hahn, J., Magee, B., Yuen, N., Sandefur, K., Tom, J. and Yap, C., 1999. Utilization of ash from municipal solid waste combustion (No. NREL/SR-570-26068). National Renewable Energy Lab., Golden, CO (US).

57. Izquierdo, M. and Querol, X., 2012. Leaching behaviour of elements from coal combustion fly ash: an overview. International Journal of Coal Geology, 94, pp.54-66.

58. Kosson, D.S., Garrabrants, A.C., DeLapp, R. and van der Sloot, H.A., 2014. pH-dependent leaching of constituents of potential concern from concrete materials containing coal combustion fly ash. Chemosphere, 103, pp.140-147.

59. McElroy, M.W., Carr, R.C., Ensor, D.S. and Markowski, G.R., 1982. Size distribution of fine particles from coal combustion. Science, 215(4528), pp.13-19.

60. Gadgil, M.R.,2006. Leachability of Trace Elements from Biomass Fly Ash Samples, M.S Thesis, University of North Dakota, Grand Forks, ND.

61. EPA Method 3052, Microwave Assisted Acid Digestion Of Siliceous And Organically Based Matrices., https://www.epa.gov/sites/production/files/2015-12/documents/3052.pdf

62. Kang, S.G., 1991. Fundamental studies of mineral matter transformation during pulverized coal combustion: Residual ash formation, PhD dissertation, Massachusetts Institute of Technology.

63. Joutsensaari, J., Kauppinen, E.I., Ahonen, P., Lind, T.M., Ylätalo, S.I., Jokiniemi, J.K., Hautanen, J. and Kilpeläinen, M., 1992. Aerosol formation in real scale pulverized coal combustion. Journal of Aerosol Science, 23, pp.241-244.

64. Senior, C.L., Bool III, L.E., Srinivasachar, S., Pease, B.R. and Porle, K., 2000. Pilot scale study of trace element vaporization and condensation during combustion of a pulverized sub-bituminous coal. Fuel Processing Technology, 63(2-3), pp.149-165.

65. Benson, S.A. and Holm, P.L., 1985. Comparison of inorganics in three low-rank coals. Industrial & engineering chemistry product research and development, 24(1), pp.145-149.

66. Bool, L.E.I. and Helble, J.J., 1995. A laboratory study of the partitioning of trace elements during pulverized coal combustion. Energy & Fuels, 9(5), pp.880-887.

67. Meij, R and Winkel, H., 2007. The emissions of heavy metals and persistent organic pollutants from modern coal-fired power stations, Atmospheric Environment 41(40), pp. 9262-9272.

68. Dean, J. A. 1992. Langes Handbook of Chemistry. (14th ed.). New York: McGraw-Hill.

69. Jones, D.R., 1995. The leaching of major and trace elements from coal ash. In Environmental aspects of trace elements in coal (pp. 221-262). Springer, Dordrecht.

70. Cornelis, G., Johnson, C.A., Gerven, T.V., Vandecasteele, C., 2008. Leaching Mechanisms of Oxyanionic Metalloid and Metal Species in Alkaline Solid Wastes: A review. Applied Geochemistry 235), pp. 955-976.

71. Kim, A.G. and Kazonich, G., 2004. The silicate/non-silicate distribution of metals in fly ash and its effect on solubility. Fuel, 83(17-18), pp.2285-2292.

72. Norman, N.C. ed., 1997. Chemistry of arsenic, antimony and bismuth. Springer Science & Business Media.

CHAPTER 4

MOBILITY OF SEMI-VOLATILE TRACE ELEMENTS IN SIZE SEGREGATED FLY ASH PARTICLES GENERATED FROM PULVERIZED COAL COMBUSTION – COMPARISON OF LEACHING RESULTS FOR BITUMINOUS AND SUB BITUMINOUS COAL SAMPLES.

Prasanna Seshadri, Dennis Sisk, Frank Bowman, Steve Benson and Wayne Seames*

Department of Chemical Engineering, University of North Dakota, Grand Forks, ND

ABSTRACT

Size segregated fly ash samples were collected from the combustion of two coals – a bituminous Illinois # 6 and a subbituminous Powder River Basin (PRB) - in a lab scale combustor. Particle Size Distribution (PSD) data for both coal fly ashes indicates a trimodal distribution comprised of submicron, fine fragment and coarse modes. However, depending on the type of coal ash, TE concentration peaks (for any given size mode) were observed at different particle sizes, indicating the possibility of differences in TE partitioning mechanisms for the two fuels. A sequential leaching process conducted on the two raw coals revealed that a majority of the TEs had mineral association in the Illinois # 6 coal, whereas, significant organic association was found in the PRB coal.

Leaching studies for TEs from fly ash particles show there could be potential health and environmental risks associated with all three trace elements and the degree of leaching was influenced by both particle size and the pH of the environment. In general, TEs associated with particles in the smaller submicron and fine fragment were found to be more soluble than TEs associated with the coarse particle fraction. Solubility data with respect to the type of coal ash showed no consistent trend for TE leaching. The presence of other major ash forming species (notably SiO_2 and CaO) influencing TE (As) partitioning and subsequent solubility has been postulated for the PRB ash. In most cases, particle size and leaching fluid pH appear to affect TE leaching more than coal rank.

Introduction and Objective

The electric power sector accounts for most of the coal consumed in the US [1] and this trend is expected to continue over the next few years [2]. One of the biggest concerns from coal fired plants is the continued stack emission of particulate matter escaping Particulate Capture Devices (PCDs) such as electrostatic precipitators (ESPs) and baghouses (BHs) and entering the atmosphere. Even though the amount of Particulate Matter (PM) leaving the stack is only a small amount compared to what is emitted from the combustion source, they still present a major risk to human health and the environment [3,4,5,6,7]. Fine particulate matter, especially those regulated as $PM_{2.5}$ (PM having aerodynamic diameter less than 2.5 μm), may be a cause of increased health risks due to inhalation into human and animal respiratory systems [6,8-11]. Depending on the collection efficiency of the PCD in use, $PM_{2.5}$ makes up around 68% of the total ash released from a power plant [8]. Knowledge of fly ash size distribution is therefore important to understand ash formation mechanisms and their overall impact downstream of the boiler.

Researchers, over the years, have proposed a multimodal distribution to describe fly ash PSD from pulverized coal (PC) combustion. Some [13-15] reported a bi-modal particle size distribution, comprising of a smaller submicron (or ultrafine) mode and a larger coarse mode, for both lab-scale and field data. Later results [12,16-19] shows that fly ash from PC combustion will yield a tri-modal

distribution, including a central fine fragment mode. The formation mechanisms for each mode is governed by multiple factors and is described in detail elsewhere [12,14,16,17,20-23]. Of importance to this study is the composition of $PM_{2.5}$ which includes both ultrafine and fine fragment modes. Some of these particles are enriched with toxic trace elements (TEs) [12, 23-26] and even though the concentrations of TEs in coal are very low, large coal consumption can result in significant emissions. Trace elements in combustion flue gas can also affect the performance of air pollution control devices such as the Selective Catalytic Reducers (SCR) [27,28]. Understanding the fate of TEs is important to assess their risk away from the boiler and develop suitable mitigation strategies.

The three TEs of interest for this study, As, Se and Sb, are known environmental toxins [12,23,29,30]. Once emitted into the atmosphere they pose health hazard for humans through inhalation and subsequent deposition in the lungs or they may deposit on the earth's surface resulting in increased levels of TEs in soil, vegetation and water [31-33]. The fate and impact of TEs in fly ash depends on fly ash particle size, chemical properties of the fly ash, and the environment they come in contact with [4,31,34]. Characterizing fly ash mass loading and elemental composition as a function of particle size provides information that can be used to help evaluate potential risks from trace and other minor elements. Determining the mobility of TEs from size segregated fly ash particles under different pH conditions provides additional insight into how these elements may be released into the environment. Submicron particles, in general, are classified as a potential health risk as they can be inhaled easily and penetrate lungs. Submicron particle health risks specific to trace elements will depend on their solubility within lung fluids, which generally have neutral pH. Hence a leaching study for sub-micron associated TEs at neutral conditions (pH = 7) can address potential risk to human health. Particles in the fine fragment size range tend to settle onto ground downwind of the stack and, depending on contact with moisture and soil pH, soluble TEs can become mobile from ash and penetrate into the soil. Here they can get absorbed into vegetation through plant roots or percolate even further down into the water table [12,31-33]. Soil pH varies based on geographic location. For example, soil in the eastern US is usually acidic and in the western US is more basic [12,31,35]. Leaching studies carried out under both these conditions can help address the impact of TEs in fine fragment particles on vegetation and groundwater. Coarse particles are usually disposed in landfills or used as asphalt filler material, sheetrock etc [12,31,36-38]. Rainwater, which is normally acidic, can dissolve soluble TEs from landfill ash piles and then percolate downwards into the water table thereby increasing dissolved contaminant levels. Because the water acidity can change depending on the pH of the ash through which it is travelling, leaching studies under a range of pH conditions are needed to assess the potential for TE release. However, TE mobility is likely not an issue for byproducts using ash unless exposed to extreme pH conditions.

Leaching studies can also help predict chemical speciation based on the degree of element solubility in a particular pH medium. TEs in coal can exhibit various oxidation states depending on their mode of occurrence and coal rank [12,39-48]. Depending on coal rank, TEs in coal may be organically associated with the carbonaceous material [12,20-23] or can be associated with the mineral portion of the fuel such as with silicates or pyrite molecules [12,20-23,49,50]. Under flame conditions, all three TEs can vaporize to varying extents [12,23,51,52]. Then as the flue gas cools the vaporized form can react with the reactive cation sites present on the surface of fly ash particles thereby transforming into the solid phase [12,23,51-54]. It is particularly important to know the speciation of TEs in fly ash as toxicity depends on their final oxidation state, which in turn depends on their partitioning mechanisms.

The two most common fly ash oxidation states of As and Sb are +3 and + 5 with the +3 form more toxic than the +5 state for both elements [41,47,48,55]. Fly ash Se normally exhibits the +4 and +6 states [43,44,45] with the +4 state being more toxic than the +6 state [41,56]. Direct measurements, such as X-ray absorption near edge structure (XANES), can determine oxidation states more directly, but are cost–prohibitive, an important consideration given the large number of samples required for size fractionated analysis. While the leaching studies do provide some indirect evidence of speciation, the primary focus of this work is TE mobility in size segregated fly ashes under various leaching environments.

Even though there has been significant interest in fly ash TE leaching studies, fundamental research in this area has been sporadic especially in the case of size segregated ash particles. Most efforts have focused on determining element mobility from bulk ash samples collected from PCD hoppers [37,38,41,42] and does not account for the effect of size fraction on the final analysis. Seames et al. previously carried out TE solubility studies on size segregated fly ashes from the combustion of five different coals burnt at the University of Arizona down fired combustor [12,23,34]. They used a Berner Low Pressure Impactor (BLPI) for particulate sampling and used a slightly modified version of the TCLP Method 1310 for solubility studies to accommodate particles captured on greased membranes. Their solubility studies were carried out at two pH conditions – 2.8 and 5.0. Later, Seames et al. [31] carried out similar studies at the University of North Dakota furnace (UND) for the combustion of Blacksville bituminous coal and co-combustion of coal and biomass. They used a Dekati Low Pressure Impactor (DLPI) to sample fly ash particles and determined TE solubility using a leaching protocol involving three pH conditions. For the study presented in this paper, fly ash TE solubility was determined and compared for the combustion of a bituminous coal (Illinois # 6) and western sub-bituminous coal (PRB). The two coals used for this study are of different ranks and hence have different properties including ash chemistry. Since the bituminous ash is acidic in nature and the PRB coal ash is basic in nature, solubility studies of TEs from these two fly ashes can address some of the above-mentioned concerns. Size segregated fly ash samples were collected from the downfired UND combustor using a DLPI. Combustion of these two coals occurred under conditions that achieved almost the same peak combustion temperature. Since combustion temperature has a significant effect on TE evolution from fuel, using the same temperature for both fuels allows coal rank effects to be evaluated more clearly. Typically, higher rank coals, such as the bituminous, will tend to produce a hotter flame compared to PRB coals for the same burner stoichiometric ratios. A combination of oxygen addition to the burner and increasing air pre-heat temperature was utilized to achieve the same combustion temperature for the PRB coal test. However, the amount of excess O_2 was maintained constant under both conditions at about 3%.

Combustion temperature recorded during these tests was higher than the temperature reported in the previous two studies [4,12,31], coming close to commercial operating conditions. This is important because combustion temperature affects the rate of refractory element (i.e. Ca and Fe) volatilization in a burning coal particle which changes the availability of active cationic surface sites for participation in subsequent downstream partitioning reactions with gas phase TE oxy-anions. Element volatility, its distribution in fly ash, and final speciation are all affected by combustion conditions, including peak temperature. Additionally, compared to the previous study carried out at the UND furnace, every single impactor stage was analyzed to obtain a more complete understanding of TE partitioning and solubility. Furthermore, while both BLPI and DLPI are cascade impactors, the DLPI has more overall stages

compared to the BLPI (13 vs 11), including more submicron particle size stages (8 vs 7) [5]. Since TE enrichment is usually higher in the smaller submicron and fine particles [6,12,20,23,57] studying all impactor stages can provide additional details on fly ash element partitioning and subsequent mobility.

EXPERIMENTAL METHODS

Fuel Analysis

Fundamental fuel properties including volatile matter, percent major elements, moisture content, percent ash, etc. were determined using ASTM methods D3172, and D3176 respectively. The composition of inorganic elements in fuel ashes were analyzed using ASTM method D3174. In addition to the above methods, a Computer Controlled Scanning Electron Microscopy (CCSEM) analysis was also carried out to determine coal mineralogy in the different fuel fractions. While the ASTM ash analysis of the coal measures total concentration (including organically bound minerals), the CCSEM analysis does not measure any organically bound species. However, chemical fractionation, a well-established analytical approach can be used to determine elements associated with the organic portion of the fuel.

Sequential leaching and acid digestion process

The mode of occurrence of elements of interest (As, Se, Sb, Ca and Fe) in coal was determined using a chemical fractionation method which involves a sequential leaching process. The leaching procedure is devised to sequentially attack specific minerals or groups of minerals, thereby providing information on the fraction of an element residing in that portion of the coal sample [58]. Data from chemical fractionation can be used to assess TE behavior under combustion conditions including the expected degree of vaporization and subsequent partitioning mechanisms. This in turn will affect TE chemical speciation and their subsequent mobility from fly ash surfaces.

The two coals used in this study were subjected to a leaching analysis to determine the forms of the selected elements in the coals. A sequential procedure developed by Finkelman et al. [23,59] was used in this process. Each step followed a similar procedure, using 50 mL of a given solvent, 18 hours of agitation, followed by filtration and one hour of drying at 100°C. First, a 10g sample of coal was placed in 50 mL of 1 N ammonium acetate solution. The solution was agitated for 18 h, and the extract was recovered by filtration using a Whatman ashless filter paper (pore size of 2.5 µm). The residue collected on the filter paper was then partially dried at 100 °C for an hour. Second, a 1:3 hydrochloric acid solution was added to the residue and the extract was agitated for 18 hours, and then filtered and partially dried. Third, this residue was extracted using a 48% solution of hydrofluoric acid, 18 hours of agitation and filtration to separate the extract from the residue. The filter residue was then rinsed with distilled water and dried. In the fourth and final step, the remaining filter residue was extracted with a 10% nitric acid solution under agitation for 18 hours, followed by filtration, rinsing with distilled water, and drying. The filtered extract collected from each extraction step was then used to determine the concentrations of soluble trace elements.

Elements that were acetate soluble are mostly present as ion-exchangeable cations in the original fuel. Hydrochloric acid (HCl) solubility indicates fraction from carbonate and mono sulfides (oxidized pyrite grains) [23,58,59], while nitric acid (HNO_3) soluble fraction indicates disulfide (pyrite) association for TEs. Hydrofluoric acid (HF) solubility indicates association with silicates or clays such as illite etc, and

this mostly represents the non-vaporizing fraction of TEs preset in the coal. Elements not leached by any of the above reagents (present in the final residue) may be organically associated or present as shielded mineral grains completely encased by the organic matrix.

Additionally, a microwave assisted acid digestion process following EPA SW – 846 Test Method 3052 [60] was used to determine the total concentration of trace and minor elements in the fuel. Element mode of occurrence in fuel was later determined as the ratio of concentration leached in a given solution to the total concentration as determined by the acid digestion method.

Furnace description and fly ash sampling

Fly ash samples were collected from a 19kW vertical downflow laboratory combustor which is 6 m tall with a 0.15 m ID. The combustor consists of a burner cap, a 1.8 m burn chamber with 4 sample ports, a 4.2 m post combustion zone with 7 additional sample ports and an ash trap located directly below the bottom of the post combustion zone. The schematic for the combustor is shown in Figure 12. The burner cap contains a top port for a water-cooled fuel probe and a side port through which hot secondary air is introduced. A honeycomb flow straightener (0.08 m long and 0.16 m diameter) helps streamline the flow of secondary air as it enters the combustor. It is made from alumina and can withstand temperatures as high as 1700 ˚C. The top half of the flow straightener is encased in the furnace cap and is located just below where secondary air is introduced to the furnace. The other half of the flow straightener sits inside the combustion chamber. The flow straightener has a 0.03 m opening in the center through which a water-cooled fuel injector is inserted into the furnace. Hot secondary air and fuel do not mix until they are both delivered inside the furnace. The fuel injector (0.72 m long) has an inner 0.015 m diameter tube surrounded by an outer 0.03 m diameter tube that is water cooled to keep the probe from overheating. Fuel is injected from the top into the inner tube and room temperature primary air is introduced to the side of the inner tube just below fuel injection. Primary air is used as transport air and is usually between 20 – 30 % of the total air required for the combustion process, depending on fuel grade. Air to the system is delivered by a compressor operating at 1100 - 1200 kPa. Rotameters (Dwyer Inc) control the rate of air/gas flow into the system. The furnace was always operated under negative pressure using a compressed air driven eductor in the flue gas ductwork.

Prior to introducing solid fuel, the furnace was preheated using external heating elements which are zonally installed along the combustion chamber. Each zone is heated by 4 heating elements arranged in series and a Watlow controller is used to control the heating rate for each zone. The elements are used to preheat the furnace to approximately 1473 K. Once the elements reach the desired set point solid fuel is fed into the furnace using an Acrison Series 105 volumetric screw feeder with feed rate adjusted using a variable voltage controller. After the furnace reaches steady state operating conditions, a refractory protected portable "R" typethermocouple probe was used to measure the gas centerline temperature.

A total of 10 specially installed sample ports along the length of the furnace allow temperature measurements and sample collection at different zones of the furnace. For this study ash samples were extracted at port 10, located near the end of the combustor but sufficiently far upstream from the un-insulated ash trap. A Dekati Low Pressure Impactor (DLPI) and a pre-separator cyclone were used to collect ash samples. The DLPI contains sonic orifices which limit the flow through the impactor and is factory calibrated at 29.01 L/min with the proper pressure of 10±0.5 kPa applied at the outlet. It has

two co-linear plates one of which has a smaller nozzle in it. The plate with the nozzle is the jet plate and the other plate is the collection plate. The sample passes through this nozzle at a high speed and makes a sharp turn with the flow in between the plates. Particles with sufficient inertia cannot remain in the flow and impact on the second plate while the smaller particles remain in the flow. An important parameter is the cut-point (aerodynamic) diameter of the impactor. It is defined as the size of the particles collected with 50 % efficiency on a given impactor stage. The DLPI can segregate ash in 13 different size fractions between 0.03 and 10 microns.

The sampling media was made up of greased polycarbonate membranes (Isopore 25 mm membrane filters, pore size 0.4 μm) which were handled using surgical gloves and tweezers to avoid contamination and weight deviations. High purity apiezon "L" type grease was dissolved in toluene in a ratio of 4 mg of grease to 20 ml of toluene. The membranes were sprayed with this solution using a Badger Type air brush with compressed air ensuring that a thin layer of the solution was applied on the surface of the membrane. Coating with grease helps to reduce particle bounce off during sampling. Before sampling, the greased foils were baked in an oven for more than 24 h at 80° C, in order to increase substrate weight stability during sampling by vaporizing residual toluene. Dried membranes were then weighed on a microbalance having a minimum measurement of 0.01 mg. Each membrane was weighed in a temperature and humidity-controlled environment at least four times and if any readings deviated from others by a value by ± 0.05 mg or more, they were reweighed. These membranes were then placed on each of the impactor stages for flue gas sample collection. Mass of ash collected combined with the flue gas sampling flow rate was then used to calculate ash loading rates for fly ash PSD. An impinger train was used downstream of the DLPI to collect gas phase samples. EPA recommended Method 29 was employed to capture vapor phase metals from the flue gas. A detailed description of the experimental facility and step by step instructions for membrane preparation, samples storage etc are shown here [5,31,61].
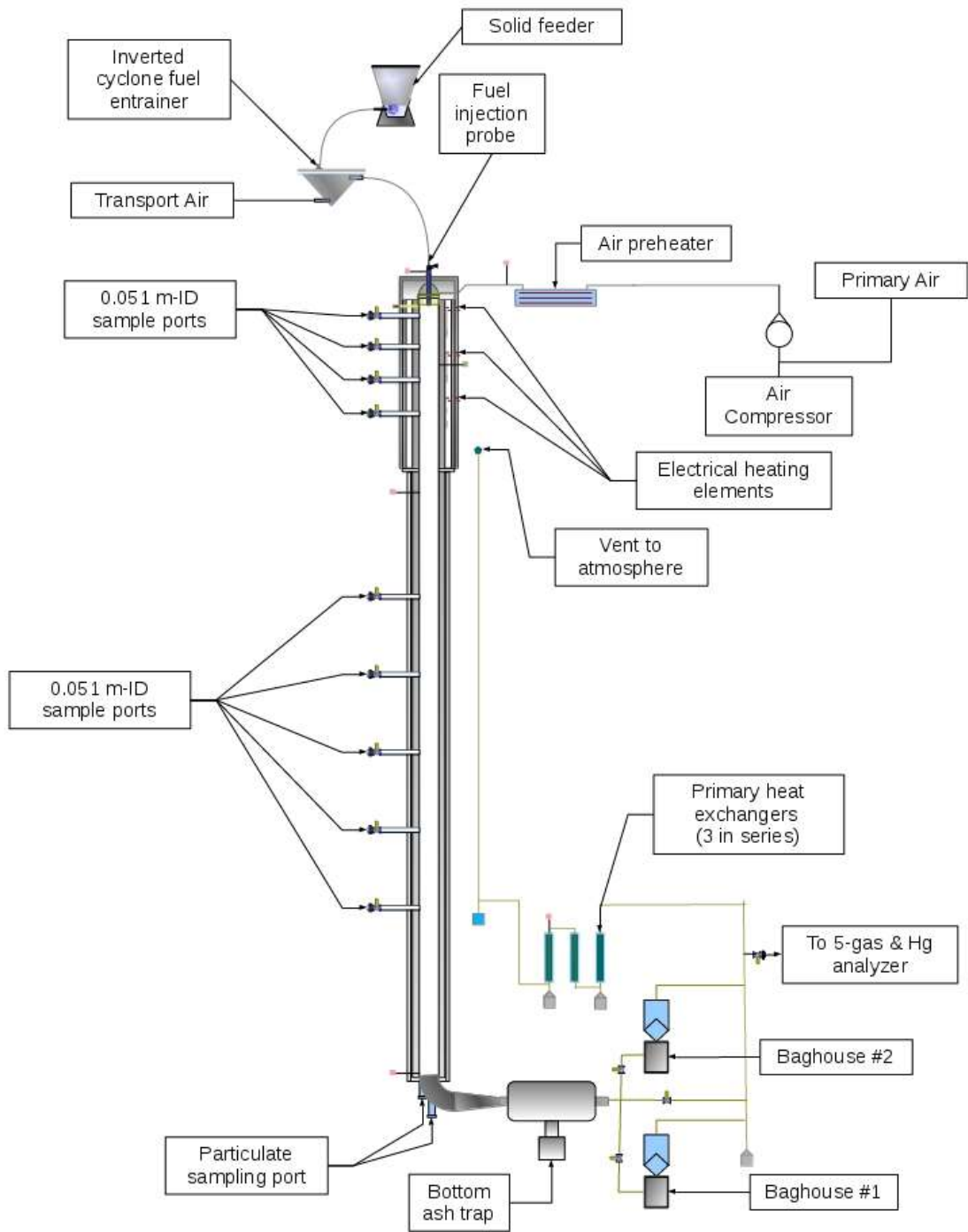
Figure 12: The University of North Dakota Chemical Engineering Department Vertical Downflow Combustion Research System

As the ash laden sample gas was drawn through the sample probe, quench nitrogen was immediately introduced at the probe entrance to dilute and cool the sample gas stream. The nitrogen quenches the reactions in the sample by diluting the sample with an inert gas and aids in rapidly cooling the sample along with the water-cooled sample probe. Otherwise the reactants will continue to react along the length of the probe and misleading results will be obtained. The sample then flows through a pre-separator cyclone (not used in all experiments as described below), the DLPI, the impinger train, a vacuum pump, a gas meter, and is then expelled into a fume hood.

Near isokinetic conditions were maintained during the entire sampling time. The goal was to extract an undisturbed laminar streamline from the furnace centerline. Sample flow rate was calculated using the centerline velocity of the flue gas, the temperature at the sample port, and the cross-sectional area of the probe inlet. The sampling rate was checked by monitoring the dilution rate of NO_x (or CO) in the sample by sending a portion of the sample exhaust to the analyzer system and comparing its concentration to the expected isokinetic diluted concentration. The expected isokinetic dilution rate is calculated by scaling the furnace NO_x or CO concentration, measured at the sample port, to include the known amount of dilution nitrogen added in the sample probe. If the dilution NO_x or CO reading is higher or lower than the desired value the sampling rate is incorrect and the nitrogen flow rate is adjusted. To verify the isokinetic sample flow rate, the DLPI was loaded with 13 blanks membranes and was run long enough to verify the right dilution N_2 rate. A sampling spreadsheet used to calculate isokinetic sampling rate is shown in Appendix D.

For the bituminous coal, fly ash samples were collected with and without the pre- separator cyclone and the combined data from both runs were used to generate a full particle size distribution (PSD) curve. When the pre-separator cyclone is used, it removes a majority of larger particles (>1 μm) from the sample gas stream. This allows a sufficient quantity of small particles to be collected in the lower DLPI (stages 1-10) and minimizes any bounce-off of larger particles which skews the data. Sampling without the pre-separator cyclone allows larger super micron particles to be collected in the top stages (11-13) of the DLPI. To assemble the entire PSD, the data from both configurations were combined and normalized. This procedure is explained in detail here [5]. This method is extremely important for the Illinois No. 6 samples as this coal does not have a high fraction of submicron particles [5,12,52] compared to the lower rank PRB coal. Steady state conditions were attained before samples were collected and sample times were maintained the same for each run with a given fuel. When using the particulate cyclone, sampling time was 15 minutes for the PRB coal and 10 minutes for the higher ash Illinois # 6 coal. At least four fly ash sample sets are required for this study – one set for analyzing total concentration of minor and trace elements of interest, and three other sets for leaching studies under three different pH conditions. A total of five sample sets were collected for each test condition and the fifth set of samples was used in case of contingency.

Sample preparation and analysis

Collected ash samples were carefully removed from the impactor and the individual membranes from each stage were weighed on a scale with 1 μg precision located in a temperature and humidity-controlled environment. The difference in the weight of membranes before and after sampling represents the amount of ash collected for each stage and these data were used to generate a PSD curve for each run. An average PSD curve for each coal was then generated from the separate runs.

The four sample sets that most closely duplicated the average PSD were selected for elemental and leaching analysis.

In order to determine total concentration of metals of interest, ash loaded membranes from each impactor stage were subjected to an acid digestion method developed by Wendt and co-workers at the University of Arizona. The complete protocol for sample preparation using this method is discussed here [12,23]. For pH dependent leaching studies, ash samples were extracted with either acidic (pH = 2.88), neutral (pH = 7), or basic (pH = 11) leaching solutions. A modified TCLP procedure was used to determine fly ash trace element mobility in the size segregated fractions. The EPA recommended TCLP Improved Method 1311 requires the use of about 100 g of fly ash [62] and a liquid to solid (L/S) ratio of 20 [34,62]. Submicron and fine particles account for only a small percentage in the total ash and collecting 100 g would require extremely long sampling times, especially in a lab scale system that burns fuel at a rate less than 2.3 kg/hr. Additionally, the TCLP Method 1311 requires loose ash samples [62] to carry out leaching studies. Fly ash particles for this study were collected using greased membranes in an impactor. Hence the modified procedure serves as a better protocol for ash in a desired size fraction, in particular the smaller sized particles. Sample pH was continuously monitored and appropriate buffers were added to maintain a constant pH value. Detailed step by step instructions for both acid digestion and leaching studies sample preparation are shown here [31].

Total digestion and leaching solution samples were analyzed using a Graphite Furnace Atomic Absorption Spectrometer (GFAAS) with Zeeman background correction (ICE 3000 Series, Thermo Electron, United Kingdom) capable of measuring concentration levels as low as 1 ppb for As and 2 ppb for Se and Sb. The minor elements in ash, including Ca and Fe, were analyzed using a Thermo Scientifics SOLAAR M6 Flame Atomic Absorption Spectrometer (FAAS) capable of measuring concentrations as low as 1 ppm. Concentration measurements are usually determined from a working curve after calibrating the instrument with standards of known concentration. The concentration of both trace and minor elements present on a greased membrane blank were analyzed in the acid mix as well as the leaching solvents. These background concentrations were then subtracted from the final element concentration data only if they were found to be greater than the minimum detection level for a given element. Elemental concentration below the recommended detection level and negative values were assumed to be zero.

RESULTS

Fuel Analysis

Table 16 shows the proximate, ultimate, ash composition and total TE concentration for the two test coals. As can be seen from this table, the Illinois No. 6 has a slightly higher ash yield whereas the PRB coal had a much higher moisture content. Another parameter that is much different between the coals is the high calcium and low iron content for the PRB coal, whereas it is the opposite for the Illinois # 6 coal. Both elements play a critical role in the retention of TEs in fly ash. Silica and alumina content were nearly the same for both coals and both are expected to be predominantly present as minerals.

Table 16: Proximate, ultimate, ash composition and TE analysis of coal samples (as received basis)

Proximate (as received)	PRB	Illinois # 6
Total Moisture	22.5	7.5
Ash	7.1	10.2
Volatile Matter	29.6	33.6
Fixed Carbon	40.8	48.7
Heating Value (BTU/lb)	9571	11332

Ultimate (as received)	PRB	Illinois # 6
Carbon	54.5	65
Hydrogen	6.3	5.3
Oxygen	30.8	15.3
Nitrogen	0.8	1.1
Sulfur	0.5	3.1

Oxide	PRB	Illinois # 6
SiO_2	47.07	52.74
Al_2O_3	21.69	18.73
TiO_2	0.93	0.96
Fe_2O_3	3.26	19.19
CaO	15.85	3.15
MgO	5.67	0.86
K_2O	1.05	2.65
Na_2O	1.31	0.32
P_2O_5	0.72	0.13
SrO	0.37	0.03
BaO	0.24	0.03
MnO_2	0.22	0.04

Trace Element	Total (ppm)	
	PRB	Illinois # 6
Arsenic	2.1	4.3
Selenium	1.8	2.6
Antimony	0.34	0.65

Data for overall concentration of TEs in both coals are also shown in Table 16. As can be seen from this table, the concentration of all three TEs in the Illinois No. 6 coal is higher than was found in the PRB coal. As these elements are commonly associated with pyrite, their concentrations are expected to be higher in the higher pyrite coal. CCSEM data from Table 17 shows that pyrite levels are much higher for the Illinois # 6 coal compared to the PRB coal.

Table 17: CCSEM mineralogical determinations for test coals (weight percent, mineral basis)

Mineral Species	Weight %	
	Illinois # 6	PRB
Quartz	15.3	37.1
Kaolinite	6.8	13.6
Illite	8.6	5.7
Pyrite	26.7	0.6
Silicates	26.6	21.9
Unclassified	10.6	12.9
Other Minor species	5.4	8.2
Total	**100**	**100**

Sequential leaching

Results for the selective leaching of the elements of interest in the raw coal are shown in Table 18 and can be used to predict their mode of occurrence in the coal. For the PRB coal there appears to be more than one mode of occurrence for the TEs, especially As and Sb. Almost 30% of these two elements were leached by HCl while minor amounts were leached by HF. Leaching by HCl may indicate an association of As and Sb with iron oxides while leaching by HF probably indicates an association with clays (possibly illite). Around 40% of both As and Sb were not leached in this coal and because most of the iron was leached, they were assumed to be organically associated. A majority of selenium was not recovered in any of the leaching fluids for the PRB coal indicating high organic association. This is consistent with findings from other researchers [23,52]. Around 55% of the iron was leached by HCl and 35% was leached by HF. Almost all the iron (97%) was leached in the four solvents indicating little or no organically-bound portion for this coal. Iron is primarily associated with iron oxides or carbonates (as indicated by leaching with HCl) and clays (as indicated by leaching with HF). Like the TEs, Ca was mostly found to be organic bound, while minor amounts were leached by acetate (present as ion exchangeable), HCl (present as carbonates and oxides) and HF soluble fractions (present in clays).

For the Illinois # 6 coal, significant amounts of all three TEs were present in the HNO_3 soluble pyrite fraction, while minor amounts were present in the HCl soluble mono-sulfide fraction as a likely result of pyrite oxidation. Most of the Fe was also derived from pyrite, while significant HF and HCl solubility indicates Ca association with clays and as carbonates. The high total percentage of elements leached suggests little (for TEs) or no organic association (for Ca and Fe) in this coal.

Table 18: Percentages of elements leached by ammonium acetate, hydrochloric acid, hydrofluoric acid, and nitric acid as compared to the total concentration of the element in the unleached coal

PRB Coal					
Element	Acetate	HCl	HF	HNO3	Total Leached
Arsenic	10%	30%	11%	9%	60%
Selenium	12%	6%	0%	3%	21%
Antimony	12%	28%	18%	8%	66%
Calcium	20%	10%	15%	0%	45%
Iron	0%	55%	35%	7%	97%
Illinois # 6 coal					
Element	Acetate	HCl	HF	HNO3	Total Leached
Arsenic	0%	13%	5%	64%	82%
Selenium	8%	8%	0%	55%	71%
Antimony	0%	22%	11%	45%	78%
Calcium	10%	35%	50%	0%	95%
Iron	7%	9%	4%	80%	100%

Fly ash particle size distributions

Fly ash particle size distributions (PSD) were determined by measuring the mass of particles impacted on the stages of the DLPI. The particle mass emissions concentration (i.e., µg/Nm3) of each stage was calculated by dividing the net mass per stage by the total sample gas flow rate. The particle size distribution curve was formed by plotting the differential mass concentration (dM) versus average particle size ($D_{p,avg}$) on a normalized $dM/dlogD_p$ basis, where $D_{p,avg}$ represents the average aerodynamic particle size of particles collected on a given stage and is calculated as the average of the cutpoint diameters of the given impactor stage and the adjacent larger stage, and where $dlogD_p$ is calculated as the difference between the log_{10} of the cutpoint diameters of these two adjacent impactor stages.

Individual PSD curves for fly ash collected from tests with the two coals are shown in Appendix B. These two figures show ash loading as a function of aerodynamic particle size for multiple runs. Data in Figures 14 & 15 (Appendix B) show good consistency in PSD data for all the replicate runs, including sample peaks, for a given size fraction. This indicates good control in both sampling conditions and furnace flows during sample collection. Minor variations, as in the case of PRB submicron fraction, could be a result of slight coal feed rate changes or fuel composition changes between sampling or from sample weight measurement variations.

The average PSD for each coal is shown in Figure 13. A trimodal ash distribution was observed for both PRB and Illinois # 6 samples with mode peaks observed at approximately the same average particle size (D_p) for both coal ashes. Based on the average PSDs shown in Figure 4 and the cut point diameters of particles for a corresponding DLPI stage, the submicron mode included particles in the size range 0.11 – 0.4 µm (stages 3-5), the fine fragment mode contains particles between 0.4 -2.5 µm (stages 6 - 9). Particles greater than 2.5µm (stages 10-12) were assigned to the coarse size mode. Material collected in the impactor at the smallest size(s) consist of both coal submicron fly ash (the

submicron fume) and vapor phase material that condenses in the sample probe during cooling [5]. As the gas cools, some of the inorganic vapors can nucleate into small particles and will be collected in the lowest stages of the DLPI. In this work we have assumed stages 1 and 2 of the DLPI, which collected particles between 0.03 and 0.11 microns, represent mixed vapor-particle mode and hence decided to not include them in leaching studies.
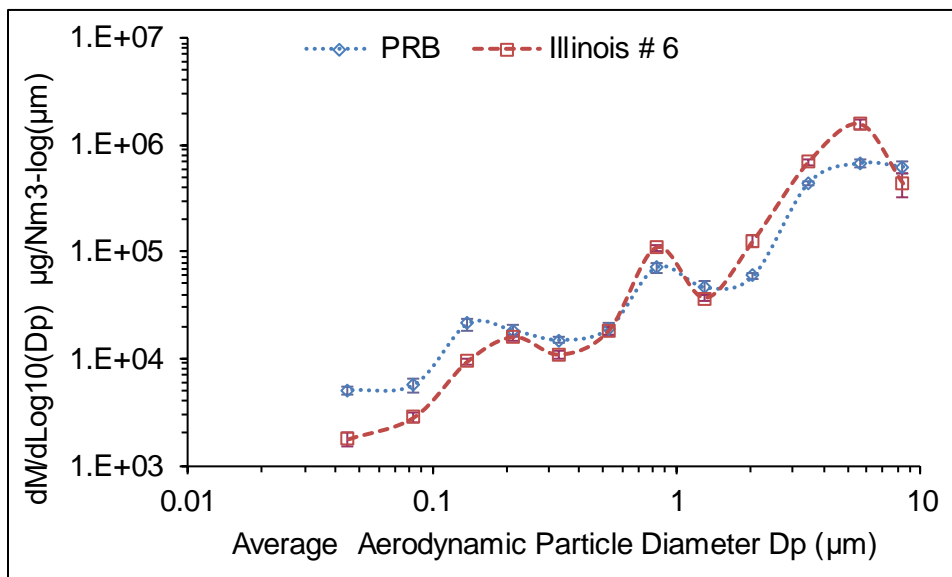
Figure 13: Comparison of average PSDs for the combustion of PRB and Illinois # 6 coals

Fly ash PSD curves for the two test coals are similar but show some variation in the relative magnitude of peaks for the different size modes. Even though the tests were carried out at the same peak combustion temperature, differences in ash content, chemistry (Table 16), and mineralogy (Table 17) influence the overall PSD curves. The sub-bituminous PRB coal was observed to have a slightly higher ash loading for particles less than 0.2 micron in size, but for the coarse mode the bituminous Illinois # 6 sample had a higher ash loading. The intermediate fine fragment mode did not show a clear trend with respect to coal rank.

Chemical fractionation data (Table 18) indicates most of the calcium in the PRB coal to have an organic association and this form will show substantial vaporization under flame operating conditions. For most low rank coals such as PRB, vaporized alkali and alkaline earth metals (Ca, Mg, Na and K) are expected to contribute significantly to the smaller submicron/ultrafine mass. This size mode will also contain low volatile elements such as the oxides of Si, Al, Fe etc as a result of vapor supersaturation and subsequent nucleation and growth. Similarly, for the low calcium and pyrite rich Illinois #6 coal, the submicron mode is expected to be mostly composed of oxides of Si, Al and Fe. Coarse mode ash for both coals is expected to be derived from clays such as kaolinite and illite.

Fly ash minor and trace element concentrations

Concentrations of Ca, Fe, As, Se and Sb in fly ash as a function of particle size are shown in Appendix B, Figures 16-20. Each figure compares elemental loading in ash for the two coals tested. Some important observations include:

- As expected, the PRB ash had higher Ca loading than the Illinois # 6 ash and it was vice versa for Fe distribution.

- As and Se loadings were higher for the Illinois # 6 ash than PRB ash in all size fractions. They are expected to be mainly derived from pyrite

- There was not a significant difference in submicron and fine fragment Sb loading for both coal ashes. However, Sb present in bulk mode was significantly more for the Illinois # 6 ash. This is expected to be derived from the non-vaporizing fraction

Leaching Studies

Results from leaching studies where ash samples were leached with solutions of varying pH to determine TE solubility are shown in Tables 19, 20 and 21 for As, Se, and Sb, respectively. DLPI stages that constitute submicron (stages #3 - #5 with cutpoint diameters 0.11 – 0.4 µm), fine fragment (stages #6 - #9, 0.4 – 2.5 µm) and coarse (stages #10 - #12, 2.5 – 10 µm) modes were all analyzed individually and an average solubility for each mode was then calculated from the individual solubilities of the stages constituting that mode   .

The reported values in Tables 19-21 are percent solubility of an element in a given leaching environment (acidic, basic or neutral) calculated as the ratio of its mass fraction in any given DLPI stage to its mass fraction for the same DLPI stage as determined by the total digestion method. It is important to recognize that these solubility values are qualitative in nature. Due to the extremely small amounts of ash involved, especially in the smaller particle modes, relatively small weighing and analytical errors can lead to a large overall relative error. A ND value indicates concentrations were below the analytical detection limit.

Table 19: Percent solubility of arsenic in the three size fractions and under the three pH conditions for bituminous and sub-bituminous fly ashes

Particle regime & coal rank	Acidic	Neutral	Basic
	pH = 2.88	pH = 7	pH = 11
Sub micron			
Bituminous - Illinois # 6	60±4	45±8	10±3
Sub-bituminous - PRB	55±4	40±6	30±4
Fine fragment			
Bituminous - Illinois # 6	65±3	50±4	15±2
Sub-bituminous - PRB	60±6	45±3	35±4
Bulk			
Bituminous - Illinois # 6	35±5	20±4	15±3
Sub-bituminous - PRB	20±3	15±3	ND

Table 20: Percent solubility of selenium in the three size fractions and under the three pH conditions for bituminous and sub-bituminous fly ashes

Particle regime & coal rank	Acidic	Neutral	Basic
	pH = 2.88	pH = 7	pH = 11
Sub micron			
Bituminous - Illinois # 6	80±8	75±4	45±6
Sub-bituminous - PRB	60±4	50±7	25±3
Fine fragment			
Bituminous - Illinois # 6	90±7	75±8	45±4
Sub-bituminous - PRB	65±3	50±5	30±5
Bulk			
Bituminous - Illinois # 6	30±4	25±6	25±3
Sub-bituminous - PRB	25±4	30±3	10±3

Table 21: Percent solubility of antimony in the three size fractions and under the three pH conditions for bituminous and sub-bituminous fly ashes

Particle regime & coal rank	Acidic	Neutral	Basic
	pH = 2.88	pH = 7	pH = 11
Sub micron			
Bituminous - Illinois # 6	90±6	60±7	35±5
Sub-bituminous - PRB	60±3	70±6	50±6
Fine fragment			
Bituminous - Illinois # 6	85±7	60±6	50±4
Sub-bituminous - PRB	65±4	75±4	55±4
Bulk			
Bituminous - Illinois # 6	45±7	25±4	10±4
Sub-bituminous - PRB	25±7	10±3	15±3

Arsenic

Arsenic was more soluble in the smaller submicron and fine fragment particles than in the coarse mode particles. Submicron and fine fragment TEs are mostly formed by a surface chemical reaction mechanism and are available for leaching whereas a significant portion of TEs present in the coarse mode will have Al-Si association and are not easily leached. Seames et al [12,31,34] have shown that differences in partitioning mechanisms has a greater effect on trace element solubility from fly ash than which size mode the trace element resides in. It was also observed that solubility decreased as the pH moved from acidic towards basic conditions and this was observed for all three size fractions. Such a trend was also observed for studies conducted by Seames et al [31,61] for TE solubility in the submicron and fine fragment regimes.

Interestingly, in the PRB coal ash arsenic was found to be slightly mobile for submicron and fine fragment particles under alkaline conditions. This result suggests that not all arsenic was associated as calcium arsenate or as ettrignite (calcium aluminate sulfate hydroxide hydrate) as both species are fairly insoluble at higher pHs [37,38,67,68]. Arsenic solubility in calcium rich fly ashes, likely present as As(V), decreases as pH approaches alkaline conditions due to the formation of insoluble complexes (12,37,38). Arsenic in the PRB supermicron fly ash is more soluble than arsenic in the Illinois # 6 fly ash for both submicron and fine fragment regions. Based on work done by Seames et. al, there is evidence of physical absorption of As_2O_3 on fly ash surfaces and subsequent oxidation to As_2O_5 resulting in increased arsenic solubility. It is therefore assumed that some of the arsenic in the PRB fly ash may have been present as $As_2O_3(s)$ formed from vapor phase As condensing on particle surfaces. Prior studies on arsenic solubility [69,70] have shown that arsenites (As (III)) are much more soluble than arsenates (As(V)) at higher pHs.

Also, PRB and Illinois # 6 arsenic had similar solubilties across submicron and fine fragment size fractions for acidic and neutral conditions. This indicates similar partitioning mechanisms across both size fractions, with calcium arsenate expected to dominate the particulate phase. However, under alkaline conditions there was more of a difference between the two coals. In the Illinois # 6 ash arsenic was not found to be very soluble for the smaller size fractions. This contrasts with the PRB ash which had somewhat higher arsenic solubiltity in the submicron and fine fragment size fractions. Chemical fractionation data for the bituminous coal shows mainly mineral association for As which can inhibit mobility under certain leaching environments.

When considering fly ash effects on human health, the chief concern is emission of submicron particulate matter into the atmosphere with flue gas which can then be inhaled by human beings and animals. For this scenario, the neutral pH solubility results are the most relevant as respiratory fluids have a pH close to 7. Arsenic solubility shows a potential for moderate health risk for both coal ashes. Regarding effects on the environment, the chief concerns are TE emissions from the fine fragment region. Fine fragment particles that settle on the ground get exposed to rainfall, runoff water, etc causing potential mobility of TEs. Depending on the geographical region, soil can be either acidic (east) or basic (west). Arsenic leaching data indicates moderate effect for both coal ashes in an acidic environment and low to moderate effect in the basic environment for the PRB ash. The environmental impact from coarse ash particles is primarily related to disposal since these particles are normally placed in landfills or used in by-products such as road asphalt, sheetrock, etc. For the acidic Illinois coal ash, the pH of rain water will drop as it seeps through the ash pile while for the PRB ash it will raise the pH of rain water. Arsenic from coarse particles in the Illinois ash may slightly leach out in a landfill ash pile while coarse fraction As in the PRB ash should pose no such risk.

Selenium

Leaching studies for selenium indicated a trend similar to arsenic. For the submicron and fine fragment particles, we observed moderate to high mobility in acidic and neutral conditions and lower solubility in alkaline conditions. For the coarse particles, only slight to partial mobility was observed under all three pH conditions. Selenium undergoes a partitioning mechanism similar to arsenic and hence it was found to be more soluble in the smaller size range. As compared to arsenic, Se was generally found to be more soluble under all three pH conditions. The Illinois #6 ash showed slightly higher solubility than the PRB ash for all three pHs in the smaller size ranges. Van Hoek et al [70,71] concluded that selenium

leaches out much better in a solution whose pH is opposite to that of the pH of the fly ash. We observed this for the alkaline PRB ash which showed higher solubility for all three size fractions at pH 2.88 than at pH 11. However, such a trend was not observed for the acidic Illinois #6 ash which was also more soluble at pH 2.88 than pH 11 for all three size fractions.

Selenium present as Fe-Se complexes (selenates) have been shown to have fairly high solubility in both acidic and neutral conditions, whereas Ca-Se complexes (selenites) have low solubility at both conditions [12,34]. While most of the selenium is expected to be present as calcium selenite in both submicron and fine fragment regions, high solubility data, especially for the Illinois # 6 ash, indicates the possibility of formation of selenates, Additional work is required to understand this particular behavior.

The neutral pH solubility results for Se in the submicron particles shows potential for moderate health risk for the PRB ash and high risk for the Illinois ash. Regarding potential effect on the environment, it is important to take into consideration Se solubility data for fine fragment particles from both acidic and basic leaching solutions. Data indicates significant risk for the PRB ash and high risk for the Illinois # 6 ash in the acidic environment and low risk for the PRB ash and moderate effect for the Illinois # 6 ash in the basic environment. The impact from coarse ash particles indicates Selenium present in the acidic Illinois ash may slightly leach out in a landfill ash pile, while coarse fraction Se in the PRB ash should pose no such risk.

Antimony

Leaching studies for antimony showed a similar trend to selenium where Sb in the bituminous ash samples was found to be more soluble in most cases than Sb in the sub bituminous ash samples. As with selenium, antimony solubility also progressively decreased for the Illinois # 6 samples as conditions went from acidic to basic, but unlike Se the PRB ash solubility remained fairly constant irrespective of pH. For the sub-micron and fine fragment fractions of the Illinois #6 ash, Sb solubility data is consistent with data reported by Norman et al. [72] where it can be very mobile under acidic conditions and moderate solubility in a neutral medium. Additionally, work done by Miravet et al., [46] on Spanish fly ashes showed Sb solubility to peak around extremely acidic pH conditions (<2), while alkaline pHs showed very poor solubility. By contrast, another study conducted by Kim et al., [73] for US coal ashes showed that some of the Sb would leach under alkaline conditions and this is very likely to be present as an oxyanion. This indicates possible differences in Sb partitioning mechanism for the two fly ashes which mainly arises from the differences in coal ash chemistry. Additionally, antimony in the smaller size fractions showed slight to partial mobility in an alkaline medium for both fly ashes. Sb, Sb_2O_4 and Sb_2O_5 all show high mobility in acidic conditions and are partially mobile close to neutral conditions [12,34]. This variation in Sb solubility was observed for the smaller particles in the Illinois # 6 ash samples, which suggests that antimony could be also present as Sb, Sb_2O_4 or Sb_2O_5.

The neutral pH solubility results for Sb in the submicron particles suggest moderate to high risk for human health while fine fragment data indicates moderate risk for the PRB ash and high environmental risk for the Illinois # 6 in an acidic medium. Both coal ashes possess medium environmental risk based on fine fragment Sb solubility under basic conditions. Coarse ash leaching data indicates medium risk of Sb leaching with rain water from acidic ash piles but should not pose any significant environmental problems from basic ash piles in landfills.

CONCLUSIONS

Leaching studies were carried out on size segregated fly ash particles for the combustion of a bituminous and a subbituminous coal to study the effect of coal rank on fly ash solubility for TEs As, Se and Sb. The main focus of this research was to measure the solubility of these TEs in the submicron, fine fragment and coarse size fractions under different pH conditions and use solubility data to assess potential risks of TE leaching from fly ash into the environment. Furnace conditions were adjusted to achieve the same peak combustion temperature for both coals to remove uncertainty of temperature effect on TE partitioning and subsequent solubility. Sequential leaching of the coals indicates mostly pyritic association for all three TEs in the bituminous coal and a combination of pyritic and organic association in the sub bituminous coal. TE distribution plots show a higher amount of TE loading for the Illinois # 6 ash samples compared to the PRB ash samples in almost all the size fractions. While inherent levels of TE in the original fuel will affect their final transformations, their fate also depends on their original mode of occurrence in the fuel and the composition of other major inorganic species in coal ash, which is mostly rank driven. The effect of rank-based chemistry on TE partitioning was identified for the PRB ash, where As data showed possible anomalous behavior with higher than expected vapor phase emissions. Elemental mass distribution data for PRB ash indicates Si-Ca interaction across a wide size range where silica may have scavenged most of the CaO thereby greatly reducing the amount of active Ca sites available for As partitioning. Based on this observation, it was postulated that some of the As vapors may have physically condensed on fly ash surfaces forming As_2O_3(s) instead of kinetically favored calcium arsenate. This needs further verification since no tests were designed in this current study to validate this claim.

Data from fly ash leaching studies indicate significant solubility for all three TEs especially in the smaller size fractions. However, only Se and Illinois # 6 Sb showed some mobility for coarse size particles. All three elements exhibited higher mobility under acidic leaching conditions compared to both neutral and basic conditions. Selenium, in all the size fractions, showed higher mobility for the Illinois # 6 samples compared to the PRB samples while no such difference was observed for arsenic. For antimony, the Illinois#6 ash samples were more soluble than the PRB ash only under acidic environment. While all three elements are expected to follow similar partitioning mechanisms in a boiler, differences in solubility data indicate the potential effect of varied speciation amongst TEs of interest. Even though multiple samples analyses were carried out, the amount of ash involved (especially for the lower stages of the impactor) is relatively small such that weighing and analytical errors can lead to a large overall relative error. Hence it is important to understand that the leaching data presented here should be seen more as a qualitative one even if percentage solubilities are presented.

With regards to the effect of human health from TE leaching, all three TEs may pose a moderate to significant risk if inhaled by human beings due to their solubility under neutral conditions. This was observed for fly ashes from both coals. As for environmental risks in both coal ashes, fine fragment solubility data indicates that all three TEs posed a moderate to high risk of leaching in acidic soils while only Se and Sb were found to be soluble under basic conditions.

APPENDIX B

SUPPLEMENTARY FIGURES, TABLES AND DISCUSSION FOR CHAPTER 4
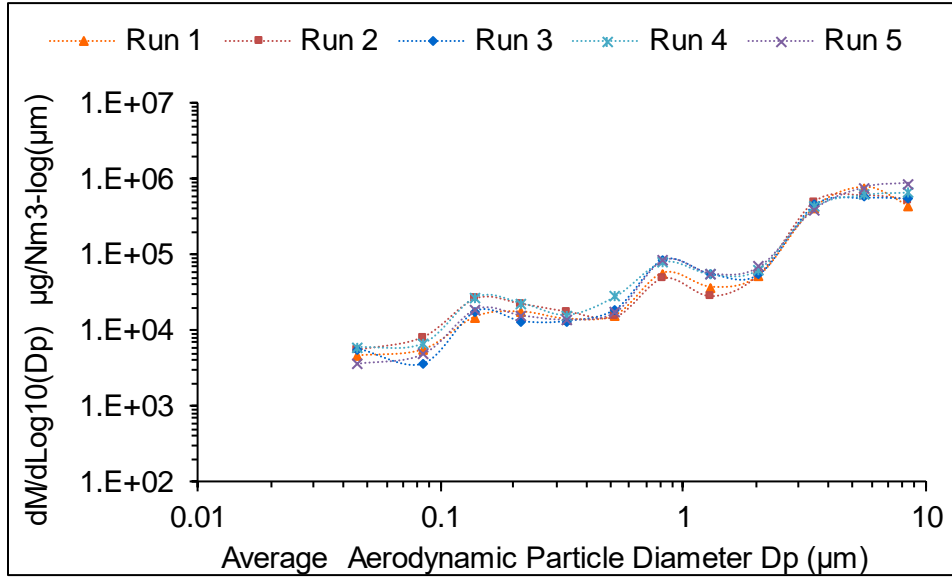
Figure 14: DLPI-generated fly ash PSD replicates for the combustion of PRB sub-bituminous coal
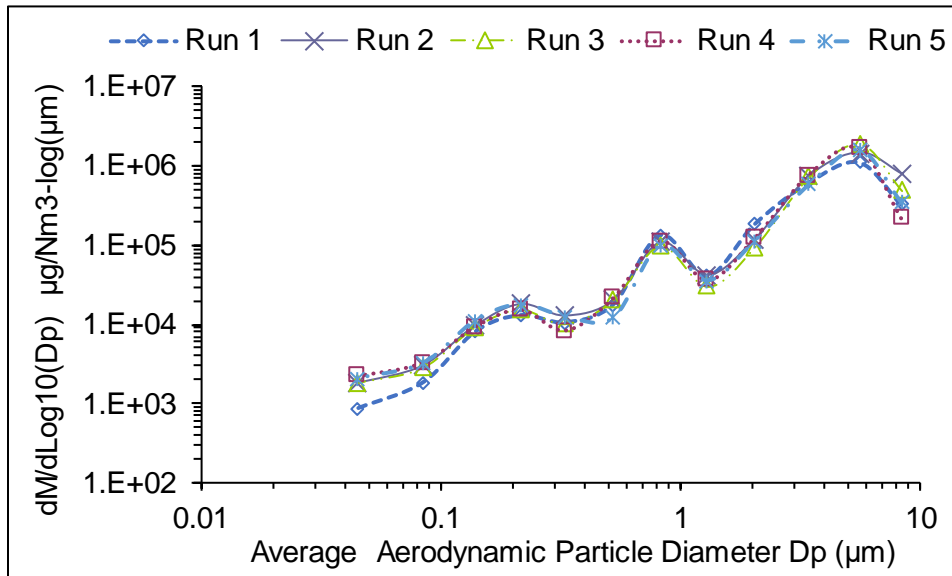
Figure 15: DLPI-generated fly ash PSD replicates for the combustion of Illinois # 6 bituminous coal

Fly ash minor and trace element concentrations

The concentration of Ca and Fe in fly ash influences vapor phase partitioning mechanisms of TEs, especially arsenic and selenium. As shown in Table 16, the PRB coal had much more calcium than the Illinois #6 coal. Consequently, and as observed from Figure 16, the PRB ash had higher loading for calcium than Illinois # 6 for all the size fractions. Additionally, submicron and fine fragment Ca peaks for the PRB coal ash mirrored the overall PSD peaks for the two size fractions. In low rank coals, such

as PRB, calcium is predominantly dispersed in the macerals and bound to carboxyl groups (organically held fraction), whereas in bituminous coals, it is present as the discrete mineral, calcite. This difference in the form of occurrence plays a major role in the behavior of calcium during combustion. The calcium that is molecularly dispersed in the macerals bound to the carboxyl group, coalesces to form CaO and some of the CaO fumes will react with clay minerals and quartz forming Ca-aluminosilicate glass and calcium silicate phases [63,64,65]. In case of the Illinois #6 coal, the combination of low calcium and high sulfur content will tend to reduce the availability of action cation sites on fly ash particle surfaces. This may reduce the fraction of trace elements that partition due to a surface reaction mechanism.
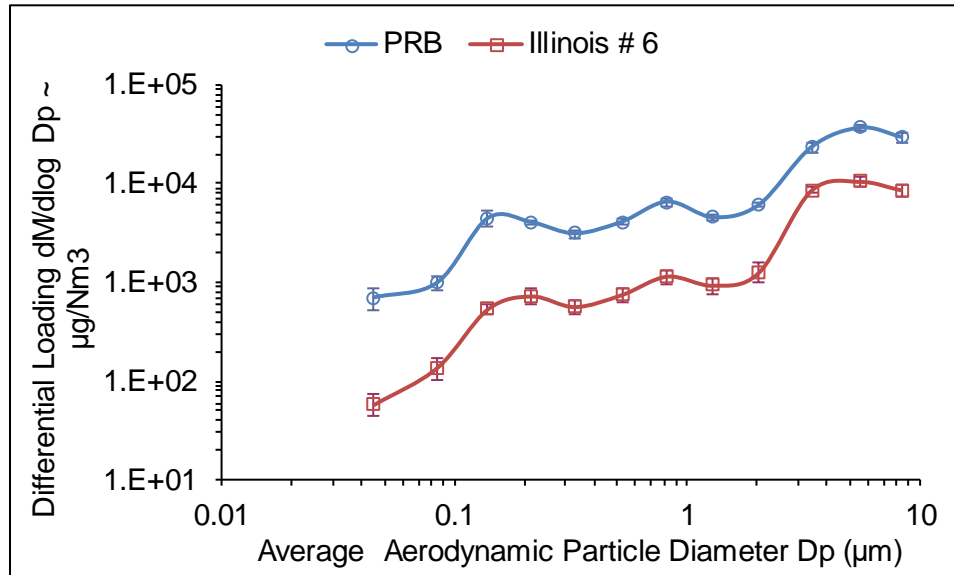
Figure 16: Differential mass loading for calcium in fly ash for the combustion of PRB and Illinois # 6 coals

Iron loading, as shown in Figure 17, in both ashes showed a contrasting trend to calcium distribution. There were much higher amounts of Fe in Illinois # 6 coal compared to PRB coal, as would be expected for a bituminous coal high in pyrite. And as seen in Figure 17, ash from the Illinois #6 coal also contained higher concentrations of Fe than the PRB ash. Similar to the PRB coal, submicron and fine fragment Fe peaks for the Illinois # 6 fly ash mirrored peaks in the overall PSD.

81
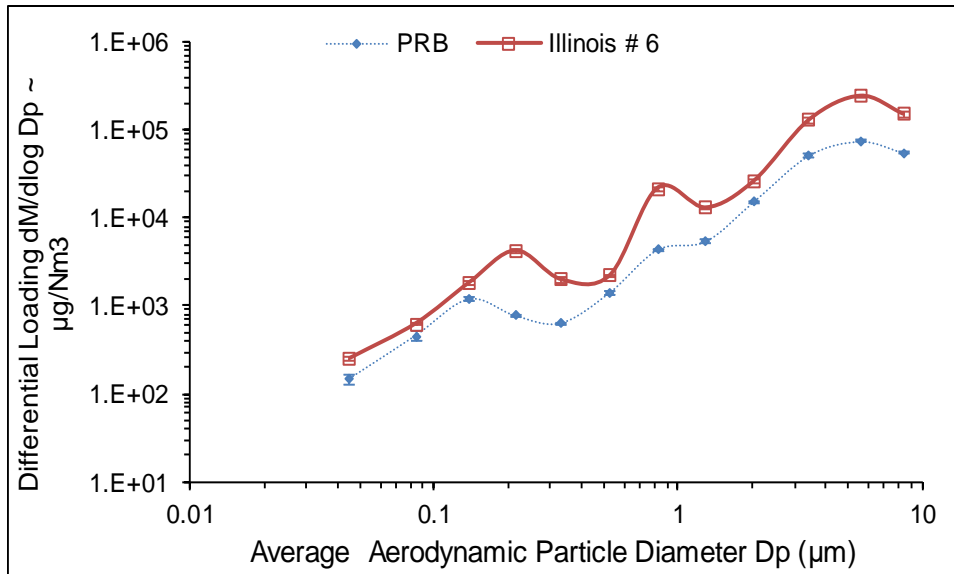
Figure 17: Differential mass loading for iron in fly ash for the combustion of PRB and Illinois # 6 coals

The arsenic distribution in each both fly ashes is shown in Figure 18. Although the forms of arsenic are different between the two coals, a significant portion of the arsenic in both coals will vaporize during the combustion process, including pyrite held arsenic. Slight low temperature oxidation of pyrite will greatly reduce the vaporization of trace species suggesting that the majority of arsenic vaporization will occur during sulfur devolatilization. Illinois # 6 ash samples had higher As for all particle sizes compared to the PRB samples. This is partly from the higher overall amounts of As present in the Illinois # 6 coal. Data also indicates the arsenic concentration in ash is not directly proportional with arsenic present in the original fuel. The Illinois coal had about two times more As than the PRB coal but the ash loading data indicates a factor of 5 to 10 times higher As than the PRB ash. This indicates the possibility of some of the vapor As from the PRB coal not transforming into solid particles in the post combustion region.

The size distribution of As in PRB ash was similar to what was observed for the Illinois # 6 samples albeit with a much lower amount for every DLPI stage analyzed. Arsenic is mostly expected to be present as calcium arsenate in both coals, especially for the smaller size fractions. The effect of high sulfur in the Illinois # 6 ash will inhibit TE partitioning on Fe surface sites [12,23,54] making calcium arsenate the most dominant product in the smaller fractions. For the low rank PRB coal, calcium is often present on the surfaces of ash particles enabling calcium arsenate formation through the reaction of vapor phase arsenic oxides with CaO. Iron arsenate is also expected to be present, especially in the larger particles, due to low sulfur in the original fuel. However, calcium and iron oxides encased in glassy matrices are usually inaccessible for reaction with vapor phase arsenic compounds. Arsenic present in coarse particles will also include the non-vaporized clay/silicate fraction and material having this association undergo very little transformation in a combustion environment and hence likely remain trapped in the ash particle [12,23,52,54].
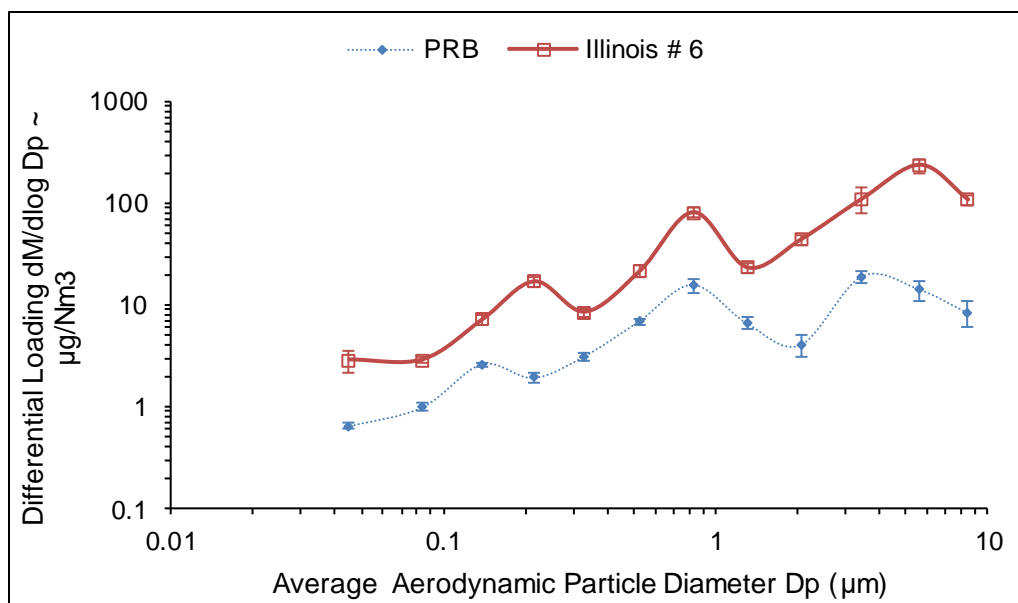
Figure 18: Differential mass loading for arsenic in fly ash for the combustion of PRB and Illinois # 6 coals

Analysis of impinger samples indicates the presence of gas phase arsenic for the PRB test, but it was in much smaller concentrations relative to the solid phase. In contrast, for the bituminous samples, gas-phase arsenic was below detection limits. Because of the low concentration of arsenic compared to other major ash forming species in the coal, most volatilized arsenic molecule will contact submicron or coarse particles and heterogeneously partition onto their surfaces. However, Seames et al., [12,23] and Bool [52] also reported the presence of vapor phase arsenic for their PRB coal tests, which suggests there might be limitations (kinetic or mass transfer) to complete calcium arsenate formation. Therefore, the presence of vapor phase arsenic especially in the calcium rich PRB coal can be possibly attributed to the high amount of SiO_2 in ash. SiO_2 in ash is primarily derived from quartz and also from clays, where it is very reactive Both vaporized and particulate forms of calcium in the flue gas can interact with silica, the most dominant species in fly ash, in a wide size range and this can potentially affect the amount of active Ca sites available as partitioning sites for As. Helble et al., [66] have shown ratio of Ca/SiO_2 in ash influences the extent of interaction between Ca in the solid matrix and arsenic oxide vapor in flue gas. This possibility is discussed in more detail at a later section of this paper.
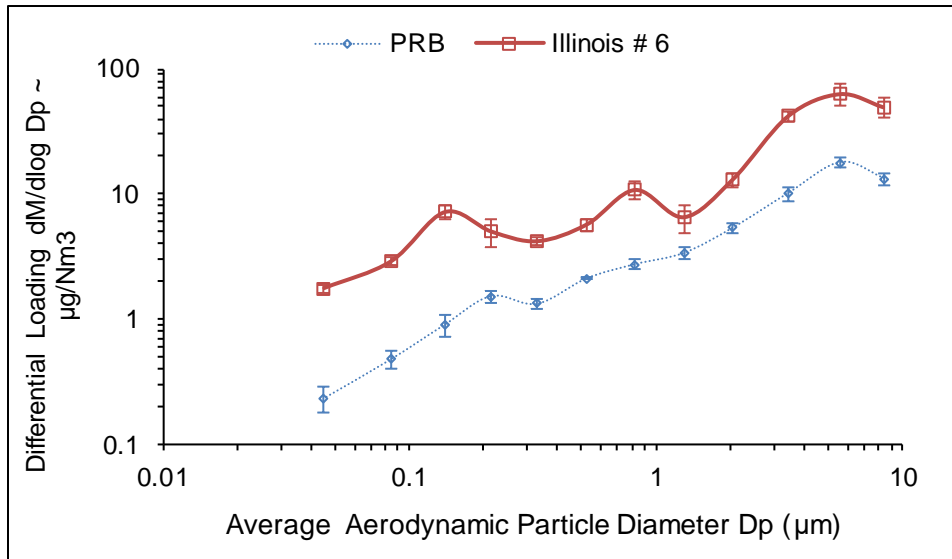
Figure 19: Differential mass loading for selenium in fly ash for the combustion of PRB and Illinois # 6 coals

Selenium distribution in fly ash

Size segregated fly ash distribution for selenium is shown in Figure 19. Similar to arsenic distribution, the Illinois # 6 samples had more Se in all the reported size fractions. The partitioning of selenium is also very similar to arsenic for the different size fractions for the Illinois # 6 sample. The individual peaks for the selenium curve is similar to the peak for calcium distribution in the Illinois # 6 ash while no such trend was seen for the PRB ash. Selenium is expected to mainly form calcium selenite and to a lesser extent, iron selenate across all the size fractions for the low sulfur PRB ash [12,23,]. However, the high sulfur in Illinois # 6 coal will inhibit selenium partitioning on active Fe sites even though they should be available in great numbers. Instead, selenium will form calcium selenite type compounds. However, some of the selenium is still expected to be present as iron selenate in the supermicron size range due to higher iron loadings in this size range and the proclivity for Se vapor towards Fe sites over Ca sites.

Analysis of impinger samples indicates the presence of gas phase Se for both coals. For the Illinois # 6 gas sample about 16% of total Se was found in the vapor phase (115 µg/l in impinger fluid) and around 7% of total Se was in vapor phase for the PRB test (48 µg/l). Selenium has a relatively high vapor pressure and some of the Se in flue gas is expected to leave the boiler in vapor phase without partitioning onto solid surfaces.
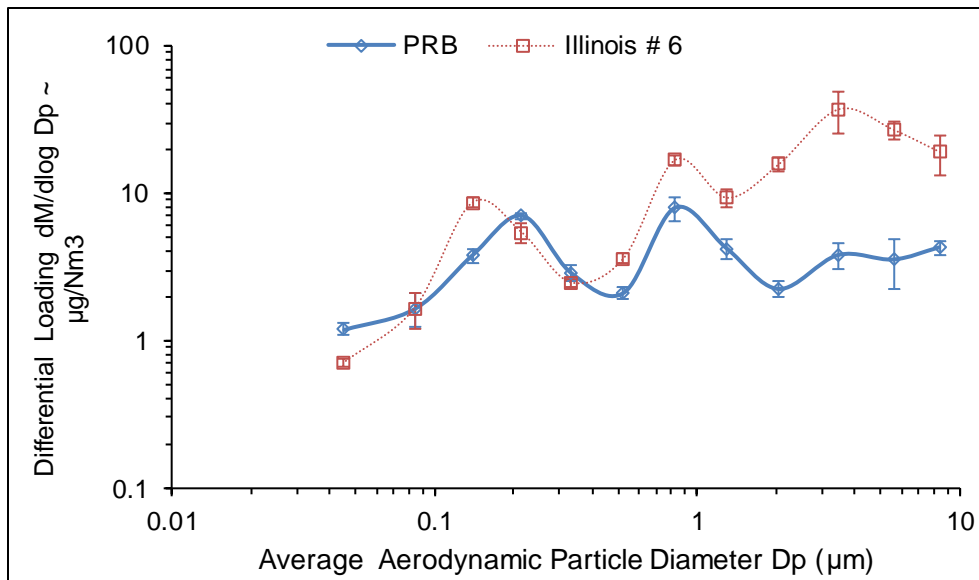
Figure 20: Differential mass loading for antimony in fly ash for the combustion of PRB and Illinois # 6 coals

Antimony distribution in fly ash

Due to the similarity in chemistry with arsenic, vapor phase antimony is expected to form an oxy-anion of the form Sb_2O_3 during coal combustion. Based on fly ash loading data shown in Figure 20, it showed trends similar to both arsenic and selenium depending on the combusting fuel and particle size fraction. The submicron fraction peak mirrored selenium peaks for both coal ashes, while fine fragment peak most closely resembled arsenic fine fragment peaks. This indicates a possibility of similar partitioning mechanism to Se for submicron Sb particles and a partitioning mechanism followed by As for fine fragment particles. Similar to As and Se, partitioning of antimony to fly ash surfaces is dependent on the availability of active cation sites on fly ash surfaces [12,23]. There was not a significant difference in submicron antimony levels between both coal ashes even though the Iliinois #6 coal had twice as much antimony than the PRB coal. This indicates the possibility of lower Sb vaporization for the Illinois # 6 coal compared to the PRB coal. However, analysis of impinger samples showed the presence of vapor phase Sb only for the Illinois # 6 coal test and not for the PRB coal. Based on this data it appears that some of the vaporized Sb in the Illinois # 6 coal did not partition on fly ash surfaces. Since Sb is the least reactive of all three TEs, it is the least likely to react with Fe and may not even have sufficient Ca sites for vapor phase partitioning.

Data indicates antimony also had a much higher coarse size fraction ash loading for the Illinois # 6 coal compared to the PRB coal. This may be due to higher inherent amounts in the original fuel with contribution from both non-volatilizing fraction, mainly derived from bigger exclusions. For most elements, the mass fraction in super micron particles is usually higher than its mass fraction for submicron and fine fragment particles. This does not seem to be the case for Sb in the PRB ash. The HF soluble fraction is nearly identical for both fuels but leaching data also indicates higher ion-exchangeable and organic association for Sb in the PRB coal than Illinois # 6 coal and this may be the reason for higher Sb in the smaller size fraction and depletion in the larger fractions. Sb present in both fractions is expected to vaporize appreciably and later react with active cation sites present in the

smaller ash size fractions. Due to its higher calcium levels and relatively low sulfur, the PRB coal ash is expected to have higher number of active cation sites than the Illinois # 6 ash in the submicron and fine fragment fractions.

Effect of CaO to SiO$_2$ ratio for PRB ash

Another interesting parameter is the ratio of CaO to SiO$_2$ in ash for the PRB coal. As mentioned earlier, TEs in vapor phase undergo a partitioning reaction on the surface of fly ash containing active Ca sites. Calcium, in PRB coal, is plentiful and given its organic association is expected to vaporize appreciably and transform into particles either through nucleation or surface condensation reactions forming active sites. However, only a small fraction of calcium in fly ash will be available as the highly reactive CaO (free lime), while calcium-silica based compounds, such as mono-calcium silicate [CaO. SiO$_2$] and di-calcium silicate [2CaO. SiO$_2$] will represent the bigger fraction of calcium in fly ash. Calcium present as calcite (CaCO$_3$), as in the case of Illinois # 6 coal, has shown only little interaction with silicate minerals and some of the calcite even remains as CaO particles in the ash. This shows the form of occurrence of calcium in the coal is very important in determining the fate of calcium and other elements.

Experiments conducted by Helble et. al. [66] showed that CaO was the best absorbent for As vapors as compared to mono and di-calcium silicates. Their data also showed that an increase in SiO$_2$ to Ca ratio in the solid reactant decreases the capture of arsenic vapors. Depending on the SiO$_2$ to Ca ratio, the number of reactive Ca sites might be limited in ash and instead mostly comprise of less reactive Ca-Si sites. However, their results demonstrate that Ca-Si solids are still capable of capturing arsenic, but with a reduction in the extent of interaction with decreasing amount of calcium. The analysis of calcium silicates product samples showed that the arsenic vapors were reacting with the calcium silicate and not with discrete calcium oxide inclusions incorporated in these solids. Lack of active cation surfaces for As and Se partitioning is important for two reasons (i) A different partitioning mechanism can impact TE speciation on fly ash surfaces (II) Different speciation can change the oxidation state of TE in ash and this affects both mobility and toxicity characteristics.

Figure 21 compares the silica and calcium loadings for the PRB ash. The concentration curves resemble each other in shape, including common peaks, indicating flue gas Ca-Si reactions and subsequent particle formation. Based on the distribution shown, it appears that calcium in all size fractions will have a certain level of silica interaction. The concentration plots for Si and Ca have similar distributions, including peaks at the same particle size consistent with post combustion reactions between the two elements. Work done by Shah et.al [63,64] and Helble et.al [65] also shows Ca-Si interaction in PRB coal ash for particles of different sizes. The high (relatively) SiO$_2$ to Ca ratio for the tested PRB ash suggests that As and Se partitioning and speciation may be influenced in this case, a possibility that can be examined further with data from leaching studies.
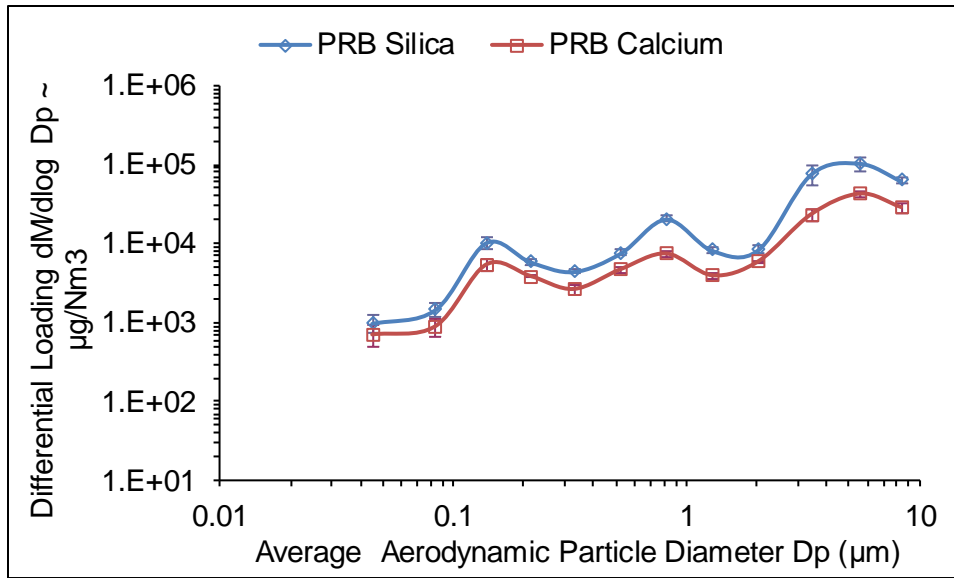
Figure 21: Comparison of differential mass loading of silica and calcium for the PRB coal ash

Table 22: Percentage solubility of TEs in the three size modes for bituminous ash samples under acidic (pH = 2.88) condition

Particle regime	Element	DLPI Stage	Cut point (µm)	% Mobility				Uncertainty in mobility (95% CL)
				Run 1	Run 2	Run 3	Average	
Submicron	Arsenic	3	0.108	53	61	63	61	4
		4	0.17	55	58	73		
		5	0.26	72	61	57		
	Selenium	3	0.108	94	84	106	81	8
		4	0.17	84	75	79		
		5	0.26	66	71	73		
	Antimony	3	0.108	86	102	83	91	6
		4	0.17	103	101	94		
		5	0.26	92	78	84		
Fine fragment	Arsenic	6	0.4	61	71	64	67	3
		7	0.65	72	59	66		
		8	1	59	71	73		
		9	1.6	78	66	61		
	Selenium	6	0.4	88	93	116	91	7
		7	0.65	103	84	106		
		8	1	72	98	91		
		9	1.6	82	71	88		
	Antimony	6	0.4	96	82	81	87	7
		7	0.65	93	84	116		
		8	1	77	73	86		
		9	1.6	102	73	77		
Bulk	Arsenic	10	2.5	46	41	37	37	5
		11	4.4	44	31	33		
		12	6.8	22	43	35		
	Selenium	10	2.5	26	21	33	31	4
		11	4.4	22	33	35		
		12	6.8	34	41	33		
	Antimony	10	2.5	55	39	44	46	7
		11	4.4	47	51	49		
		12	6.8	56	57	19		

Table 23: Percentage solubility of TEs in the three size modes for bituminous ash samples under neutral (pH = 7) condition

Particle regime	Element	DLPI Stage	Cut point (µm)	% Mobility				Uncertainty in mobility (95% CL)
				Run 1	Run 2	Run 3	Average	
Submicron	Arsenic	3	0.108	56	58	66	46	8
		4	0.17	53	40	33		
		5	0.26	29	33	46		
	Selenium	3	0.108	69	73	82	73	4
		4	0.17	66	74	63		
		5	0.26	81	72	74		
	Antimony	3	0.108	58	61	59	60	7
		4	0.17	69	77	73		
		5	0.26	52	44	49		
Fine fragment	Arsenic	6	0.4	61	52	51	52	4
		7	0.65	49	67	46		
		8	1	57	55	51		
		9	1.6	32	54	49		
	Selenium	6	0.4	81	73	89	76	8
		7	0.65	74	79	68		
		8	1	58	61	49		
		9	1.6	99	93	91		
	Antimony	6	0.4	58	53	51	60	6
		7	0.65	64	83	77		
		8	1	73	51	54		
		9	1.6	58	47	49		
Bulk	Arsenic	10	2.5	11	26	22	19	4
		11	4.4	13	23	29		
		12	6.8	16	14	17		
	Selenium	10	2.5	23	37	31	23	6
		11	4.4	11	32	33		
		12	6.8	19	12	13		
	Antimony	10	2.5	17	12	19	23	4
		11	4.4	24	22	31		
		12	6.8	22	33	23		

Table 24: Percentage solubility of TEs in the three size modes for bituminous ash samples under basic (pH = 11) condition

Particle regime	Element	DLPI Stage	Cut point (μm)	% Mobility				Uncertainty in mobility (95% CL)
				Run 1	Run 2	Run 3	Average	
Submicron	Arsenic	3	0.108	11	17	19	12	3
		4	0.17	8	13	12		
		5	0.26	6	9	15		
	Selenium	3	0.108	61	47	42	46	6
		4	0.17	36	57	51		
		5	0.26	36	43	39		
	Antimony	3	0.108	31	37	48	33	5
		4	0.17	26	39	22		
		5	0.26	24	32	41		
Fine fragment	Arsenic	6	0.4	22	19	16	16	2
		7	0.65	15	11	17		
		8	1	18	13	6		
		9	1.6	21	16	18		
	Selenium	6	0.4	54	43	36	43	4
		7	0.65	46	32	54		
		8	1	48	31	44		
		9	1.6	46	41	36		
	Antimony	6	0.4	44	42	49	48	4
		7	0.65	51	57	43		
		8	1	61	49	37		
		9	1.6	44	39	55		
Bulk	Arsenic	10	2.5	13	22	19	14	3
		11	4.4	17	8	12		
		12	6.8	21	11	7		
	Selenium	10	2.5	31	22	29	24	3
		11	4.4	28	21	23		
		12	6.8	19	14	25		
	Antimony	10	2.5	16	23	9	12	4
		11	4.4	13	7	17		
		12	6.8	12	5	8		

Table 25: Percentage solubility of TEs in the three size modes for sub-bituminous ash samples under acidic (pH = 2.88) condition

Particle regime	Element	DLPI Stage	Cut point (µm)	% Mobility				Uncertainty in mobility (95% CL)
				Run 1	Run 2	Run 3	Average	
Submicron	Arsenic	3	0.108	49	47	45	56	4
		4	0.17	66	58	59		
		5	0.26	61	57	59		
	Selenium	3	0.108	61	54	66	61	4
		4	0.17	62	58	56		
		5	0.26	56	71	66		
	Antimony	3	0.108	64	59	66	62	3
		4	0.17	59	69	67		
		5	0.26	61	57	59		
Fine fragment	Arsenic	6	0.4	48	66	61	62	6
		7	0.65	73	51	54		
		8	1	62	49	46		
		9	1.6	77	69	83		
	Selenium	6	0.4	71	73	64	63	3
		7	0.65	68	57	59		
		8	1	66	63	58		
		9	1.6	59	64	57		
	Antimony	6	0.4	71	64	73	64	4
		7	0.65	59	53	66		
		8	1	56	81	63		
		9	1.6	54	61	69		
Bulk	Arsenic	10	2.5	23	21	26	19	3
		11	4.4	22	16	18		
		12	6.8	12	19	16		
	Selenium	10	2.5	22	19	28	23	4
		11	4.4	28	19	30		
		12	6.8	22	27	11		
	Antimony	10	2.5	24	41	43	23	7
		11	4.4	17	19	8		
		12	6.8	16	26	13		

Table 26: Percentage solubility of TEs in the three size modes for sub-bituminous ash samples under neutral (pH = 7) condition

Particle regime	Element	DLPI Stage	Cut point (µm)	% Mobility				Uncertainty in mobility (95% CL)
				Run 1	Run 2	Run 3	Average	
Submicron	Arsenic	3	0.108	54	36	52	40	6
		4	0.17	26	41	39		
		5	0.26	41	29	46		
	Selenium	3	0.108	55	47	31	52	7
		4	0.17	52	59	66		
		5	0.26	41	67	53		
	Antimony	3	0.108	91	55	73	69	6
		4	0.17	59	64	66		
		5	0.26	74	66	69		
Fine fragment	Arsenic	6	0.4	46	54	52	47	3
		7	0.65	49	47	47		
		8	1	46	41	39		
		9	1.6	54	36	52		
	Selenium	6	0.4	49	47	45	53	5
		7	0.65	57	71	62		
		8	1	41	54	51		
		9	1.6	63	50	43		
	Antimony	6	0.4	74	68	76	74	4
		7	0.65	71	79	74		
		8	1	83	71	92		
		9	1.6	68	67	70		
Bulk	Arsenic	10	2.5	24	11	15	14	3
		11	4.4	14	10	13		
		12	6.8	21	12	9		
	Selenium	10	2.5	24	39	31	31	3
		11	4.4	28	34	37		
		12	6.8	26	28	31		
	Antimony	10	2.5	6	11	15	11	3
		11	4.4	14	9	7		
		12	6.8	12	18	7		

Table 27: Percentage solubility of TEs in the three size modes for sub-bituminous ash samples under basic (pH = 11) condition

Particle regime	Element	DLPI Stage	Cut point (µm)	% Mobility				Uncertainty in mobility (95% CL)
				Run 1	Run 2	Run 3	Average	
Submicron	Arsenic	3	0.108	33	26	24	28	4
		4	0.17	39	16	27		
		5	0.26	33	28	22		
	Selenium	3	0.108	33	26	22	23	3
		4	0.17	26	18	17		
		5	0.26	28	19	21		
	Antimony	3	0.108	58	40	66	48	6
		4	0.17	41	49	37		
		5	0.26	55	43	39		
Fine fragment	Arsenic	6	0.4	36	33	32	35	4
		7	0.65	21	39	20		
		8	1	34	43	39		
		9	1.6	41	39	37		
	Selenium	6	0.4	31	36	35	29	5
		7	0.65	37	27	39		
		8	1	33	31	22		
		9	1.6	31	8	12		
	Antimony	6	0.4	58	68	51	53	4
		7	0.65	47	57	42		
		8	1	49	59	53		
		9	1.6	46	57	51		
Bulk	Arsenic	10	2.5	1	1	3	1	1
		11	4.4	0	0	2		
		12	6.8	2	1	0		
	Selenium	10	2.5	9	13	13	12	3
		11	4.4	14	10	21		
		12	6.8	16	7	8		
	Antimony	10	2.5	10	18	17	13	3
		11	4.4	22	17	11		
		12	6.8	8	6	12		

REFERENCES

1. EIA Report - https://www.eia.gov/coal/annual/pdf/table26.pdf.

2. EIA Report - https://www.eia.gov/outlooks/aeo/pdf/AEO2018.pdf.

3. Bachmann, J.D., Damberg, R.J., Caldwell, J.C., Edwards, C., and Koman, P.D., "Review of the National Ambient Air Quality Standards for Particulate Matter: Policy Assessment of Scientific and Technical Information," (OAQPS Staff Paper), EPA- 452/R-96-013 (NTIS PB97-115406), Washington, DC (1996).

4. Wolff, G.T., Closure by the Clean Air Scientific Advisory Committee (CASAC) on the staff paper for particulate matter, EPA-SAB-CASAC-LTR-96-008, U.S. Environmental Protection Agency, Washington, DC, June 13, 1996.

5. Chunmei Wang, Wayne S. Seames, Mandar Gadgil, Jason Hrdlicka & Gregory Fix (2008) Comparison of Coal Ash Particle Size Distributions from Berner and Dekati Low Pressure Impactors, Aerosol Science and Technology, 41:12, 1049-1062.

6. William P. Linak, Jong-Ik Yoo, Shirley J. Wasson, Weiyan Zhu, Jost O.L. Wendt, Frank E. Huggins, Yuanzhi Chen, Naresh Shah, Gerald P. Huffman, M. Ian Gilmour, Ultrafine ash aerosols from coal combustion: Characterization and health effects, Proceedings of the Combustion Institute, Volume 31, Issue 2, 2007, Pages 1929-1937.

7. Gregory Fix, Wayne Seames, Michael Mann, Steve Benson, Dean Miller, The effect of combustion temperature on coal ash fine-fragmentation mode formation mechanisms, Fuel, Volume 113, 2013, Pages 140-147.

8. USEPA. 1998. Particulate matter research needs for human health risk assessment to support future reviews of the national ambient air quality standards for particulate matter. U.S. Environmental Protection Agency, Report No. EPA/600/R97/132F.

9. Gauderman WJ, Avol E, Gilliland F, Vora H, Thomas D, Berhane K, et al. The effect of air pollution on lung development from 10 to 18 years of age. N Engl J Med 2004; 351:1057–67.

10. Seaton, A., Godden, D., MacNee, W. et al. 1995. Particulate air pollution and acute health effects. The Lancet 345, pp 176-178.

11. Dockery DW, Pope CA, Xu X, Spengler JD, Ware JH, Fay ME et al. An association between air pollution and mortality in six US cities. 1993; 329: 1753–9.

12. Seames, W.S., 2000.The partitioning of trace elements during pulverized coal combustion, Ph.D. dissertation, University of Arizona, Tucson, AZ.

13. Sarofim, A. F., Howard, J. B., and Padia, A. S., Combust. Sci. Technol. 16:187 (1977).

14. Quann, R. J., Neville, M., Janghorbani, M., Mims, C. A., Sarofim, A. F., 1982. Mineral Matter and Trace Element Vaporization in a Laboratory-Pulverized Coal Combustion System. Environ.Sci.Technology 16, pp 776-781.

15. McElroy, M.W., Carr, R.C.; Ensor, D.S., Markowski, G.R. Size Distribution of Fine Particles from Coal Combustion; Science 1982, 215(4528),13-19.

16. Helble, J. J., and Sarofim, A. F., Combustion & Flame 76:183 (1989).

17. S.G. Kang, Ph.D. Thesis, Department of Chemical Engineering, MIT, 1991.

18. Jorma Joutsensaari, Esko I. Kauppinen, Petri Ahonen, Terttaliisa M. Lind, Sampo I. Ylätalo, Jorma K. Jokiniemi, Jukka Hautanen, Markku Kilpeläinen, Aerosol formation in real scale pulverized coal combustion, Journal of Aerosol Science, Volume 23, Supplement 1, 1992, Pages 241-244.

19. Linak, W. P., Miller, A. C., Seames, W. S., Wendt, J. O. L., Ishinomori, T., Endo, Y., Miyamae, S. 2002. On Trimodal Size Distribution in Fly Ash from Pulverized-Coal Combustion. In Proceedings of The Combustion Institute.

20. R.J. Quann, Ph.D. Thesis, Ash vaporization under simulated pulverized coal combustion conditions, Department of Chemical Engineering, MIT, 1982.

21. Quann, R. J., Sarfoim, A. F. 1982. Vaporization of Refractory Oxides during Pulverized Coal Combustion. In The Combustion Institute.

22. Neville, M., Quann, R. J., Haynes, B. S., Sarofim, A. F. 1981. Vaporization and Condensation of Mineral Matter During Pulverized Coal Combustion. In The Combustion Institute.

23. Senior, C.L., et.al., 1999. Toxic Substances from Coal Combustion – A Comprehensive Assessment. Final Report, July 2001, pp 1-786.

24. Gao Y, Nelson ED, Field MP, Ding Q, Li H, Sherrell RM, Gigliotti CL, Van Ry DA, Glenn TR, Eisenreich SJ. Characterization of atmospheric trace elements on PM2. 5 particulate matter over the New York–New Jersey harbor estuary. Atmospheric Environment. 2002 Feb 1;36(6):1077-86.

25. Linak WP, Miller CA, Wendt JO. Comparison of particle size distributions and elemental partitioning from the combustion of pulverized coal and residual fuel oil. Journal of the Air & Waste Management Association. 2000 Aug 1;50(8):1532-44.

26. Srinivasachar, S., Bease, P. R., Porle, K., Mauritzson, C., Haythornthwaite, S., 1997. Ultra-high efficiency ESP for fine particulate and air toxics control, 1-17.

27. Senior, C.L., Lignell, D, O., Sarofim, A, F., Mehta, A., Modeling arsenic partitioning in coal-fired power plants, Combustion and Flame 3, 209-221.

28. Crocker, C.R., Benson, S. A., Laumb, J, D., SCR catalyst blinding due to sodium and calcium sulfate formation, American Chemical Soceity, 169-172.

29. Natusch, D. F. S., Wallace, J. R., Evans Jr., C. A., Toxic Trace Elements: Preferential Concentration in Respirable Particles, Science 18, 202-204.

30. Mu-Qing, Yu., Gui-Qin, Liu., Determination of trace arsenic, antimony, selenium and tellurium in various oxidation states in water by hydride generation and atomic-absorption spectrophotometry after enrichment and separation with thiol cotton 4, 265-270.

31. Seames, W.S., Gadgil, M., Wang, C and Fetsch, J. 2006. Impacts on Trace Metal Leaching from Fly Ash Due to the Co-Combustion of Switch Grass with Coal in 23rd International Pittsburgh Coal Conference, Pittsburgh, PA, United States.

32. David W. Evans, James G. Wiener & John H. Horton (2012) Trace Element Inputs from a Coal Burning Power Plant to Adjacent Terrestrial and Aquatic Environments, Journal of the Air Pollution Control Association, 30:5, 567-573.

33. Swaine, D. J., 1994. Trace elements in coal and their dispersal during combustion. Fuel Processing Technology 39, pp 121–137.

34. Seames, W.S., Sooroshian, J. and Wendt, J.O.L. Assessing the solubility of inorganic compounds from size-segregated coal fly ash aerosol impactor samples. 2001. Aerosol Science 33, pp 77-90.

35. Charles Wortmann, Martha Mamo, and Charles Shapiro, Management Strategies to Reduce the Rate of Soil Acidification, University of Nebraska Extension NebGuide G03-1503-A.

36. C.M. Jones, J.L. Hahn, B.H. Magee, N.Q.S. Yuen, K. Sandefur, J.N. Tom, and C. Yap, Utilization of Ash from Municipal Solid Waste Combustion, Final Report, Phase II, September 1999, NREL/SR-570-26068.

37. Izquierdo, M., Querol, X., 2012. Leaching Behavior of Elements from Coal Combustion Fly Ash, International Journal of Coal geology 94, pp 54-66.

38. Hassett, D.J., Pflughoeft-Hassett, D.F., Heebink, L.V., 2005, Leaching of CCBs: Observations from over 25 years of Research. Fuel 84, pp 1378-1383.

39. Shah, P., Strezov, V., Stevanoc, C., Nelson, P.F., 2007. Speciation of Arsenic and Selenium in Coal Combustion Products. Energy & Fuels 21. pp 506-512.

40. Monahan –Pendergast, MT., Przybylek, M., Lindblad, M., Wilcox, J., 2008. Theorotical predictions of arsenic and selenium species under atmospheric conditions. Atmospheric Environment 42, pp 2349-2357.

41. Wang, T., Wang, J., Tang, Y., Shi, H and Ladwig, K. 2009. Leaching Characteristics of Arsenic and Selenium from Coal Fly Ash: Role of Calcium, Energy & Fuels, 23, pp 2959-2966.

42. Jankowski, J., Ward, C.R., French, D., Groves, S., 2006. Mobility of trace elements from selected Australian fly ashes and its potential impact on aquatic ecosystems. Fuel 85. pp 243 – 256.

43. Huggins, F.E., Senior. C.L., Chu, P., Ladwig, K., Huffman, G.P., 2007. Selenium and Arsenic Speciation in Fly Ash from Full Scale Coal-Burning Utility Plants. Environmental Science Technology 41, 3284-3289.

44. Narukawa, T., A. Takatsu, K. Chiba, K.W. Riley, and D.H. French. 2005. Investigation on chemical species of arsenic, selenium, and antimony in fly ash from coal fuel thermal power stations. J. Environ. Monit. 7:1342–1348.

45. Jackson, B.P., and W.P. Miller. 1999. Soluble arsenic and selenium species in fly ash/organic waste-amended soils using ion chromatography-inductively coupled plasma mass spectrometry. Environ. Sci. Technol. 33:270–275.

46. Miravet, R., Lopez-Sanchez, J.F., Rubio, R., 2006. Leachability and analytical speciation of antimony in coal fly ash. Analytica Chimica Acta 576, 200-206.

47. Matusiewicz, H., Krawczyk, M., 2008. Determination of total antimony and inorganic antimony species by hydride generation in situ trapping flame atomic absorption

spectrometry: a new way to (ultra) trace speciation analysis. Journal of Analytical Atomic Spectrometry 23, pp 43-53.

48. Varrica, D., Bardelli, F., Dongarra, G., Tamburo, E., 2013. Speciation of Sb in airborne particulate matter, vehicle brake linings, and brake pad wear residues. Atmospheric Environment 64. Pp 18-24.

49. Raeva, Anna & Klykov, Oleg & Kozliak, Evguenii & T. Pierce, David & Seames, Wayne. (2011). In Situ Evaluation of Inorganic Matrix Effects on the Partitioning of Three Trace Elements (As, Sb, Se) at the Outset of Coal Combustion. Energy & Fuels. 25 (10).

50. Raeva, Anna & Dongari, Nagaraju & Artemyeva, Anastasia & Kozliak, Evguenii & T. Pierce, David & Seames, Wayne. (2014). Experimental simulation of trace element evolution from the excluded mineral fraction during coal combustion using GFAAS and TGA–DSC. Fuel. 124. 28–40.

51. Senior, C. L., Bool III, L. E., Srinivasachar, S., Pease, B. R., Porle, K., 2000. Pilot scale study of trace element vaporization and condensation during combustion of a pulverized sub-bituminous coal. Fuel Processing Technology 63, pp 149-165.

52. Bool III, L. E., Helble, J. J., 1995. A Laboratory Study of the Partitioning of Trace Elements during Pulverized Coal Combustion. Energy & Fuels 9, pp 880-887.

53. Senior, C. L., Helble, J. J., Sarofim, A, F., Emissions of mercury, trace elements, and fine particles from stationary combustion sources, Fuel Processing Technology 65-66, 263-288.

54. Seames, W.S and Wendt, J.O.L. 2007. Regimes of association of arsenic and selenium during pulverized coal combustion. Proceedings of the Combustion Institute 31, pp 2839-2846.

55. Goodarzi, F., Huggins, F.E., 2001. Monitoring the species of arsenic, chromium and nickel in milled coal, bottom ash and fly ash from a pulverized coal – fired power plant in western Canada. Journal of Environmental Monitoring 1. Pp 1-6.

56. Goldberg, S., Martens, D.A., Forster, H.S., Herbel, M.J., 2006. Speciation of Selenium (IV) and Selenium (VI) using Coupled Ion Chromatography – Hydride Generation Atomic Absorption Spectrometry. Soil Science Society of America Journal 70, pp 41-47.

57. Xu M, Yan R, Zheng C, Qiao Y, Han J, Sheng C. Status of trace element emission in a coal combustion process: a review. Fuel Processing Technology. 2004 Feb 15;85(2-3):215-37.

58. Kolker. A, et.al., 2002. Toxic Substances from Coal Combustion- A Comprehensive Assessment, Phase II: Element Modes of Occurrence for the Ohio 5/6/7, Wyodak, and North Dakota Coal Samples, Open-File Report 02-224.

59. Finkelman, R.B.,1994. Modes of occurrence of potentially hazardous elements in coal: levels of confidence, Fuel Processing Technology 39, pp 21-32.

60. https://www.epa.gov/sites/production/files/2015-12/documents/3052.pdf.

61. Gadgil, M.R.,2006. Leachability of Trace Elements from Biomass Fly Ash Samples, M.S Thesis, University of North Dakota, Grand Forks, ND.

62. https://www.epa.gov/sites/production/files/2015-12/documents/1311.pdf.

63. Shah, A. D., Huffman, G. P., Huggins, F. E., Shah, N., 1993. Role of Calcium During Combustion Revisited. American Chemical Society Preprints 38, pp 1210-1216.

64. Huffman, G. P., Huggins, F. E., Shah, N., and Shah, A. D., Behavior of basic elements during coal combustion, Progress in energy and combustion science, 16 #4, 293-302 (1990).

65. Helble, J. J., Srinivasachar, S., Boni, A. A., Kang, S. G., Graham, K. A,, Sarofim, A. F., Beer, J. M, Gallagher, N. B., Bool, L. E., Peterson, T. W., Wendt, J. 0. L., Shah, N., Huggins, F. E., and Huflinan, G. P., Mechanism of ash evolution – A fundamental study. Part I: Low-rank coals and the role of calcium. Proceedings, Engineering Foundation Conference on Inorganic Transformation and Ash Deposition, (Palm Coast, FL), pp. 209-228, Benson, S. A. (Ed.) (1991).

66. J.J. Helble, R.O. Sterling, Reaction of arsenic vapor species with fly ash compounds: kinetics and speciation of the reaction with calcium silicates, Chemosphere,Volume 51, Issue 10,2003,Pages 1111-1119.

67. Dean, J. A. 1992. Langes Handbook of Chemistry. (14th ed.). New York: McGraw-Hill.

68. Jones, D.R.,1995. The leaching of major and trace elements from coal ash, Swain., Goodarzi, F(Eds)., Environmental aspects of trace elements in coal, Springer.

69. Raven, K.P., Jain, A. and Loeppert, R.H., 1998. Arsenite and arsenate adsorption on ferrihydrite: kinetics, equilibrium, and adsorption envelopes. Environmental Science & Technology, 32(3), pp.344-349.

70. Van der Hoek, E.E., Bonouvrie, P.A., Comans, R.N.J., 1994. Sorption of As and Se on mineral components of fly ash: Relevance for leaching processes. Applied Geochemistry 9, 403-412. Smedley, P.L. and Kinniburgh, D.G., 2002. A review of the source, behaviour and distribution of arsenic in natural waters. Applied geochemistry, 17(5), pp.517-568.

71. Modeling Arsenic and Selenium Leaching from Acidic Fly Ash by Sorption on Iron Hydroxide in the Fly Ash Matrix Eline E. Van der Hoek and and Rob N. J. Comans, Environmental Science & Technology 1996 30 (2), 517-523.

72. Norman, N. C.,1998. Chemistry of Arsenic, Antimony, and Bismuth. New York: Blackie Academic and Professional.

73. Kim, A.G., Kazonich, G., 2004. The silicate/non-silicate distribution of metals in fly ash and its effect on solubility. Fuel 83, 2285-2292.

CHAPTER 5

TRACE ELEMENT SOLUBILITY IN SIZE-SEGREGATED FLY ASH PARTICLES COLLECTED ACROSS A WET SCRUBBER FROM A FULL-SCALE PULVERIZED COAL UTILITY BOILER

Prasanna Seshadri, Dennis Sisk, Frank Bowman, Steve Benson, and Wayne Seames*

University of North Dakota, Department of Chemical Engineering, 241 Centennial Drive Stop 7101, Grand Forks, ND 58201

ABSTRACT

Size segregated fly ash samples were collected at both the inlet and exit of a wet flue gas desulfurization scrubber attached to a utility sized boiler burning a mixture of two Powder River Basin sub-bituminous coals. Fly ash samples collected in a low-pressure impactor were used to generate particle size distribution curves. Additional size segregated samples were subjected to a series of solvents to determine overall trace element availability and solubility in three different leaching environments – acidic, neutral and basic.

Of particular interest in this study were the fly ash solubility characteristics of three trace elements namely, arsenic, selenium and antimony. Results indicate that the scrubber was able to capture most of these trace elements across a wide size range. However, selenium emissions showed a slight increase at the scrubber outlet for particles present in the smaller submicron mode, represented in the particle size range 0.11 – 0.65 μm, suggesting potential displacement reactions within the scrubber and subsequent Se vapor to solid partitioning resulting in a changed form. Leaching studies of fly ash particles shows TEs to be mobile under some of the test conditions. However, the degree of mobility was influenced by both particle size and the pH of the environment.

BACKGROUND

Fly ash generated from pulverized coal combustion has a wide size range including some fine aerosols. Some of these particles can affect boiler performance by forming fireside ash deposits [1,2] while others may pose health and environmental hazards [3,4,5]. Particulate control equipment (PCE) such as electrostatic precipitators (ESPs) are less efficient in capturing fine particles especially those in the size range of 0.1 – 1 μm [6,7,8]. Fly ash particles that escape PCEs enter the atmosphere with the flue gas stream and can stay suspended in air or settle downwind of the stack onto soil surfaces and water bodies inducing adverse health effects [9]. Aside from health and environmental impacts, some of the elements present in fly ash can also impact the performance of air pollution control technologies such as Selective Catalytic Reduction (SCR) by causing catalyst deactivation [10,11].

The most common mineral forms in coals include quartz, alumino silicate clays, calcite and pyrite. [12,13,14,15]. During combustion, these minerals can undergo physical and/or chemical transformations producing intermediate gases, liquids and solids. Of importance in assessing an elements role for environmental effects is knowledge of its composition in the different fly ash size fractions. This in turn depends on the elements original mode of association in the coal and furnace operating conditions, amongst other factors..

Earlier studies, including work done by McElroy [16], Quann [17] and Kauppinen et al. [18], reported fly ash size distribution from coal combustion to be bimodally distributed. The two modes include a larger bulk size mode usually centered around diameters > 4 μm [19,20] and a smaller submicron (or ultrafine) mode typically centered around diameters < 0.4 μm [21]. However, Kang [22] suggested that ash particles from pulverized coal combustion may have a trimodal distribution which includes a central fine fragment mode. Joutsensaari et al. [23] also observed this central mode for ash PSDs generated using real scale power plant data. Later work done by Linak et al., [24] and Seames et al. [9,25] suggest that coal fly ash particle formation is more accurately described by a trimodal particle size distribution which includes a distinct central or fine fragment mode centered at approximately 2.0 μm. Compared to both submicron and bulk size modes, the formation of the fine fragment mode might be the consequence of multiple mechanisms including heterogenous vapor condensation, shedding of char, fragmenting of larger fly ash particles and particle-to-particle impaction [24,26,27,28]. The relative importance of composition based on size is an important part of fly ash research and could serve to inform appropriate control and mitigation strategies.

Of particular concern is the abundance and solubility of some of the trace elements (TE) present in fly ash, mainly As, Se and Sb, which are classified environmental toxins [9,29,30,31]. They tend to be enriched in the smaller submicron and fine fragment size fractions of ash [6,9,31,32] which increases the potential risk of increased TE emissions in the environment through stack emissions.

Arsenic, selenium, and antimony occur naturally in coal, albeit in variable concentrations depending on their source, but their levels usually do not exceed 100 ppmw [33,34]. They can be bonded to the carboxylic and phenolic groups of the coal maceral. This form of occurrence is referred to as the organically associated fraction [12,31,35]. TEs can also be present as mineral inclusions contained with the carbonaceous matrix or as discrete exclusions which are mostly free of organic matter [31,36,37].

Because of their semi-volatile nature, all three trace elements (As, Se and Sb) can vaporize during combustion primarily forming oxy-anions [9,31,38]. The extent of volatilization primarily depends on their mode of occurrence in coal and the combustion environment. Material associated with the organic structure of the coal or in small inclusions will experience very high temperatures and can vaporize with a high efficiency as it diffuses out of the burning char particle and into the bulk gas phase. Elements associated with excluded mineral grains do not experience as high a temperature and TEs contained in them are less likely to volatilize and may remain trapped in these particles [9,38,39].

Vaporized TEs partition back to the solid phase mainly through a surface chemical reaction on existing fly ash particles where they are sorbed to an active cation site [9,38]. These active sites, mainly provided by Ca and Fe cations, are mainly the result of major element vaporization and their subsequent nucleation/coagulation or heterogenous condensation onto existing ash particles [9,12,31,38]. If these sites are not available, the dominant mechanism is adsorption and a much lower fraction of the vaporized TEs will partition back to the PM. Due to their surface morphology, most of the smaller sized submicron and fine fragment particles have fairly high surface to volume ratios and particle number densities (as compared to bulk ash particles) and hence can offer more active surface sites for TE heterogeneous transformation reactions. Additional explanations of TE partitioning is available in the literature [9,31,38,40,41,42].

While most TE partitioning reactions are well understood, it is also important to consider the presence of other major species in the flue gas, notably sulfur oxides (SO_X) and chlorides, and their potential effects on TE transformations. Most of the Sulfur (S) present in fuel is released during combustion but only a fraction of the total fuel S is emitted as gas phase stack emissions. Most of it is retained in ash particles through vapor to solid transformation reactions, which includes both homogeneous nucleation/coagulation [28,43] and heterogeneous condensation reactions [28,43,44,45,46,47]. Sulfur present in the gas phase will compete with other vaporized species (including TEs) for active cation sites (preferentially Fe when available and Ca after Fe sites are exhausted) present on fly ash surfaces, mainly through heterogeneous condensation/adsorption reactions [9,28]. This is especially true for sulfur present in the fine fragment region, where, TE transformation reactions are also controlled by the availability of active cation sites on existing fly ash surfaces.

The gas-solid partitioning mechanisms of TEs have an impact on the solubility of trace element-containing species formed during combustion. Large quantities of fly ash are either stored temporarily in stockpiles or disposed of in landfills or lagooned where it can come into contact with run-off water [9,48]. Some of the elements contained in fly ash may be released to the environment (ground water, rivers, etc.) when ash comes into contact with water raising concerns of contamination. Trace elements present on the smaller submicron and fine fragment particles and those present on the surface of bulk ash particles have a high solubility potential, whereas elements present inside the cores of bulk ash particles are less likely to be mobile unless they come into contact with strong acids. [9,39,48]. Those TEs forming oxy-anions in the gas phase will have significant partitioning back to the PM surface.. The oxidation state of the TE after its partitioning back to the PM surface has an effect on both solubility and toxicity in a particular aqueous environment. For example, selenium on fly ash surfaces, may be present as either a selenate (SeO_4^{2-}, +6 oxidation state) or selenites (SeO_3^{2-}, with a +4-oxidation state) oxy-anion. The selenite forms are typically more soluble in aqueous solutions, but the selenite forms are usually more toxic than the comparable selenates [3,49,50].

LEACHING STUDIES

Laboratory leaching studies are a qualitative means to assess potential environmental impacts from combustion generated PM. Leaching studies are simple lab scale tests, wherein a sample of collected PM is dissolved under different pH conditions and the concentration of each element in the leaching solution is then measured. Whether or not certain toxic elements in fly ash are stable and do not impact the surrounding environment depends on their solubility in the specific pH conditions encountered [48]. Data from leaching studies can be used to assess the severity of threat in particular environments. Fly ash enters the environment through three main pathways: bulk ash piles, deposition downwind and inhalation.

Bulk ash particles collected by pollution control equipment are typically disposed of in landfills or utilized as a sheetrock or asphalt filler material [3,48,51]. During rainstorms, water percolates through the ash pile, absorbing water-soluble material and thereby changing water pH substantially. Only the TEs present on the surface of bulk particles are generally mobile, as most of the TEs in these particles are fused within the refrozen solid spheres that characterize this ash fraction. Depending on the pH of the ash, the pH of water can be lower than the original rain source (acidic ash) or higher (basic ash). Since the ash in this study was alkaline, leaching results from bulk particles under basic conditions will be the most important for this size fraction.

Trace elements contained in the fine particulate mode account for only a small portion of the mass of ash disposed of in the landfill but have the potential to be easily dissolved as a result of their presence on the surface of particles. Since the collection efficiencies for ESPs and Baghouses (BHs) is lower for particles in this size range as compared to bulk ash particles, they will represent the majority of the particulate matter (PM) mass emitted with the flue gas. These particles leaving with the flue gas will settle out onto the ground downwind of the combustor. Ground moisture and rainfall may dissolve soluble trace element-containing compounds and carry them into the soil. These compounds may then be absorbed into plants through roots in the soil or percolate downwards to the water table [3,9,39]. The solubility will depend primarily upon the pH of the soil where the particles deposit, rather than the pH of the ash itself [3,9,39]. Fine particulate solubility data in an acidic medium can demonstrate TE solubility in acidic soil, such as that in the eastern United States, whereas solubility data in a basic medium can represent TE solubility in more alkaline soils, such as that typical of the western U.S.

Finally, airborne particles that have not yet settled to the ground can be inhaled into human and animal respiratory systems [3, 21,39]. Particles in the submicron mode pose the greatest inhalation health risk due to their longer atmospheric residence times (mean residence times of 100-1000 hours compared to 10-100 hours for super-micron particles) [39,52,53] and their ability to penetrate deeper into the lungs. Solubility data under neutral conditions represents the pH environment of respiratory fluids and can be used to determine potential TE exposure through inhalation.

RESEARCH OBJECTIVES

Leaching characteristics of TEs from fly ash have been studied by a host of other researchers both under lab scale and utility scale conditions. Wang et al [54] and Schwartz et al [55] studied fly ash TE leachability for samples collected from utility boilers. However, such tests were conducted for ash samples drawn directly from a ESP or BH and do not account for any size dependent effects on element mobility.

Seames et al [3] developed a modified Toxicity Characteristic Leaching Procedure (TCLP) protocol to study TE mobility for size segregated coal fly ashes collected on greased membranes from a lab-scale combustor. They reported data for element mobility for two fly ash size fractions (submicron and supermicron/bulk) and under two pH conditions – 2.9 and 5. Additionally, Seames et al [39] also reported fly ash TE mobility data for samples collected from a lab-scale furnace burning bituminous coal. Their study reported fly ash TE mobility for all three size fractions and under three leaching conditions.

While extensive research data is readily available for TE mobility for ash from both lab-scale and utility boilers, data are reported mostly for loose ash samples collected from PCEs. However only limited data is available for size segregated fly ash samples, especially for samples collected from utility-scale boilers. Senior et al [56] conducted sampling work in a utility boiler and used a cascade impactor to quantify particle bound selenium distribution across a wet scrubber. Leaching behavior, however, was not the focus of their work and selenium was the only trace metal of interest.

The main objectives of this research project, therefore, were to characterize fly ash particles upstream and downstream of a wet scrubber from a utility scale boiler and determine the composition for three trace elements, As, Se and Sb, as well as for major elements such as Ca and Fe in the ash fractions. Short term leaching tests were then conducted to determine the relative solubility of these trace

elements in size segregated fly ash under three pH environments. Of particular importance are TE mobility data for ash samples collected after the scrubber, since this ash has the potential to come into direct contact with the environment due to continuous stack emissions. The scope of the work focused on studying selected fly ash characteristics, including size distribution, composition and solubility, for particles collected upstream and downstream of the scrubber and did not address the overall performance of the scrubber itself.

EXPERIMENTAL METHODS

Size segregated PC combustion fly ash samples were collected upstream and downstream of the wet scrubber of a utility scale boiler. The unit was running at full load during sample collection. A 1:1 (by weight) blend of two different PRB coals was fired during testing and the two coals will be referred to as coal 1 and coal 2. The relevant properties for the two coals including proximate, ultimate and ash composition analysis are shown in Table 28. The two coals have very similar properties including heating value and volatile content. Based on ash composition Coal 1 has more calcium and also slightly higher iron than coal 2. These two cations play a very important role in TE post combustion speciation. For low rank fuels such as PRB coals, chemical fractionation data has shown [22,31] that most of the total Ca is either organically associated or present in an ion-exchangeable form, both of which are extremely reactive under flame conditions.

In addition to the above analysis, a microwave assisted acid digestion was also performed to determine the total concentration of TEs in coal. This was carried out following an EPA recommended method at an outside laboratory. Results of this analysis are also shown in Table 28. Data shows TE concentration levels comparable for other PRB coals as reported by other researchers [9,31]

Table 28: Relevant properties of the two coals including TE and major ash element analysis reported on a SO$_3$ free basis

				Ash Composition (% SO$_3$-free basis)		
Proximate (as received)	**Coal 1**	**Coal 2**		**Oxide**	**Coal 1**	**Coal 2**
Total Moisture	24.59	24.58		SiO$_2$	30.94	29.09
Ash	4.59	3.82		Al$_2$O$_3$	13.33	17.12
Volatile Matter	31.59	31.23		TiO$_2$	1.1	1.14
Fixed Carbon	39.23	40.37		Fe$_2$O$_3$	6.35	4.94
Btu/lb	9086	9427		CaO	25.67	18.77
				MgO	5.4	4.99
Ultimate (as received)	**Coal 1**	**Coal 2**		K$_2$O	0.77	1.41
Carbon	53.96	55.69		Na$_2$O	1.95	5.4
Hydrogen	6.51	6.63		P$_2$O$_5$	0.95	0.25
Nitrogen	0.78	0.67		SrO	0.4	0.8
Total Sulfur	0.25	0.32		BaO	0.66	0.99
Oxygen by difference	33.91	32.87		MnO$_2$	0.02	0.05

Element	Concentration (μg/g)	±
As	2.3	0.25
Se	1.2	0.1
Sb	0.4	0.15

The coals were also analyzed by computer-controlled scanning electron microscopy (CCSEM) to determine mineral types, abundance, and sizes within the coal and these results are shown in Table 29. Only those minerals whose levels were found to be significant in the coal are reported here. For both coals quartz (SiO_2) and clay minerals (including kaolinite, montmorillonite, K-Al silicate, Ca-Al silicate, Aluminosilicate etc) were the most abundant. Coal 2 had significant amounts of pyrite and this is important for two reasons:

1. Pyritic association is one of the common modes of TE presence in coal especially for As, Se and Sb

2. Higher amounts of pyrite indicates the possibility of more Fe in the fly ash which can become active sites for TE transformation reactions.

Table 29: CCSEM analysis of the two test coals expressed as weight percentage on a mineral basis.

Coal	MINERAL	Particle Size, microns						
		1.0 - 2.2	2.2 - 4.6	4.6 - 10	10 - 22	22- 46	46 - 400	Totals
Coal 1	QUARTZ	0.5	8.1	6.6	8	2.7	1.8	27.7
	KAOLINITE	0.2	3.2	2.3	6.7	2.3	1.4	16.1
	MONTMORILLONITE	0	0.2	0.7	3.2	0.8	0.8	5.7
	K-Al-SILICATE	0.1	0.1	0.4	0.4	0.2	0.1	1.3
	Ca-Al-SILICATE	0.1	1.6	0.4	1.1	0.1	0	3.3
	ALUMINOSILICATE	0	0.3	0.2	0.7	0.4	0.6	2.2
	PYRITE	0	0.7	0.1	1.9	1	0.5	4.2
	Ca-Al-P	0.1	1	1.6	1.9	0.1	0	4.7
	Si-RICH	0.8	2.6	0.8	0.7	0.4	0.6	5.9
	OTHER MINOR SPECIES	0 - 0.2	0 - 1.4	0 - 0.4	0 - 0.3	0 - 0.2	0	4.6
	UNCLASSIFIED	1.9	13.6	4.1	4.4	0.3	0	24.3
Coal 2	QUARTZ	0.4	1.9	3.1	3.3	2.1	1.8	18.6
	KAOLINITE	0.7	2.2	3.9	6.2	7.1	9.3	23.4
	MONTMORILLONITE	0.1	0.5	0.5	0.9	1.1	0.5	3.6
	K-Al-SILICATE	0	0.9	0.6	0.7	0.6	0.4	3.2
	Ca-Al-SILICATE	0.1	0.6	0.3	0.3	0.4	0.7	2.4
	ALUMINOSILICATE	0	0	0.2	0.5	0.4	0.5	1.6
	PYRITE	0.4	0.5	1.5	3	3.2	2	10.6
	Ca-Al-P	0.1	1	1.4	0.5	0.8	0.4	4.2
	Si-RICH	0.2	1.2	0.5	0	0.3	0.8	3
	OTHER MINOR SPECIES	0 - 0.1	0 - 1	0 - 1.4	0 - 0.5	0 - 0.8	0 - 0.4	6.3
	UNCLASSIFIED	1.5	6.1	5.5	4.6	3.8	1.6	23.1

Both coals had a significant amount of unclassified minerals which are those that do not fit into any of the known mineral classifications. The unclassified minerals are those that do not fit into any of the known mineral classifications and account for 24.3 wt% of the minerals found in Coal 1 and 23.1%

minerals found in coal 2. In coal 1 most of them were 2.2 to 4.6 microns in size whereas in coal 2 they were fairly evenly divided over the different size bins except for the smallest size (1.0 to 2.2 microns). The nature of mineral matter in coal determines its transformation into ash during combustion and the nature of the resulting ash (e.g. chemical composition and particle size distribution) which could be useful to predict TE transformations. Additionally, CCSEM data can be used to detail mineral matter transformations important to boiler fouling and slagging [57].

Fly ash sampling methods

Fly ash sampling was conducted using a modified EPA Method 5 sample train with the heated filter section replaced by a cyclone and multi-stage impactor. A heated, stainless steel (SS) isokinetic sample probe consisting of a probe sheath, probe liner and pitot ends (all SS, Model # M5-S1, Environmental Supply Company, Inc., USA) was used to sample ash-laden flue gas. Flue gas from the probe entered a pre-separator cyclone which efficiently removes the majority of ash particles greater than 5 μm. Downstream of the cyclone a Dekati Low Pressure Impactor (DLPI) collected size segregated ash particles on greased pre-weighed membranes (Millipore). The DLPI is a state-of-the-art 13-stage cascade impactor for measuring gravimetric particle size distribution of very small particles. It size-classified particles from 10 microns (μm) to 30 nm. A filter stage accessory enabled collection of particles smaller than 30 nm in diameter. Membrane properties and the method of preparation for fly ash collection have been described in detail elsewhere [39].

Moisture concentration was determined by drawing a measured volume of the duct gas through a set of chilled impingers (placed in an ice-bath). The total weight gain of the impingers and the volume of gas sampled were measured to calculate the moisture concentration in the duct gas. The entire sampling train was leak checked prior to any sampling and again after each run. The probe was placed in the wet scrubber inlet and the system was allowed to heat to the desired temperature. Static pressure, temperature and velocity of the flue gas were all measured at the sampling location. Sampling commenced only after the probe and DLPI assembly reached sampling temperature. Five sets of impactor samples were collected upstream of the scrubber and 4 sets were collected downstream of it. The sampling time at the inlet was 15 minutes per sample while outlet sampling occurred over a 60-minute time period due to lower ash loading downstream of the scrubber. Collected samples were carefully placed in petri dishes and stored in air tight desiccator jars.

Analysis methods for TEs and other major elements in fly ash

Collected DLPI membranes were analyzed to determine both total concentration and environment-specific solubility of TEs in size segregated fly ash particles. Ash-laden membranes from each sample set were carefully weighed (precision of ±0.01 mg) and the total mass of ash collected on each stage was calculated. The DLPI has a constant flow rate of 30 normal L/min, which allowed the overall ash concentration (μg ash / Nm^3 flue gas) for each DLPI stage to be calculated. This data was used to generate particle size distribution (PSD) curves which represent fly ash loading as a function of average

particle aerodynamic diameter. The PSD curves were also used to identify the separate PM modes of occurrence in the coal.

Membranes from one sample set were digested in individual sample vials following the method of Seames and Wendt [9,38]. An acid solution containing 300 ml hydrofluoric (HF) acid, 100 ml nitric acid (HNO_3) and 100 ml hydrochloric acid (HCl) in 500 ml of ultrapure water was used as the primary digestion fluid. All three acids were of TE grade and were acquired from Fisher Scientific, USA. Four ml of this dissolving acid mixture was added to each of the polycarbonate vials containing the sample membranes and then sealed. Vials were then sonicated (unheated) for 12 minutes and allowed to rest for 24 hours. Then they were sonicated another 12 minutes after which four ml of boric acid solution (prepared by dissolving 56.6g of boric acid crystals in 1000 ml ultrapure water) was added to the vials to break the fluorosilicate bonds formed during the initial acid dissolving step. The vials were sonicated again for another five minutes. The extracted solution was then used to determine the total concentration of trace elements (As, Se and Sb) and other major elements (Ca and Fe) on each stage. An additional vial containing only a pre-weighed plain greased membrane was also dissolved using the above steps to perform a blank correction for TEs and other major elements of analysis. Sulfur analysis was performed using a Scanning Electron Microscope (SEM) where a morphological analysis was carried out to completely characterize ash particles.

In addition to this total digestion analysis, three other sample sets were used in leaching studies to determine how much of the total mass of each element is soluble under different pH conditions. One set of samples was leached in an acidic environment (pH = 2.88), the second set in a neutral environment (pH = 7), and the last set in a basic environment (pH = 11). In this procedure, individual impactor membranes were place into 10ml polycarbonate vials and 5ml of the leaching fluid were then added and the pH was checked. If the pH changed from the target value, a buffer solution was added drop-wise until the pH was restored. The pH was rechecked after 20 minutes and then after every hour to make sure it remained constant. Capped vials were placed in a test tube wrist shaker for about 18 hours. After 18 hours the samples were removed from the shaker and allowed to rest for an hour. The solution was then decanted from this vial into another vial. Trace amounts of fluids entrained in the membranes were removed by placing the membrane into a syringe without a tip and squeezing out the moisture. The liquid recovered by the syringe was then transferred into the vial containing the leachate. Similar to the earlier acid digestion method, blank corrections for TE leaching in a given medium (acidic, neutral or basic) wer performed by following the above steps for three pre-weighed plain greased membranes in three individual vials (one for each leaching fluid).

Sample analysis of leachates was carried out using a SOLAAR Flame Atomic Absorption Spectrometry (FAAS, Model M6, Thermo Electron Corporation, United Kingdom) for Ca and Fe and using Graphite Furnace Atomic Absorption Spectrometry (GFAAS, Model GF95Z, Thermo Electron Corporation, United Kingdom) with Zeeman background correction for trace elements analysis (As, Se and Sb). Four pre-weighed greased membranes were used to make blank corrections during elemental analysis. One was digested in the acidic mix and the other three were digested in the respective leaching solutions. Sample extract solutions from each particular sample were analyzed at least three times for each element for QA purposes. Final elemental concentrations (μg TE / Nm^3 flue gas) were calculated using the average mass fraction (from replicate analysis) for that particular DLPI stage times the overall ash loading for that given impactor stage.

The mass fraction of solubility material of an element in a given leaching environment (acidic, basic or neutral) was calculated as the ratio of its mass fraction in any given DLPI stage to its mass fraction for the same DLPI stage as determined by the total digestion method and reported as a percentage. Once the degree of solubility of a given TE for all thirteen stages were calculated, single stage solubility values from all stages comprising a given size fraction, i.e., submicron, fine fragment and bulk, were averaged together to give an average solubility for that size fraction. This averaging was done to account for variability resulting from measurement uncertainty. However, solubility values for individual impactor stages within a particular size fraction were often found to be within 10% of each other. This is because trace elements found in a particular size fraction are expected to undergo the same partitioning mechanism in the post combustion environment and their final forms are expected to have similar solubility characteristics. It must be emphasized that even though element solubility is quantified, the results should be treated as qualitative. The particle sample weight was so small that measurement uncertainty was significant in some cases, with percentage solubility of more than 100% calculated for some samples.

RESULTS AND DISCUSSION

Particle Size Distribution

The average mass size distribution of particulate collected upstream and downstream of the scrubber is illustrated in Figure 22. Error bars in the data represent 95% confidence intervals based on five runs at the scrubber inlet and 4 runs at the scrubber outlet. Results show a trimodal distribution – a smaller submicron mode, an intermediate fine fragment mode and a larger bulk mode - in both inlet and outlet samples. Based on the overall PSD curve, at both the scrubber inlet and outlet, DLPI stages 3-5 are defined as the submicron particle mode, 6-9 as the fine particulate mode, and stages 10-12 as the bulk particle size mode. The scrubber removed particles across the entire size range of fly ash. The fine fragment mode with a peak at about 0.8 μm is not removed as well as the other modes. Relative to the bulk particle size mode, the fine fragment and submicron modes are usually enriched with toxic trace metals [6,9,31,32,42].
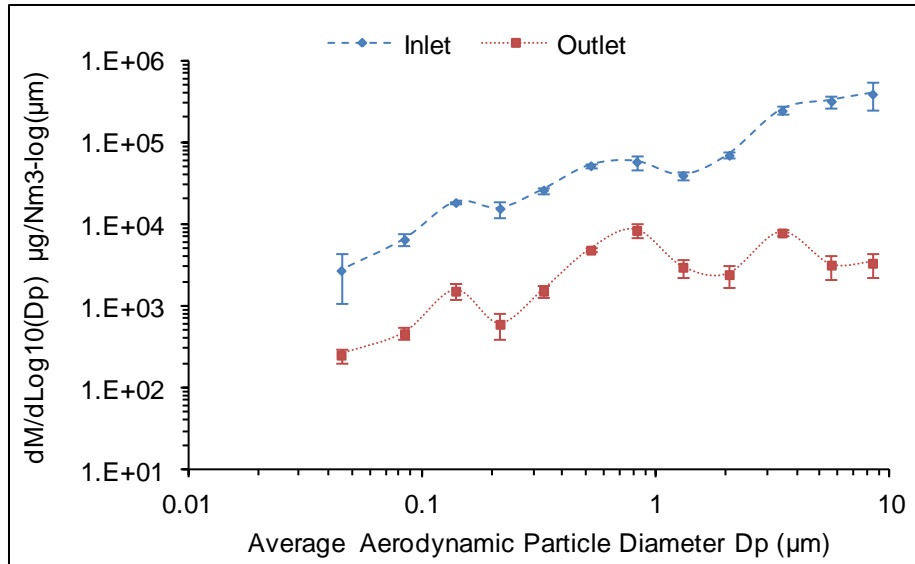
Figure 22: Average Particle Size Distribution (PSD) for fly ash particles collected upstream and downstream of the wet scrubber

Composition of fly ash

The compositions of the size segregated fly ash samples collected using the DLPI are presented for the elements of interest - Ca, Fe, S, As, Se and Sb at both scrubber inlet and outlet and also for S (at inlet only). The complete mass distribution data for elements of interest is provided in the Appendix.C Figures 24-29, respectively. Some important important observations are summarized below:

- Calcium and iron both mirrored overall PSD distribution curves especially for submicron and fine fragment particles, indicating efficient removal across the scrubber.

- Most of the sulfur in fly ash was distributed in the smaller submicron and fine fragment particles, indicating vaporization and subsequent condensation/sorption/reaction mechanisms for vapor partitioning to fly ash surfaces. Sulfur will compete with TEs for both Fe and Ca sites.

- Both, As and Sb had similar distributions at both inlet and outlet including matching peaks for both submicron and fine fragment regions. Additionally, these peaks matched Ca peaks for both inlet and outlet data indicating the possibility of Ca-As and Ca-Sb species in fly ash.

- Se, on the other hand, exhibited anomalous behavior compared to both As and Sb, especially at the scrubber outlet. Data, as shown in figure 4, indicates a slight increase in submicron selenium at scrubber outlet compared to inlet concentrations. Possible reasons for this behavior are discussed in the below section.

While most of the vaporized Se is expected to partition onto solid surfaces, a very small amount is expected to stay in vapor phase because of its relatively high vapor pressure. Any vapor phase selenium entering the scrubber is expected to dissolve in the slurry and enter the liquid phase or leave the stack with the flue gas. To a varying degree, both forms of selenium i.e. (Se(IV) and Se(VI)) are known to be soluble in the scrubber slurry, but distinguishing between them is not possible in this case.

Fly ash data at the scrubber outlet shows an interesting trend for selenium, especially in the smaller submicron and fine particulate mode. For the smaller size fractions, between 0.1-0.5 µm, selenium showed increases in concentrations at the scrubber outlet compared to inlet levels. Even though the scrubber does not efficiently capture smaller sub-micron sized particles, it will still remove a considerable fraction of the particles in this size range as shown in the case of calcium, iron and arsenic distributions. However, we do not see a similar trend for selenium. An increase in loading for Se in sub-micron sized particles could be attributed to any of the following factors or a combination there-of:

1. Displacement reactions in the scrubber where sulfur present in the FGD solution reacts with the cations that were holding the selenium oxy-anion and thereby liberating Se back in the gas phase. Released Se vapor can then nucleate/coagulate or even condense forming very small particles. This is somewhat akin to mercury re-emission in wet FGDs, where operating conditions, amongst other factors, can directly result in some of the captured mercury (typically present as Hg^{2+} in the FGD slurry) reduced to its elemental form, causing it to exit with the flue gas. While elemental Hg is not easily captured on particulate surfaces, Se oxyanions readily partition from its vapor phase.

2. Gas-to-particle conversion of selenium vapor across the scrubber as evidenced by Senior et al [56] in a study conducted on a utility boiler burning bituminous coal. Although most of the vaporized Se is expected to partition onto solid surfaces prior to reaching PCDs, a very small amount is expected to stay in vapor phase and is expected to dissolve in the FGD slurry or leave as flue gas vapor. This creates the possibility of a portion of vapor phase Se transforming to solid phase as the cool flue gas exits the scrubber.

3. A combination of mechanisms1 and 2.

4. About 50% of the fly dust emitted through the stack originates in evaporative droplets saturated with gypsum [59]. A significant portion of Se in the FGD can be associated with the gypsum [60] and this can be entrained with the flue gas exiting the FGD and can be collected as fine PM.

Factors affecting Se partitioning on solid particulate surfaces in a wet scrubber are not fully understood yet and may require additional data on Se in the scrubber slurry, gypsum stream and chloride purge. Such an analysis is outside the scope of work presented in this paper.

Based on data from both sampling locations, it is clear selenium in flue gas is influenced by FGD operation and it seems to be independent of coal rank. Such behavior can have implications on overall selenium emissions through the stack as well as transfer into the aqueous phase, which is critical for meeting Effluent Limitation Guidelines (ELG) requirements.
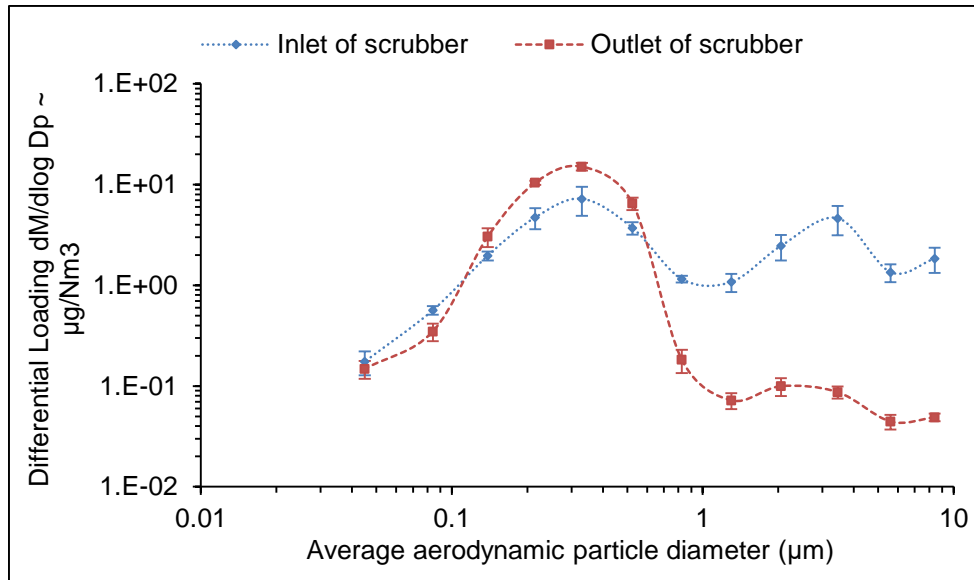
Figure 23: Fly ash loading for selenium in combustion flue gas collected upstream and downstream of the wet scrubber

LEACHING STUDIES

Results from the leaching studies are shown in Tables 30, 31 and 32 for arsenic, selenium and antimony, respectively. Uncertainty in data was calculated using a 95% confidence interval for the average value. For a given size fraction in a specific leaching fluid, the average mobility was calculated from individual mobilities for all the stages comprising that size fraction. Leaching data for individual stages were in turn averages based on the number of sample replicates during instrumental analysis. Data in these tables are used to consider the effect of particle model of occurrence and leaching fluid pH on TE mobility. A ND value indicates element solubility was below detection limits.

Table 30: Relative solubilities of arsenic from three size fractions of coal fly ash sampled at scrubber inlet and outlet (%)

Particle regime & sample location	Acidic pH = 2.88	Neutral pH = 7	Basic pH = 11
Sub micron			
Scrubber inlet	68±4	56±3	ND
Scrubber outlet	77±8	51±7	6±2
Fine fragment			
Scrubber inlet	77±3	61±5	ND
Scrubber outlet	76±6	57±5	ND
Bulk			
Scrubber inlet	24±3	13±3	5±1
Scrubber outlet	22±3	11±2	5±2

Table 31: Relative solubilities of selenium from three size fractions of coal fly ash sampled at scrubber inlet and outlet (%)

Particle regime & sample location	Acidic pH = 2.88	Neutral pH = 7	Basic pH = 11
Sub micron			
Scrubber inlet	67±3	55±4	21±3
Scrubber outlet	92±6	76±6	37±2
Fine fragment			
Scrubber inlet	71±3	49±3	27±2
Scrubber outlet	92±4	73±3	39±4
Bulk			
Scrubber inlet	25±5	21±2	11±2
Scrubber outlet	21±3	19±3	9±2

Table 32: Relative solubilities of antimony from three size fractions of coal fly ash sampled at scrubber inlet and outlet (%)

Particle regime & sample location	Acidic pH = 2.88	Neutral pH = 7	Basic pH = 11
Sub micron			
Scrubber inlet	75±5	61±2	54±3
Scrubber outlet	69±5	60±3	60±6
Fine fragment			
Scrubber inlet	80±5	67±3	61±4
Scrubber outlet	81±5	63±3	57±3
Bulk			
Scrubber inlet	15±3	11±2	ND
Scrubber outlet	14±3	16±2	ND

Effect of particle size fraction

For all three trace elements, solubility was much higher in the smaller submicron and fine particulate fractions as compared to the larger bulk fly ash particles. This is mainly due to surface partitioning mechanisms resulting in TE enrichment on small particle surfaces. TEs present on the surface of ash are more soluble compared to those trapped inside the ash as in the case of silicate association or the non-vaporized fraction present in bulk ash particles. These are tightly bound and are not soluble unless they encounter extremely acidic environmental conditions.

All three TEs showed about equal solubility in the submicron and fine particulate size regimes under all three environmental conditions. This indicates the possibility of the same partitioning mechanism for both size fractions for that particular TE. Furthermore, with the exception of selenium, there was no clear distinction in element solubility between scrubber inlet and outlet for both As and Sb in all three

111

size modes. This indicates that these TEs haven't changed form/species across the scrubber and that the decrease in mass loading is solely due to the physical scrubbing of the PM out of the flue gas and not due to any effect from the FGD solvent. However, for Se, the increase in mobility for both submicron and fine fragment fractions across the scrubber is mainly due to change in speciation as explained in the earlier section. If sulfur had replaced Se in the Fe-SeO$_x$ and Ca-SeO$_x$ complexes on the surfaces of the particles, the Se is probably now in the form of SeOH or SeO$_2$ and thus more soluble in all fluids. Additionally, physically adsorbed species tend to have a higher mobility than chemically adsorbed species due to relatively weaker attractive forces between the adsorbent and the adsorbate molecule.

Effect of leaching fluid pH

All three TEs were more soluble in an acidic environment as compared to both neutral and basic environments. For both As and Se, relative solubility progressively decreased as the pH increased from acidic to basic conditions. This was observed especially for the smaller submicron and fine particulate size fractions. Arsenic, in particular, was almost completely insoluble under basic conditions for all particle sizes. Researchers have identified the formation of insoluble precipitates such as Ca$_3$(AsO$_4$)$_2$ as a reason for reduced dissolved arsenic in high pH solutions [48,51]. Formation of ettringite [48,51,61,62] can also reduce arsenic solubility at high pH levels. Selenium, on the other hand, showed slight solubility under alkaline conditions in both submicron and fine particulate fractions.

Antimony, similar to As and Se, had higher solubility in an acidic environment for the smaller size fractions. However, unlike As and Se, Sb solubility decreased only slightly with increasing pH and it showed similar solubility characteristics under both neutral and alkaline conditions. Antimony solubility in a basic solution indicates that it could potentially be present also in the form of oxyanions, which are normally highly soluble in alkaline solutions [48].

Effect of TE solubility on control and immobilization strategies

Based on the TE solubility data presented in Tables 30-32 and an understanding of how fly ash materials are distributed in the environment, inferences can be made regarding potential environmental and human health impacts which can help design cost effective designs to mitigate any such threats. Additionally, gaining a better understanding of the underlying reasons for TE mobility can also aid in better control on environmental impacts for a wide variety of utilization and disposal practices.

Data shows that for As and Sb, the FGD removes a majority of the PM from the flue gas with no change in the form of the As or Sb. Thus, the FGD has a positive environmental impact for these TEs. For Se, data shows a substantial reduction in the mass of Se emitted with the flue gas. However, the Se in this emission will be somewhat more mobile in all three solvents, although the overall effect is still likely to be positive from using an FGD to decrease Se emission impacts. However, as mentioned earlier, it is important to recognize that the leaching data is qualitative.

When considering fly ash effects on human health, the chief concern is emission of submicron particulate matter into the atmosphere with flue gas which can then be inhaled by human beings and animals. For this scenario, the neutral pH solubility results are the most relevant as respiratory fluids have a pH close to 7. Data from Tables 3-5 show that a substantial fraction of all three TEs in submicron particles were soluble under neutral pH conditions.

Tables 30-32 indicate that all three TEs in the fine particulate mode were extremely soluble under acidic conditions, while they showed slightly reduced solubility under neutral conditions. Arsenic was completely insoluble in basic conditions whereas selenium showed slight solubility. Antimony, on the other hand, showed significant to fairly high solubility under all three conditions. All three TEs in the fine fragment mode can pose a significant amount of risk in the eastern part of the US where the soil is acidic. They can either directly enter the water table with the rain water or can be absorbed by plant roots which can then be consumed by other living beings causing TE ingestion into their system. Fine fragment antimony may cause the same concern in the western part of United States because of the soil's alkaline nature there. Selenium however was only mildly soluble under the same conditions and is not expected to be a big concern in the western U.S. Arsenic was found to be completely insoluble in alkaline solution and is not expected to leach from the ash in western U.S. soil whose pH is basic.

Since this coal ash is alkaline, it will raise the pH of water that seeps through the ash pile. Based on data in Tables 3-5, for bulk size particles all three TEs had only slight to no solubility under basic conditions and hence should not be expected to pose a significant environmental problem if disposed of in a landfill. TE solubility is likely not an issue for by-products using ash, such as concrete mixes, because these will be trapped deep within the concrete matrix and will not become mobile unless exposed to extreme pH conditions [9,39]

CONCLUSIONS

Size segregated fly ash samples were collected at both scrubber inlet and outlet for a utility boiler burning a mixture of two PRB coals. PSD curves show a tri-modal distribution for fly ash at both scrubber inlet and outlet. Ash samples, from both scrubber inlet and outlet, were analyzed to determine the concentration of the three TEs of interest for this study – As, Se and Sb. The scrubber had an overall positive impact by removing a majority amount of all three elements. In the case of As and Sb, removal across the scrubber occurred without change in form (physical scrubbing) as evidenced by both mass distribution and mobility data. However, Se data indicates there has been a change in form from scrubber operating conditions resulting in slightly increased emissions for the submicron range. This was further confirmed by differences in mobility data between inlet and outlet conditions. The scrubber still removed a significant portion of the Selenium yielding an overall positive effect for emission impacts. Results from leaching indicate all three TEs may be solubilized in lungs after subsequent inhalation. Further, all three TEs present in the fine fragment mode may become mobile in acidic soils, while both Se and Sb can also become partially mobile in alkaline soils. All three TEs found in the bulk particle mode showed no significant solubility indicating less potential for serious health or environmental risks from this size range.

APPENDIX C

SUPPLEMENTARY FIGURES, TABLES AND DISCUSSION FOR CHAPTER 5

Mass Size Distributions for Major and TEs

As shown in Figure 24, calcium data from the scrubber outlet indicates a trimodal distribution with peak diameters similar to those observed for the overall fly ash distribution (0.14, 0.8 & 3.45 μm) although a similar level of correspondence was not observed for the inlet data. Similar to calcium, iron loading at the scrubber outlet, shown in Figure 25, also had submicron and fine fragment mode peaks at 0.14 and 0.8 μm, respectively, but without a clear bulk mode peak. Removal of Ca and Fe is generally similar to removal of the overall ash, with comparable removal fractions for all but bulk mode Fe.

Calcium, iron, and sulfur present in the smaller ash size fractions is expected to play a critical role in TE transformation reactions in combustion flue gas. For these high Ca coals, partitioning of vapor phase TE to particulates is expected to be governed by the number of active Ca and Fe sites available on the surface of fly ash particles and particle morphology for reactions within the particle pores.

Figure 24: Fly ash loading for calcium in combustion flue gas collected upstream and downstream of the wet scrubber

Figure 25: Fly ash loading for iron in combustion flue gas collected upstream and downstream of the wet scrubber

As mentioned earlier, the presence of sulfur in flue gas (mainly as SO_3) will impact the availability of active Fe and Ca cations for vapor to solid TE transformation reactions. One of the mechanisms for sulfur vapor to solid transformation is reaction with surface cations (mainly iron and calcium) on fly ash particles and these reactions proceed much faster than TE sorption reactions. This mechanism is mostly observed for sulfur present in the smaller submicron and fine fragment particles where active sites are readily available. However, unlike TEs, homogeneous nucleation and heterogeneous condensation with other volatile species such as Na, K etc promotes sulfur vapor to particle transformations in the very fine particles (<0.1 µm).

Figure 26 shows the sulfur distribution in fly ash collected upstream of the wet scrubber. Even though the data shown is derived from SEM based analysis, the results can still be used to understand S distribution in the various size fractions of fly ash. Of particular importance is the distribution of sulfur in the smaller size range between 0.1 – 2 µm where competing reactions with TEs are likely to take place. The observed submicron and fine fragment peaks (at 0.22 and 0.52 µm, respectively) were the same for both Ca and S indicating the possibility of sulfation of calcium sites in the smaller sizer fractions. The concentration of the S in the bulk mode is lower than the fine fragment mode and seems to be nearly independent of particle size.

Figure 26: Fly ash loading for sulfur in combustion flue gas collected upstream of the wet scrubber

Arsenic data (Figure 27), shows submicron and fine fragment peaks that closely resemble those of calcium at inlet conditions. This suggests vapor phase arsenic partitioning on reactive and readily available calcium fly ash sites, where it would be expected to mainly form calcium arsenate. Formation of calcium arsenate, containing the As(V) oxyanion, has been reported by a host of other researchers [9,10,24,31,32]. However, for a low sulfur coal such as the one in our tests, arsenic can also partition onto iron fly ash sites (forming iron arsenate) depending on availability [9,31,38]. Arsenic exhibits a relatively small bulk mode peak than seen for Ca, Fe, and bulk ash, consistent with preferential partitioning to smaller sizes with greater (relative) surface area. Arsenic present in the bulk size mode includes species formed as a result of a surface chemical reaction (or within the pores of the particle) and will also include the non-vaporizing portion from the parent coal, which is expected to be associated mainly with silicates and aluminosilicates as well as iron rich particles derived from pyrite. While arsenic can partition to both calcium and iron sites, calcium-based compounds and complexes are expected to dominate arsenic distribution in fly ash due to much higher amounts of calcium, in comparison to iron, both in the original fuel and final fly ash particles. A significant amount of this calcium is expected to be present as reactive sites on the surface of fly ash based on its original mode of occurrence in the fuel.

Arsenic at the scrubber outlet had submicron and fine fragment mode peaks 0.14 and 0.8 µm, similar to both calcium and iron modes, which further indicates the presence of calcium arsenate and also, possibly, iron arsenate in the fly ash stream
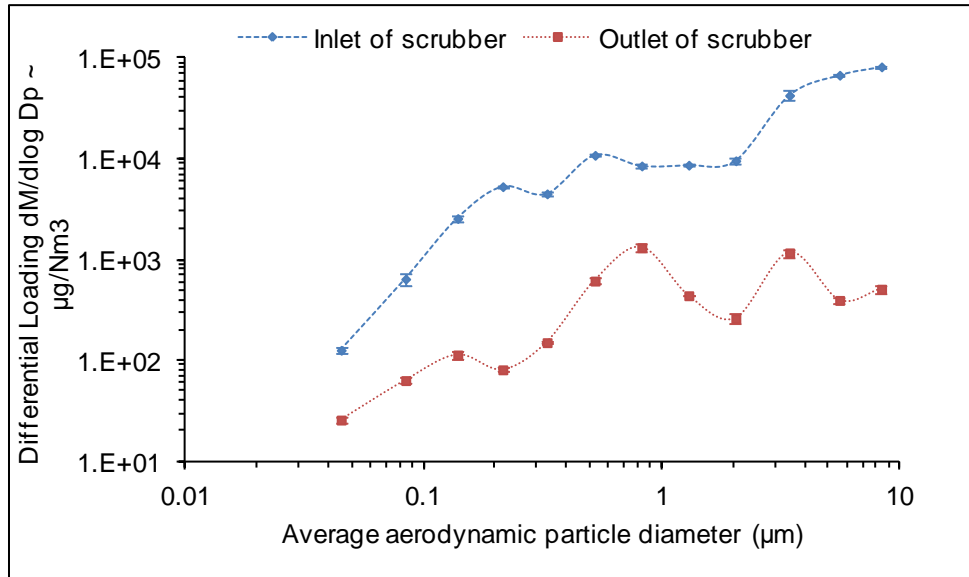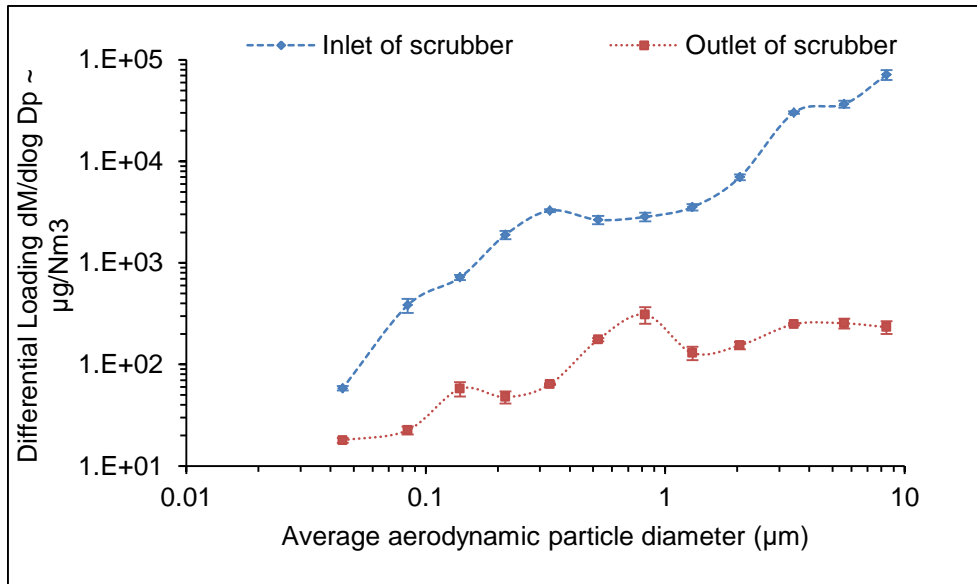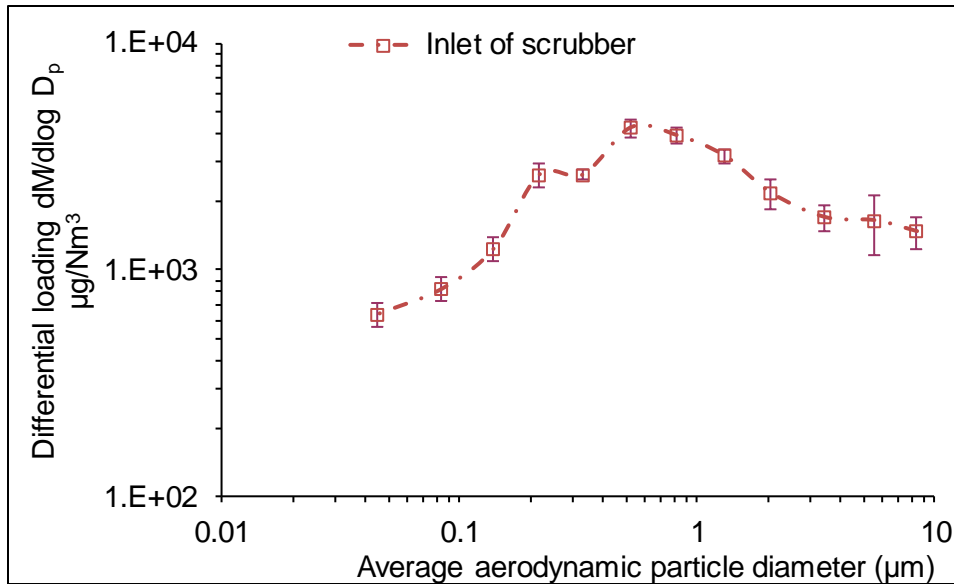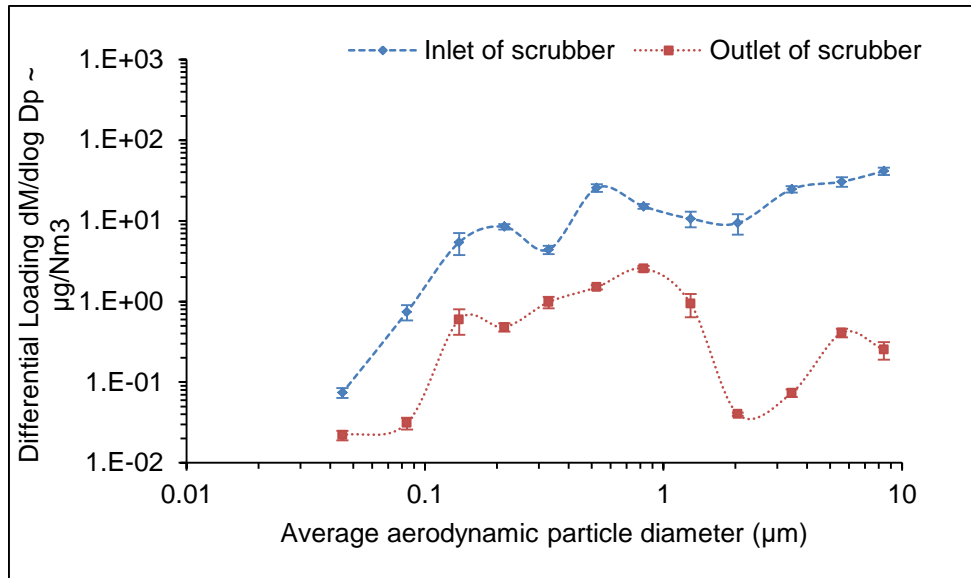
Figure 27: Fly ash loading for arsenic in combustion flue gas collected upstream and downstream of the wet scrubber

Figure **Error! Reference source not found.**28 shows the selenium concentration versus size distribution in fly ash particles before and after the scrubber. Research work done by Seames, et al. [9,31,38] showed selenium vapors preferentially partition to iron over calcium when both sites are available. Selenium data at the scrubber inlet support that observation. Both selenium and iron (Figure 5) exhibit inlet distributions with fine fragment and bulk mode peaks at 0.33 and 3.45 µm, respectively, as would be expected if selenium is associating with iron. This also suggests possible selenium speciation with iron in fly ash. However, as with the case of arsenic, calcium-selenium complexes are also expected to be present due to high amounts of calcium in the ash and its distribution across a wide size range. Selenium present in the bulk size mode will mostly consist of metal (calcium and iron) selenate complexes and may also include a small portion of non-vaporized fraction from the original fuel. Mechanisms governing the transformation of vapor phase selenium and arsenic onto fly ash particles into the different size regimes has been clearly explained by other researchers elsewhere [9,31,32,38,40].
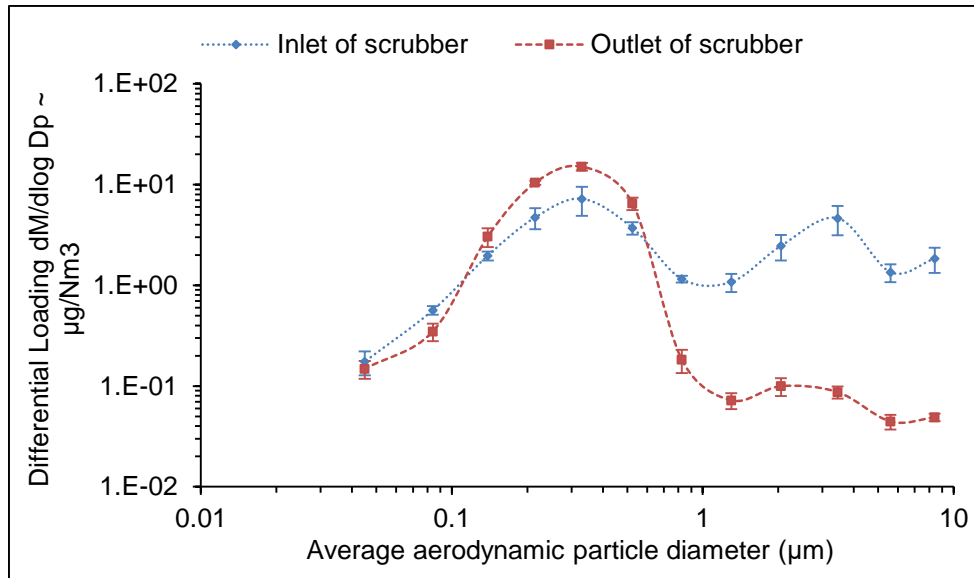
Figure 28: Fly ash loading for selenium in combustion flue gas collected upstream and downstream of the wet scrubber

Figure 29 shows the distribution of antimony in fly ash collected at the scrubber inlet and outlet. Antimony exhibits similar behavior to arsenic in a combustion system. Once in the vapor phase, antimony can react with active cationic sites (e.g., calcium oxide) incorporated on particle surfaces and partition onto the solid phase [9,31,42]. Peaks at submicron and fine particulate regions were observed for the same size fraction as observed for arsenic. This indicates the possibility of a similar partitioning mechanism as both elements are present in the same group of the periodic table and are expected to exhibit similar behavior in a combustion environment. Antimony in the bulk size fraction could be the result of the non-vaporized portion in the original fuel [9,42,58].

Scrubber outlet data showed submicron and fine fragment mode peaks at 0.14 and 0.8 µm, where similar peaks were observed for both arsenic and the overall ash distribution. Antimony present in the bulk mode had no well-defined peak and was efficiently removed by the scrubber.
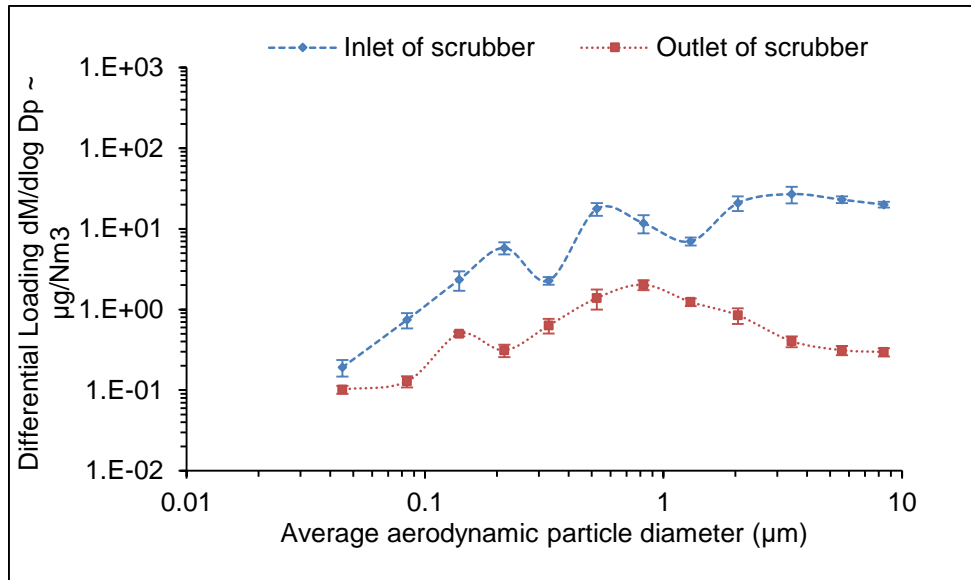
Figure 29: Fly ash loading for antimony in combustion flue gas collected upstream and downstream of the wet scrubber

Table 33: Percentage solubility of TEs in the three size modes for scrubber inlet samples under acidic (pH = 2.88) condition

Particle regime	Element	DLPI Stage	Cut point (µm)	% Mobility				Uncertainty in mobility (95% CL)
				Run 1	Run 2	Run 3	Average	
Submicron	Arsenic	3	0.108	64	63	59	68	4
		4	0.17	76	81	74		
		5	0.26	66	68	65		
	Selenium	3	0.108	66	69	71	67	3
		4	0.17	59	64	66		
		5	0.26	74	66	69		
	Antimony	3	0.108	91	79	74	75	5
		4	0.17	69	73	82		
		5	0.26	66	74	63		
Fine fragment	Arsenic	6	0.4	68	76	77	77	3
		7	0.65	83	73	86		
		8	1	69	76	68		
		9	1.6	84	79	81		
	Selenium	6	0.4	69	81	83	71	3
		7	0.65	67	68	71		
		8	1	66	67	74		
		9	1.6	68	70	62		
	Antimony	6	0.4	93	96	92	80	5
		7	0.65	79	81	77		
		8	1	84	83	81		
		9	1.6	66	63	69		
Bulk	Arsenic	10	2.5	33	31	22	24	3
		11	4.4	24	22	17		
		12	6.8	18	22	24		
	Selenium	10	2.5	37	23	39	25	5
		11	4.4	24	22	31		
		12	6.8	12	21	19		
	Antimony	10	2.5	13	21	23	15	3
		11	4.4	18	11	13		
		12	6.8	11	12	12		

Table 34: Percentage solubility of TEs in the three size modes for scrubber inlet samples under neutral (pH = 7) condition

Particle regime	Element	DLPI Stage	Cut point (µm)	% Mobility				Uncertainty in mobility (95% CL)
				Run 1	Run 2	Run 3	Average	
Submicron	Arsenic	3	0.108	51	54	62	56	3
		4	0.17	61	57	59		
		5	0.26	54	48	59		
	Selenium	3	0.108	62	54	57	55	4
		4	0.17	66	58	59		
		5	0.26	49	47	45		
	Antimony	3	0.108	57	61	62	61	2
		4	0.17	62	58	56		
		5	0.26	61	66	64		
Fine fragment	Arsenic	6	0.4	56	59	53	61	5
		7	0.65	46	58	55		
		8	1	71	64	73		
		9	1.6	56	61	83		
	Selenium	6	0.4	42	44	49	49	3
		7	0.65	46	48	54		
		8	1	57	55	51		
		9	1.6	49	53	41		
	Antimony	6	0.4	64	59	66	67	3
		7	0.65	64	66	59		
		8	1	73	71	69		
		9	1.6	62	78	77		
Bulk	Arsenic	10	2.5	21	16	14	13	3
		11	4.4	8	18	16		
		12	6.8	11	7	9		
	Selenium	10	2.5	17	22	21	21	2
		11	4.4	21	16	18		
		12	6.8	23	26	28		
	Antimony	10	2.5	11	14	12	11	2
		11	4.4	9	13	8		
		12	6.8	10	12	6		

Table 35: Percentage solubility of TEs in the three size modes for scrubber inlet samples under basic (pH = 11) condition

Particle regime	Element	DLPI Stage	Cut point (μm)	% Mobility			Average	Uncertainty in mobility (95% CL)
				Run 1	Run 2	Run 3		
Submicron	Arsenic	3	0.108	2	0	0	1	0
		4	0.17	1	1	0		
		5	0.26	1	0	0		
	Selenium	3	0.108	16	17	19	21	3
		4	0.17	26	27	31		
		5	0.26	22	19	16		
	Antimony	3	0.108	54	51	49	54	3
		4	0.17	53	56	58		
		5	0.26	54	49	62		
Fine fragment	Arsenic	6	0.4	3	1	1	1	0
		7	0.65	1	0	1		
		8	1	1	1	0		
		9	1.6	1	0	0		
	Selenium	6	0.4	33	28	29	27	2
		7	0.65	26	22	30		
		8	1	24	26	21		
		9	1.6	31	22	29		
	Antimony	6	0.4	68	53	66	61	4
		7	0.65	56	71	59		
		8	1	48	59	61		
		9	1.6	59	66	69		
Bulk	Arsenic	10	2.5	7	7	3	5	1
		11	4.4	5	2	8		
		12	6.8	5	2	7		
	Selenium	10	2.5	6	10	12	11	2
		11	4.4	17	9	13		
		12	6.8	11	8	9		
	Antimony	10	2.5	0	1	0	1	0
		11	4.4	1	1	2		
		12	6.8	0	1	0		

Table 36: Percentage solubility of TEs in the three size modes for scrubber outlet samples under acidic (pH = 2.88) condition

Particle regime	Element	DLPI Stage	Cut point (µm)	% Mobility			Average	Uncertainty in mobility (95% CL)
				Run 1	Run 2	Run 3		
Submicron	Arsenic	3	0.108	103	89	84	77	8
		4	0.17	69	73	74		
		5	0.26	66	74	63		
	Selenium	3	0.108	83	79	81	92	6
		4	0.17	105	101	93		
		5	0.26	94	96	99		
	Antimony	3	0.108	58	61	59	69	5
		4	0.17	69	77	73		
		5	0.26	71	72	79		
Fine fragment	Arsenic	6	0.4	99	93	91	76	6
		7	0.65	74	71	78		
		8	1	68	65	72		
		9	1.6	62	61	76		
	Selenium	6	0.4	96	93	111	92	4
		7	0.65	93	84	87		
		8	1	88	90	96		
		9	1.6	82	89	93		
	Antimony	6	0.4	83	74	78	81	5
		7	0.65	77	73	86		
		8	1	71	66	88		
		9	1.6	97	91	93		
Bulk	Arsenic	10	2.5	26	22	31	22	3
		11	4.4	22	24	21		
		12	6.8	11	19	19		
	Selenium	10	2.5	17	22	21	21	3
		11	4.4	21	16	18		
		12	6.8	19	29	28		
	Antimony	10	2.5	18	19	11	14	3
		11	4.4	15	17	17		
		12	6.8	8	13	6		

Table 37: Percentage solubility of TEs in the three size modes for scrubber outlet samples under neutral (pH = 7) condition

Particle regime	Element	DLPI Stage	Cut point (µm)	% Mobility				Uncertainty in mobility (95% CL)
				Run 1	Run 2	Run 3	Average	
Submicron	Arsenic	3	0.108	49	34	36	51	7
		4	0.17	63	59	54		
		5	0.26	49	64	53		
	Selenium	3	0.108	78	96	84	76	6
		4	0.17	72	68	77		
		5	0.26	68	71	73		
	Antimony	3	0.108	66	63	58	60	3
		4	0.17	59	64	57		
		5	0.26	48	59	63		
Fine fragment	Arsenic	6	0.4	51	62	47	57	5
		7	0.65	49	47	45		
		8	1	71	64	73		
		9	1.6	62	54	57		
	Selenium	6	0.4	71	76	77	73	3
		7	0.65	69	68	74		
		8	1	74	59	68		
		9	1.6	81	79	76		
	Antimony	6	0.4	55	59	61	63	3
		7	0.65	63	56	58		
		8	1	71	69	64		
		9	1.6	62	68	71		
Bulk	Arsenic	10	2.5	8	13	17	11	2
		11	4.4	11	7	6		
		12	6.8	11	14	9		
	Selenium	10	2.5	23	22	26	19	3
		11	4.4	19	14	16		
		12	6.8	11	18	22		
	Antimony	10	2.5	22	14	19	16	2
		11	4.4	13	16	19		
		12	6.8	10	12	18		

Table 38: Percentage solubility of TEs in the three size modes for scrubber outlet samples under basic (pH = 11) condition

Particle regime	Element	DLPI Stage	Cut point (μm)	% Mobility			Average	Uncertainty in mobility (95% CL)
				Run 1	Run 2	Run 3		
Submicron	Arsenic	3	0.108	7	7	11	6	2
		4	0.17	6	1	4		
		5	0.26	7	3	8		
	Selenium	3	0.108	36	41	34	37	2
		4	0.17	33	39	43		
		5	0.26	32	37	39		
	Antimony	3	0.108	77	54	51	60	6
		4	0.17	73	51	54		
		5	0.26	66	49	61		
Fine fragment	Arsenic	6	0.4	0	0	1	0	0
		7	0.65	0	0	1		
		8	1	0	0	0		
		9	1.6	1	0	0		
	Selenium	6	0.4	36	33	31	39	4
		7	0.65	46	41	39		
		8	1	54	36	52		
		9	1.6	43	32	29		
	Antimony	6	0.4	59	51	65	57	3
		7	0.65	48	46	52		
		8	1	56	61	66		
		9	1.6	56	64	59		
Bulk	Arsenic	10	2.5	7	8	11	5	2
		11	4.4	6	4	4		
		12	6.8	2	2	3		
	Selenium	10	2.5	11	10	7	9	2
		11	4.4	8	9	16		
		12	6.8	6	7	11		
	Antimony	10	2.5	2	3	1	1	1
		11	4.4	0	1	0		
		12	6.8	0	0	0		

REFERENCES

1. EIA Report, Electricity Net Generation: Total (All Sectors), Table 7.2a - https://www.eia.gov/totalenergy/data/monthly/pdf/sec7_5.pdf

2. EIA Report, Coal Production and Number of Mines by State and Coal Rank, 2016, Table 6 - https://www.eia.gov/coal/annual/pdf/table6.pdf

3. Li, Z.M., Sun, F.Z., Ma, L., Wei, W. and Li, F., 2016. Low-pressure economizer increases fly ash collection efficiency in ESP. Applied Thermal Engineering, 93, pp.509-517.

4. Seames, W.S., 2000. The partitioning of trace elements during pulverized coal combustion, Ph.D. dissertation, University of Arizona, Tucson, AZ.

5. Fix, G., Seames, W., Mann, M., Benson, S. and Miller, D., 2013. The effect of combustion temperature on coal ash fine-fragmentation mode formation mechanisms. Fuel, 113, pp.140-147.

6. Zellagui, S., Trouvé, G., Schönnenbeck, C., Zouaoui-Mahzoul, N. and Brilhac, J.F., 2017. Parametric study on the particulate matter emissions during solid fuel combustion in a drop tube furnace. Fuel, 189, pp.358-368.

7. Linak, W.P., Yoo, J.I., Wasson, S.J., Zhu, W., Wendt, J.O., Huggins, F.E., Chen, Y., Shah, N., Huffman, G.P. and Gilmour, M.I., 2007. Ultrafine ash aerosols from coal combustion: Characterization and health effects. Proceedings of the Combustion Institute, 31(2), pp.1929-1937.

8. Wang, C., Seames, W.S., Gadgil, M., Hrdlicka, J. and Fix, G., 2007. Comparison of coal ash particle size distributions from Berner and Dekati low pressure impactors. Aerosol Science and Technology, 41(12), pp.1049-1062.

9. Yan, R., Gauthier, D., Flamant, G. and Badie, J.M., 1999. Thermodynamic study of the behaviour of minor coal elements and their affinities to sulphur during coal combustion. Fuel, 78(15), pp.1817-1829.

10. Schwartz, G.E., Hower, J.C., Phillips, A.L., Rivera, N., Vengosh, A. and Hsu-Kim, H., 2018. Ranking Coal Ash Materials for Their Potential to Leach Arsenic and Selenium: Relative Importance of Ash Chemistry and Site Biogeochemistry. Environmental Engineering Science, 35(7), pp. 728-738

11. Environmental Protection Agency, Mercury and Air Toxics Standards (MATS) Electronic Reporting Requirements., 2017. 40 CFR Part 63, https://www.gpo.gov/fdsys/pkg/FR-2017-04-06/pdf/2017-06884.pdf.

12. Zhu, C., Tian, H., Cheng, K., Liu, K., Wang, K., Hua, S., Gao, J. and Zhou, J., 2016. Potentials of whole process control of heavy metals emissions from coal-fired power plants in China. Journal of Cleaner Production, 114, pp.343-351.

13. Senior, C.L., Huggins, F., Huffman, G.P., Shah, N., Yap, N., Wendt, J.O., Seames, W., Ames, M.R., Sarofim, A.F., Swenson, S. and Lighty, J.S., 2001. Toxic substances from coal combustion-a comprehensive assessment. Physical Sciences Inc. pp. 1-786.

14. Huang, Q., Li, S., Li, G. and Yao, Q., 2017. Mechanisms on the size partitioning of sodium in particulate matter from pulverized coal combustion. Combustion and Flame, 182, pp.313-323.

15. De Santiago, A., Longo, A.F., Ingall, E.D., Diaz, J.M., King, L.E., Lai, B., Weber, R.J., Russell, A.G. and Oakes, M., 2014. Characterization of selenium in ambient aerosols and primary emission sources. Environmental science & technology, 48(16), pp.8988-8994.

16. USEPA. 1998. Particulate matter research needs for human health risk assessment to support future reviews of the national ambient air quality standards for particulate matter. U.S. Environmental Protection Agency, Report No. EPA/600/R97/132F

17. Seames, W.S., Sooroshian, J. and Wendt, J.O., 2002. Assessing the solubility of inorganic compounds from size-segregated coal fly ash aerosol impactor samples. Journal of aerosol science, 33(1), pp.77-90.

18. Seames, W.S., Gadgil, M., Wang, C. and Fetsch, J., 2006, September. Impacts on trace metal leaching from fly ash due to the co-combustion of switch grass with coal. In Proceedings of 23rd Pittsburgh coal Conference paper (pp. 40-4).

19. David W. Evans, James G. Wiener & John H. Horton., 2012. Trace Element Inputs from a Coal Burning Power Plant to Adjacent Terrestrial and Aquatic Environments, Journal of the Air Pollution Control Association, 30(5), pp. 567-573.

20. Yao, Z.T., Ji, X.S., Sarker, P.K., Tang, J.H., Ge, L.Q., Xia, M.S. and Xi, Y.Q., 2015. A comprehensive review on the applications of coal fly ash. Earth-Science Reviews, 141, pp.105-121.

21. Wang, C., Liu, H., Zhang, Y., Zou, C. and Anthony, E.J., 2018. Review of arsenic behavior during coal combustion: Volatilization, transformation, emission and removal technologies. Progress in Energy and Combustion Science, 68, pp.1-28.

22. Hu, G., Liu, G., Wu, D. and Fu, B., 2018. Geochemical behavior of hazardous volatile elements in coals with different geological origin during combustion. Fuel, 233, pp.361-376.

23. Bustaffa, E., Stoccoro, A., Bianchi, F. and Migliore, L., 2014. Genotoxic and epigenetic mechanisms in arsenic carcinogenicity. Archives of toxicology, 88(5), pp.1043-1067..

24. Agency for Toxic Substances and Disease Registry (ATSDR). 2003. Toxicological profile for Selenium. Atlanta, GA: U.S. Department of Health and Human Services, Public Health Service.

25. Sun, H.J., Rathinasabapathi, B., Wu, B., Luo, J., Pu, L.P. and Ma, L.Q., 2014. Arsenic and selenium toxicity and their interactive effects in humans. Environment international, 69, pp.148-158.

26. De Miguel, E., Izquierdo, M., Gómez, A., Mingot, J. and Barrio‐Parra, F., 2017. Risk assessment from exposure to arsenic, antimony, and selenium in urban gardens (Madrid, Spain). Environmental toxicology and chemistry, 36(2), pp.544-550.

27. Zhao, X., Xing, F., Cong, Y., Zhuang, Y., Han, M., Wu, Z., Yu, S., Wei, H., Wang, X. and Chen, G., 2017. Antimony trichloride induces a loss of cell viability via reactive oxygen species-dependent autophagy in A549 cells. The international journal of biochemistry & cell biology, 93, pp.32-40.

28. Shah, P., Strezov, V., Stevanov, C. and Nelson, P.F., 2007. Speciation of arsenic and selenium in coal combustion products. Energy & Fuels, 21(2), pp.506-512.

29. Deonarine, A., Kolker, A., Foster, A.L., Doughten, M.W., Holland, J.T. and Bailoo, J.D., 2016. Arsenic speciation in bituminous coal fly ash and transformations in response to redox conditions. Environmental science & technology, 50(11), pp.6099-6106.

30. Wang, T., Wang, J., Tang, Y., Shi, H. and Ladwig, K., 2009. Leaching characteristics of arsenic and selenium from coal fly ash: role of calcium. Energy & Fuels, 23(6), pp.2959-2966.

31. Schwartz, G.E., Rivera, N., Lee, S.W., Harrington, J.M., Hower, J.C., Levine, K.E., Vengosh, A. and Hsu-Kim, H., 2016. Leaching potential and redox transformations of arsenic and selenium in sediment microcosms with fly ash. Applied Geochemistry, 67, pp.177-185.

32. Hu, H., Liu, H., Chen, J., Li, A., Yao, H., Low, F. and Zhang, L., 2015. Speciation transformation of arsenic during municipal solid waste incineration. Proceedings of the Combustion Institute, 35(3), pp.2883-2890.

33. Sun, W., Renew, J.E., Zhang, W., Tang, Y. and Huang, C.H., 2017. Sorption of Se (IV) and Se (VI) to coal fly ash/cement composite: Effect of Ca 2+ and high ionic strength. Chemical Geology, 464, pp.76-83.

34. Huggins, F.E., Senior, C.L., Chu, P., Ladwig, K. and Huffman, G.P., 2007. Selenium and arsenic speciation in fly ash from full-scale coal-burning utility plants. Environmental science & technology, 41(9), pp.3284-3289.

35. Liu, Y.T., Chen, T.Y., Mackebee, W.G., Ruhl, L., Vengosh, A. and Hsu-Kim, H., 2013. Selenium speciation in coal ash spilled at the Tennessee Valley Authority Kingston site. Environmental science & technology, 47(24), pp.14001-14009.

36. Roy, B., Choo, W.L. and Bhattacharya, S., 2013. Prediction of distribution of trace elements under oxy-fuel combustion condition using Victorian brown coals. Fuel, 114, pp.135-142.

37. Tian, H., Zhou, J., Zhu, C., Zhao, D., Gao, J., Hao, J., He, M., Liu, K., Wang, K. and Hua, S., 2014. A comprehensive global inventory of atmospheric antimony emissions from anthropogenic activities, 1995–2010. Environmental science & technology, 48(17), pp.10235-10241.

38. Matusiewicz, H. and Krawczyk, M., 2008. Determination of total antimony and inorganic antimony species by hydride generation in situ trapping flame atomic absorption spectrometry: a new way to (ultra) trace speciation analysis. Journal of Analytical Atomic Spectrometry, 23(1), pp.43-53.

39. Varrica, D., Bardelli, F., Dongarra, G. and Tamburo, E., 2013. Speciation of Sb in airborne particulate matter, vehicle brake linings, and brake pad wear residues. Atmospheric environment, 64, pp.18-24.

40. Peng, Y., Li, J., Si, W., Luo, J., Wang, Y., Fu, J., Li, X., Crittenden, J. and Hao, J., 2015. Deactivation and regeneration of a commercial SCR catalyst: Comparison with alkali metals and arsenic. Applied Catalysis B: Environmental, 168, pp.195-202.

41. Niu, Y., Wang, S., Shaddix, C.R. and Hui, S.E., 2016. Kinetic modeling of the formation and growth of inorganic nano-particles during pulverized coal char combustion in O 2/N 2 and O 2/CO 2 atmospheres. Combustion and Flame, 173, pp.195-207.

42. Quann, R. J., Neville, M., Janghorbani, M., Mims, C. A., Sarofim, A. F., 1982. Mineral Matter and Trace Element Vaporization in a Laboratory-Pulverized Coal Combustion System. Environ.Sci.Technol 16, pp. 776-781

43. Raeva, A.A., Pierce, D.T., Seames, W.S. and Kozliak, E.I., 2011. A method for measuring the kinetics of organically associated inorganic contaminant vaporization during coal combustion. Fuel processing technology, 92(7), pp.1333-1339.

44. Raeva, A.A., Klykov, O.V., Kozliak, E.I., Pierce, D.T. and Seames, W.S., 2011. In situ evaluation of inorganic matrix effects on the partitioning of three trace elements (As, Sb, Se) at the outset of coal combustion. Energy & Fuels, 25(10), pp.4290-4298.

45. James, D.W., Krishnamoorthy, G., Benson, S.A. and Seames, W.S., 2014. Modeling trace element partitioning during coal combustion. Fuel Processing Technology, 126, pp.284-297.

46. Linak, W.P., Miller, C.A., Seames, W.S., Wendt, J.O., Ishinomori, T., Endo, Y. and Miyamae, S., 2002. On trimodal particle size distributions in fly ash from pulverized-coal combustion. Proceedings of the Combustion Institute, 29(1), pp.441-447.

47. Yu, D., Xu, M., Yao, H., Liu, X., Zhou, K., Li, L. and Wen, C., 2009. Mechanisms of the central mode particle formation during pulverized coal combustion. Proceedings of the Combustion Institute, 32(2), pp.2075-2082.

48. Seames, W.S., 2003. An initial study of the fine fragmentation fly ash particle mode generated during pulverized coal combustion. Fuel Processing Technology, 81(2), pp.109-125.

49. Smith, R.D., Campbell, J.A. and Nielson, K.K., 1979. Characterization and formation of submicron particles in coal-fired plants. Atmospheric Environment (1967), 13(5), pp.607-617.

50. Baxter, L.L., 1992. Char fragmentation and fly ash formation during pulverized-coal combustion. Combustion and Flame, 90(2), pp.174-184.

51. Yu, D., Xu, M., Yao, H., Liu, X. and Zhou, K., 2008. A new method for identifying the modes of particulate matter from pulverized coal combustion. Powder Technology, 183(1), pp.105-114.

52. Taylor, D.D. and Flagan, R.C., 1981. The influence of combustor operation on fine particles from coal combustion. Aerosol Science and Technology, 1(1), pp.103-117.

53. Zeng, T., Sarofim, A. F., Senior, C. L., 2001. Vaporization of arsenic, selenium and antimony during coal combustion. Combustion and Flame 126, pp. 1714-1724.

54. Liu, J., Dai, S., He, X., Hower, J.C. and Sakulpitakphon, T., 2017. Size-dependent variations in fly ash trace element chemistry: examples from a Kentucky power plant and with emphasis on rare earth elements. Energy & Fuels, 31(1), pp.438-447.

55. Wortmann, C.S., Mamo, M. and Shapiro, C.A., 2003. Management strategies to reduce the rate of soil acidification. Cooperative Extension, Institute of Agriculture and Natural Resources, University of Nebraska-Lincoln.

56. Jones, C., Hahn, J., Magee, B., Yuen, N., Sandefur, K., Tom, J. and Yap, C., 1999. Utilization of ash from municipal solid waste combustion (No. NREL/SR-570-26068). National Renewable Energy Lab., Golden, CO (US).

57. Izquierdo, M. and Querol, X., 2012. Leaching behaviour of elements from coal combustion fly ash: an overview. International Journal of Coal Geology, 94, pp.54-66.

58. Kosson, D.S., Garrabrants, A.C., DeLapp, R. and van der Sloot, H.A., 2014. pH-dependent leaching of constituents of potential concern from concrete materials containing coal combustion fly ash. Chemosphere, 103, pp.140-147.

59. McElroy, M.W., Carr, R.C., Ensor, D.S. and Markowski, G.R., 1982. Size distribution of fine particles from coal combustion. Science, 215(4528), pp.13-19.

60. Gadgil, M.R.,2006. Leachability of Trace Elements from Biomass Fly Ash Samples, M.S Thesis, University of North Dakota, Grand Forks, ND.

61. EPA Method 3052, Microwave Assisted Acid Digestion Of Siliceous And Organically Based Matrices., https://www.epa.gov/sites/production/files/2015-12/documents/3052.pdf

62. Kang, S.G., 1991. Fundamental studies of mineral matter transformation during pulverized coal combustion: Residual ash formation, PhD dissertation, Massachusetts Institute of Technology.

63. Joutsensaari, J., Kauppinen, E.I., Ahonen, P., Lind, T.M., Ylätalo, S.I., Jokiniemi, J.K., Hautanen, J. and Kilpeläinen, M., 1992. Aerosol formation in real scale pulverized coal combustion. Journal of Aerosol Science, 23, pp.241-244.

64. Senior, C.L., Bool III, L.E., Srinivasachar, S., Pease, B.R. and Porle, K., 2000. Pilot scale study of trace element vaporization and condensation during combustion of a pulverized sub-bituminous coal. Fuel Processing Technology, 63(2-3), pp.149-165.

65. Benson, S.A. and Holm, P.L., 1985. Comparison of inorganics in three low-rank coals. Industrial & engineering chemistry product research and development, 24(1), pp.145-149.

66. Bool, L.E.I. and Helble, J.J., 1995. A laboratory study of the partitioning of trace elements during pulverized coal combustion. Energy & Fuels, 9(5), pp.880-887.

67. Meij, R and Winkel, H., 2007. The emissions of heavy metals and persistent organic pollutants from modern coal-fired power stations, Atmospheric Environment 41(40), pp. 9262-9272.

68. Dean, J. A. 1992. Langes Handbook of Chemistry. (14th ed.). New York: McGraw-Hill.

69. Jones, D.R., 1995. The leaching of major and trace elements from coal ash. In Environmental aspects of trace elements in coal (pp. 221-262). Springer, Dordrecht.

70. Cornelis, G., Johnson, C.A., Gerven, T.V., Vandecasteele, C., 2008. Leaching Mechanisms of Oxyanionic Metalloid and Metal Species in Alkaline Solid Wastes: A review. Applied Geochemistry 235), pp. 955-976.

71. Kim, A.G. and Kazonich, G., 2004. The silicate/non-silicate distribution of metals in fly ash and its effect on solubility. Fuel, 83(17-18), pp.2285-2292.

72. Norman, N.C. ed., 1997. Chemistry of arsenic, antimony and bismuth. Springer Science & Business Media.

CHAPTER 6

CONCLUSIONS AND SUGGESTIONS FOR FUTURE WORK

Understanding the fate of trace elements (TEs) in fly ash generated during pulverized coal combustion is a necessary component in assessing potential risks, including health effects of any respirable ash particles, and in the subsequent implementation of suitable control measures. Of particular interest to this study is the leaching potential of the three TEs in coal combustion fly ash – As, Se and Sb. All three TEs have been classified as hazardous pollutants under the amended clean air act and As and Se are two of the species regulated to meet the proposed ELG requirements for electric utilities. Their tendency to be enriched in the $PM_{2.5}$ size range makes them a potential threat in the solid phase as well.

Because of their semi-volatile nature, all three TEs tend to vaporize under flame conditions and undergo post combustion partitioning reactions on the surface of existing fly ash particles. Both kinetic considerations and mass transfer limitations influence TE availability and speciation on ash particles. Previous research has shown that fly ash particle size plays a significant role in both TE partitioning reactions and the control of their overall mobility under different leaching environments.

A series of experiments were conducted to evaluate the environmental impact, in terms of element mobility, of these three important trace elements in coal. This study examined the effect of certain parameters affecting ash particle size distribution including changes to combustion temperature, difference in coal ash chemistries etc and its effect on both TE availability and its subsequent mobility. Collection of fly ash particles using cascade impactors, such as the DLPI, has provided the versatility necessary for detailed characterization of mobility based on different size ranges.

This work demonstrated a relatively easy, inexpensive technique that can be utilized in specific studies to qualitatively assess the environmental impact of PC combustion generated fly ash. While only three TEs were included in this demonstration study, a much richer suite of TEs can be evaluated using these techniques.

CONCLUSIONS

1   All three TEs showed moderate to high mobility in the smaller submicron and fine fragment particles mainly under acidic and neutral environments. This was observed irrespective of combustion conditions and coal rank, indicating mainly surface presence of TEs on these particles

2   Bulk mode mobility was comparatively lower for all TEs under most test conditions.

3   Changes to combustion temperature increased TE mass loadings in particle matter in the submicron and fine fragment regime size ranges. However, TE solubilities in a given leaching solution and for a particular size mode remained unaffected for the test coal. This suggests that the increase in mass loadings was due to an increase in available cation surface sites rather than from a change to TE partitioning mechanism.

4   With respect to the effect of coal rank, differences in mobility were observed only for Se suggesting potential speciation differences for the two test coals. Arsenic mobility showed no significant difference between the two coals and antimony results were inconclusive.

5   Tests conducted in a full-scale utility boiler showed the scrubber had an overall positive impact by removing a majority amount of all three elements. In the case of As and Sb, removal across the scrubber occurred without change in form (physical scrubbing) as evidenced by both mass distribution and mobility data. However, Se data indicates there has been a change in form from scrubber operating conditions resulting in slightly increased emissions for the submicron range. This was further confirmed by differences in mobility data between inlet and outlet conditions.

RECOMMENDATIONS

1   An effort to determine the actual speciation (oxidation state) of TEs in both coal and fly ash. While mobility data can be used to predict possible TE speciation in ash, such predictions are often speculative since two or three species can have similar solubility characteristics in a given leaching environment. An improvement on the existing modified TCLP method is highly recommended to determine TE oxidation state especially in size segregated ash.

2   A detailed investigation to study the impacts of sulfation (catalyzed by iron) on the partitioning and subsequent mobility of trace elements of interest.

3   A detailed investigation to study the effect of varying Ca to Si ratios and the subsequent effect on TE speciation and mobility. This was postulated as a possible reason for high vapor phase As concentrations and merits further investigation, especially fly ash SiO_2 derived from clays.

4   An investigation of the effects of halogen addition (mainly bromine and Iodine) to coal on fly ash TE speciation and mobility. Reports indicate that halogen added to coal (for Hg oxidation) also resulted in an increase in vapor phase selenium concentration. However, no such data is available for either As or Sb. A more detailed investigation should be conducted to understand this effect on all three TEs. Also, there could be a potential a trade-off between Hg oxidation and increased Se in the FGD slurry.

5   An extended study to further investigate selenium speciation across the wet scrubber, especially for another coal. This could be an Illinois basin coal which typically has high amounts of both sulfur and selenium. A selenium balance can be constructed across the FGD by also including Se in gypsum and chloride purge. Consider the impact of recycle (causes build-up) and a leaching study of the gypsum by-product is also recommended.

6   An investigation of TE mobility in international coals, especially Indian coals, where coal is still a major source of power. Coals in this region are typically very high ash and can also contain significant levels of TEs such as As. Reports of high As concentration in vegetation and rice plantations has been previously reported as fly ashes are mostly disposed in open ash ponds. The potential for leaching seems to be high and mobility studies for size segregated ash particles is recommended.

APPENDIX D

Particulate sampling in the laboratory scale furnace

The particulate sampling system is used to generate size segregated particulate samples from the furnace centerline. A portable, stainless steel, water cooled, iso-kinetic sampling probe and vacuum pump are used to extract particulate from the furnace centerline. The 1.25" OD particulate probe is sealed to the sample port using a 2" threaded union. The probe internals consist of a ¼" OD cooling water dip tube, a ¼" OD cooling water exit line, a ¼" nitrogen dilution line, and the 3/8" sample line. The cooling water from a water manifold station enters the dip tube and exits through the outlet on the handle end of the probe. The inlet to the sample tube faces up during sampling to extract an undisturbed streamline sample from the furnace centerline.

A furnace sample is extracted from the furnace centerline into the probe and immediately diluted with nitrogen at the probe inlet and cooled which minimizes reaction processes within the probe and tubing so that the composition in the samples reflects the composition in the furnace. Also, the rapid cooling in the probe causes some material that is in the vapor phase at the furnace temperature to nucleate in the probe. Dilution inhibits coagulation and agglomeration in the probe so that the particle size distribution (PSD) generated by the LPI can be consistently related to the actual PSD in the furnace. The sample is then pulled into the LPI using a vacuum pump (Rietschie – SV 25, 0.5 hp). The low-pressure impactor bottom stages act as sonic orifices to control the total flow rate from the sampling probe at approximately 30 actual L/min (alpm).

The dilution ratio is defined as the volumetric flow rate ratio of the dilution nitrogen into the sampling probe to the combustion gas extracted from the furnace through the sampling probe. Isokinetic sampling is monitored by the concentration of NO_x (or CO). The expected isokinetic NO_x (or CO) concentration is calculated by scaling the furnace NO_x (or CO) concentration measured at the sample port to include the dilution nitrogen added in the sample probe.

Steps for iso-kinetic sampling in the laboratory scale combustor

1.   Measure and record O_2, CO, and temperature at the desired sample port.

2.   Input the measurements from step 1 into the coal operations spreadsheet. Run the program to determine the required N_2 flowrate into the probe. The program also gives the dilution ratio and the diluted concentration for CO through the impactor.

3.   Load impactor with blank foils.

4.   Connect impactor and cyclone with particulate probe.

5.   Turn on particulate probe cooling water.

6.   Turn on N_2 and set the flowrate close to the required value as determined in step 2.

7.   Insert particulate probe into the sample port.

8.   Turn on vacuum pump.

9.   Record CO measurement and adjust N_2 flow to obtain the desired diluted concentration as determined in step 2.

Table 39: Example iso-kinetic sampling rate calculation flow sheet for the laboratory furnace

SAMPEL PORT TEMPERATURE →	825	°C				
FLUE GAS FLOW RATE →	2020	ft^3/hr				
→	0.561	ft^3/s				
FURNACE CROSS SECTIONAL AREA →	0.196	ft^2				
AVERAGE VELOCITY →	10288	ft/hr				
→	2.858	ft/s				
CENTER-LINE VELOCITY →	3.175	ft/s				
PROBE INLET DIAMETER →	0.0254	ft				
PROBE INLET CROSS SECTIONAL AREA →	0.0005	ft^2				
SAMPLE FLOW RATE INTO PROBE →	0.0016	ft^3/s				
→	0.00040	Sft^3/s				
→	0.011347	NL/s				
MOLAR FLOW RATE IN FURNACE→	0.000389	lbmol/s				
OBSERVED LPI MAXIMUM FLOW RATE →	29.98	NL/m				
N$_2$ MASS FLOW CONTROLLER OFFSET →	0.6	NL/m				
ACTUAL LPI MAXIMUM FLOW RATE →	29.38	NL/m				
→	0.490	NL/s				
→	0.0173	Sft^3/s				
DESIRED N$_2$ FLOW RATE →	0.0169	Sft^3/s				
→	28.699	NL/m				
N$_2$ SETPOINT →	29.299	NL/m				
DILUTION RATIO →	42.15					
REFERENCE CONCENTRATION →	12					
DESIRED OBSERVED READING →	0.28					

FOR CALCULATING THE ISOKINETIC SAMPLE RATE

O$_2$ CONC AT SAMPLE PORT →	4.9	%				
DIFFERENCE IN O$_2$ CONC →	1.100	%				

STEPS TO INCORPORATE LEAKAGE INTO THE ISOKINETIC SET POINT CALCULATION
1. BACK CALCULATE THE FUEL FEED RATE USING THE OXYGEN CONCENTRATION AT THE TOP OF THE FURNACE.
2. CHECK THE OXYGEN READING AT THE SAMPLE PORT AND INPUT INTO (B35).
3. GOALSEEK THE DIFFERENCE IN OXYGEN CONC (B36) TO ZERO BY CHANGING THE EXCESS AIR ESTIMATE (I-0 C9).